Technological Advances in Conservation Biology

Anne Cathrine Linder

Master's Thesis

June 2022

AALBORG UNIVERSITY
STUDENT REPORT

Title:
Technological Advances in Conservation Biology

Theme:
Master's thesis

Project Period:
Fall 2021 - Spring 2022

Participants:
Anne Cathrine Linder

Supervisors:
Cino Pertoldi
Dan Bruhn

Number of Pages: 102

Date of Completion: June 1, 2022

Preface

This master's thesis demonstrates the use of three different conservation technologies for wildlife monitoring, nature management, and wildlife research. These conservation technologies include drones with thermal imaging for monitoring populations, automated camera–based monitoring systems developed to mitigate the impact of wind turbines on protected avian species, and virtual fencing systems for conservation grazing. The use of these conservation technologies has not previously been demonstrated in Denmark and Sweden, where the studies included in this thesis took place. The first study demonstrates the use of drones with thermal imaging to monitor European hare (*Lepus europaeus*) populations. To my knowledge, the use of drones with thermal imaging to conduct population counts over a larger area has not previously been demonstrated for small mammals. This study is, therefore, the first to demonstrate the use of drones with thermal imaging to monitor European hare populations. Thus, providing imperative information on the appropriate flight methodology. The second and third study utilize data from an automated camera–based monitoring system, to quantify flight behavior in association with turbine collision risk. These studies are the first to use this unique data to describe avian flight behavior and by using this data it was possible to quantify trivial flight behaviors, which to my knowledge has not been done previously. The last study demonstrated the use of virtual fencing as an effective tool for confining a herd of cattle in Denmark. This technology is currently illegal in Denmark due to welfare concerns and this study, therefore, provides legislators with crucial evidence that virtual fencing does not compromise animal welfare and is, therefore, a viable alternative to physical electrical fencing for conservation grazing in Denmark.

The second article *Quantifying Raptors' Flight Behavior to Assess Collision Risk and Avoidance Behavior to Wind Turbines* is based on a semester project that was conducted in the fall semester, 2020. The entire article has since been thoroughly restructured and revised, including the addition of a multivariate analysis to assess which variables affect flight behaviors influencing collision risk. The third article *Modeling Species-Specific Collision Risk of Birds with Wind Turbines: A Behavioral Approach* is based on another semester project that was conducted in the spring semester, 2021. The semester project was based on data collected over a six month period from the middle of February, 2020 to the middle of August, 2020. As part of this master's project seven additional months of data were included in the analysis, i.e., the revised article included in this thesis is based on data from the middle of February, 2020 to the end of March, 2021. Thus, the methods, results, and discussion sections of the article previously submitted as a semester project have been revised according to the new data analysis.

Contents

Introduction

Conservation technology is an emerging field within wildlife research. Technology can provide wildlife researchers with the opportunity to collect more and better data. Thereby, potentially improving wildlife monitoring and assisting in management decisions [1]. Throughout the past decade, drones have been increasingly used by biologists as a noninvasive method for surveying wildlife [2–6]. Drones can be used in environments that are difficult to monitor with traditional methods. Moreover, drones equipped with thermal cameras have recently become readily available, thus, broadening the possibilities with drone surveys to include surveying nocturnal species [7]. However, most studies demonstrating the use of drone surveys with thermal imaging, have focused on larger mammals, such as, deer spp. (Cervidae), alpaca (*Vicugna pacos*), and long–tailed macaque (*Macaca fascicularis*) [7–11]. There is a need for studies assessing the use of drones equipped with thermal cameras as a monitoring tool for smaller mammals, such as, the European hare (*Lepus europaeus*), which has been a species of conservation interest in Denmark since the mid 1900s [12–14]. Moreover, the value of drone surveys is dependent on the recording method along with a number of flight parameters, such as, flight altitude and speed. Thus, for different species groups, based on size, shape, behavior, and habitat, it is necessary to assess how different flight parameters affect species identification and population counts.

Technological advances have not only led to the the development new surveillance methods, but have also yielded new tools within nature management. Recently, some technologies have even been specifically developed to contribute to nature management, such as, automated camera–based monitoring systems mitigating the impact of wind turbines on protected bird species [15]. However, the actual collision risk is presumably determined by multiple other factors, such as, flight behavior, flight morphology, and weather conditions [16–19]. Knowledge on the flight behavior of protected species, such as eagles and red kites, and how their behavior can be affected by environmental factors is, therefore, crucial to improving curtailment decisions. Curtailing wind turbines is expensive, hence, energy companies would benefit from the development of behavior specific curtailment models which may result in more companies investing in this type of technology and contributing to avian conservation. Moreover, flight behavior is likely linked to species–specific foraging behavior, flight behavior, and morphology [20–22]. Quantifying species–specific differences in flight behavior could also contribute to improving curtailment models. The development of camera–based monitoring systems has also effectuated the collection of large amounts of data on wind farms, including flight trajectories based on spatial coordinates and images of individual birds throughout their flight trajectories. Thus, giving the unique opportunity of assessing flight behavior based on both flight trajectories and image based behavioral observations.

Another recent technological advance contributing to nature management is virtual fencing. Virtual fencing has been developed as an alternative to physical fencing for conservation grazing. This fencing type uses GPS technology and could provide a flexible fencing option for extensive grazing of large areas, such as, in rewilding projects [23–25]. Physical electric fencing has previously been described as a limitation in nature management because of its inflexibility and the negative effects of physical boundaries on wildlife [26–29]. Virtual fencing systems provide boundaries without physical barriers. Virtual fencing works by attaching a collar to each animal that can administer auditory warnings and low energy electric impulses. However, this is currently illegal in a number of European countries, including Denmark, due to welfare concerns [30]. Therefore, to determine whether this technology is suitable for use in nature conservation it must be ensured that welfare is not compromised.

This study will assess the use of three different conservation technologies for wildlife monitoring and nature management. The first article will investigate the potential use of a drone equipped with a thermal camera as a tool for monitoring the European hare (*Lepus europaeus*) population in Denmark. The second article will investigate how the flight behavior of raptors can be quantified by using unique data from the IdentiFlight system, demonstrating how this type of data can be used to assess general flight behavior and investigate site and species–specific avoidance behavior. The third article will further utilize the data collected with the IdentiFlight system to investigate how the flight behavioral traits; head position, active flight, track tortuosity, and track symmetry can be used to model collision risk for twelve different bird species along with weather and temporal factors. The last article will assess the use of the Nofence© virtual fencing system to keep a group of twelve Angus cows (*Bos taurus*) within a virtual enclosure with minimal welfare implications.

References

1. Berger-Tal, O.; Lahoz-Monfort, J.J. Conservation technology: The next generation. *Conservation Letters* **2018**, *11*, e12458. doi:10.1111/conl.12458.

2.   Sweeney, K.L.; Helker, V.T.; Perryman, W.L.; LeRoi, D.J.; Fritz, L.W.; Gelatt, T.S.; Angliss, R.P. Flying beneath the Clouds at the Edge of the World: Using a Hexacopter to Supplement Abundance Surveys of Steller Sea Lions (*Eumetopias Jubatus*) in Alaska. *Journal of Unmanned Vehicle Systems* **2016**, *4*, 70–81. doi:10.1139/juvs-2015-0010.

3.   Bech-Hansen, M.; M. Kallehauge, R.; Bruhn, D.; H. Funder Castenschiold, J.; Beltoft Gehrlein, J.; Laubek, B.; F. Jensen, L.; Pertoldi, C. Effect of Landscape Elements on the Symmetry and Variance of the Spatial Distribution of Individual Birds within Foraging Flocks of Geese. *Symmetry* **2019**, *11*. doi:10.3390/sym11091103.

4.   Rahman, D.A.; Sitorus, A.B.Y.; Condro, A.A. From Coastal to Montane Forest Ecosystems, Using Drones for Multi-Species Research in the Tropics. *Drones* **2021**, *6*, 6. doi:10.3390/drones6010006.

5.   Wen, D.; Su, L.; Hu, Y.; Xiong, Z.; Liu, M.; Long, Y. Surveys of Large Waterfowl and Their Habitats Using an Unmanned Aerial Vehicle: A Case Study on the Siberian Crane. *Drones* **2021**, *5*, 102. doi:10.3390/drones5040102.

6.   Castenschiold, J.H.F.; Bregnballe, T.; Bruhn, D.; Pertoldi, C. Unmanned Aircraft Systems as a Powerful Tool to Detect Fine-Scale Spatial Positioning and Interactions between Waterbirds at High-Tide Roosts. *Animals* **2022**, *12*. doi:10.3390/ani12080947.

7.   Lee, S.; Song, Y.; Kil, S.H. Feasibility Analyses of Real-Time Detection of Wildlife Using UAV-Derived Thermal and RGB Images. *Remote Sensing* **2021**, *13*, 2169. doi:10.3390/rs13112169.

8.   Chrétien, L.P.; Théau, J.; Ménard, P. Visible and thermal infrared remote sensing for the detection of white-tailed deer using an unmanned aerial system. *Wildlife Society Bulletin* **2016**, *40*, 181–191. doi:10.1002/wsb.629.

9.   Obermoller, T.R.; Norton, A.S.; Michel, E.S.; Haroldson, B.S. Use of Drones with Thermal Infrared to Locate White-tailed Deer Neonates for Capture. *Wildlife Society Bulletin* **2021**, *45*, 682–689. doi:10.1002/wsb.1242.

10. Rahman, D.A.; Setiawan, Y.; Wijayanto, A.K.; Rahman, A.A.A.F.; Martiyani, T.R. An Experimental Approach to Exploring the Feasibility of Unmanned Aerial Vehicle and Thermal Imaging in Terrestrial and Arboreal Mammals Research. *E3S Web of Conferences* **2020**, *211*, 02010. doi:10.1051/e3sconf/202021102010.

11. Rahman, D.A.; Setiawan, Y. Possibility of Applying Unmanned Aerial Vehicle and Thermal Imaging in Several Canopy Cover Class for Wildlife Monitoring – Preliminary Results. *E3S Web of Conferences* **2020**, *211*, 04007. doi:10.1051/e3sconf/202021104007.

12. Schmidt, N.M.; Asferg, T.; Forchhammer, M.C. Long-term patterns in European brown hare population dynamics in Denmark: effects of agriculture, predation and climate. *BMC Ecology* **2004**, *4*, 1–7. doi:10.1186/1472-6785-4-15.

13. Misiorowska, M.; Wasilewski, M. Survival and causes of death among released brown hares (*Lepus europaeus* Pallas, 1778) in Central Poland. *Acta Theriologica* **2012**, *57*, 305–312. doi:10.1007/s13364-012-0081-1.

14. Nationalt Center for Miljø og Energi, A.U. *Forvaltningsplan for hare*, 2013.

15. McClure, C.J.W.; Martinson, L.; Allison, T.D. Automated Monitoring for Birds in Flight: Proof of Concept with Eagles at a Wind Power Facility. *Biological Conservation* **2018**, *224*, 26–33. doi:10.1016/j.biocon.2018.04.041.

16. Garvin, J.C.; Jennelle, C.S.; Drake, D.; Grodsky, S.M. Response of Raptors to a Wind farm. *Journal of Applied Ecology* **2011**, *48*, 199–209. doi:365-2664.2010.01912.X.

17. Dahl, E.L.; May, R.; Hoel, P.L.; Bevanger, K.; Pedersen, H.C.; Røskaft, E.; Stokke, B.G. White-Tailed Eagles (*Haliaeetus albicilla*) at the Smøla Wind-Power plant, Central Norway, Lack Behavioral Flight Responses to Wind Turbines. *Wildlife Society Bulletin* **2013**, *37*, 66–74. doi:10.1002/wsb.258.

18. Cook, A.S.C.P.; Humphreys, E.M.; Masden, E.A.; Burton, N.H.K. The Avoidance Rates of Collision Between Birds and Offshore Turbines - BTO Research Report No. 656. *Scottish Marine and Freshwater Science* **2014**, *5*.

19. Marques, A.T.; Batalha, H.; Rodrigues, S.; Costa, H.; Pereira, M.J.R.; Fonseca, C.; Mascarenhas, M.; Bernardino, J. Understanding Bird Collisions at Wind Farms: An Updated Review on the Causes and Possible Mitigation Strategies. *Biological Conservation* **2014**, *179*, 40–52. doi:10.1016/j.biocon.2014.08.017.

20. Barrios, L.; Rodríguez, A. Behavioural and Environmental Correlates of Soaring-bird Mortality at On-shore Wind Turbines. *Journal of Applied Ecology* **2004**, *41*, 72–81. doi:10.1111/j.1365-2664.2004.00876.x.

21. Drewitt, A.L.; Langston, R.H.W. Assessing the Impacts of Wind Farms on Birds. *Ibis* **2006**, *148*, 29–42. doi:10.1111/j.1474-919X.2006.00516.x.

22. de Lucas, M.; Janss, G.F.E.; Whitfield, D.P.; Ferrer, M. Collision Fatality of Raptors in Wind Farms does not Depend on Raptor Abundance. *Journal of Applied Ecology* **2008**, *45*, 1695–1703. doi:10.1111/j.1365-2664.2008.01549.x.

23. Campbell, D.L.M.; Lea, J.M.; Farrer, W.J.; Haynes, S.J.; Lee, C. Tech-Savvy Beef Cattle? How Heifers Respond to Moving Virtual Fence Lines. *Animals* **2017**, *7*, 72. doi:10.3390/ani7090072.

24. Campbell, D.L.M.; Ouzman, J.; Mowat, D.; Lea, J.M.; Lee, C.; Llewellyn, R.S. Virtual Fencing Technology Excludes Beef Cattle from an Environmentally Sensitive Area. *Animals* **2020**, *10*, 1069. doi:0.3390/ani1006106.

25. Lomax, S.; Colusso, P.; Clark, C.E. Does Virtual Fencing Work for Grazing Dairy Cattle? *Animals* **2019**, *9*, 429. doi:10.3390/ani9070429.

26. Jachowski, D.S.; Slotow, R.; Millspaugh, J.J. Good Virtual Fences Make Good Neighbors: Opportunities for Conservation. *Animal Conservation* **2014**, *17*, 187–196. doi:10.1111/acv.12082.

27. Osipova, L.; Okello, M.M.; Njumbi, S.J.; Ngene, S.; Western, D.; Hayward, M.W.; Balkenhol, N. Fencing Solves Human-Wildlife Conflict Locally but Shifts Problems Elsewhere: A Case Study Using Functional Connectivity Modelling of the African Elephant. *Journal of Applied Ecology* **2018**, *55*, 2673–2684. doi:10.1111/1365-2664.13246.

28. Campbell, D.L.M.; Lea, J.M.; Keshavarzi, H.; Lee, C. Virtual Fencing is Comparable to Electric Tape Fencing for Cattle Behavior and Welfare. *Frontiers in Veterinary Science* **2019**, *6*, 445. doi:10.3389/fvets.2019.00445.

29. Umstatter, C. The Evolution of Virtual Fences: A Review. *Computers and Electronics in Agriculture* **2011**, *75*, 10–22. doi:10.1016/j.compag.2010.10.005.

30. Stampa, E.; Zander, K.; Hamm, U. Insights into German Consumers' Perceptions of Virtual Fencing in Grassland-Based Beef and Dairy Systems: Recommendations for Communication. *Animals* **2020**, *10*, 2267. doi:10.3390/ani10122267.

Using Drones with Thermal Imaging to Estimate Population Trends of European Hare (*Lepus europaeus*) in Denmark

Anne Cathrine Linder [1]*

1   Department of Chemistry and Bioscience — Section of Biology and Environmental Science, Aalborg University, Fredrik Bajers Vej 7, 9220 Aalborg, Denmark

Abstract: Drones have over the past decade emerged as a noninvasive tool for surveying wildlife populations. More recently, drones equipped with thermal cameras have become readily available, thus, broadening the possibilities with drone surveys. Due to the reliance of animals' body heat, drone surveys with thermal imaging are ideal for monitoring nocturnal species. The European hare (*Lepus europaeus*) is a nocturnal species that is closely monitored in Denmark, due to populations declining since the mid 1900s. The limitations of current population assessments, based on spotlight counts and hunting game statistics, could be overcome by relying on drone surveys with thermal imaging for population counts. The aim of this study was to investigate the possible use of a drone equipped with a thermal camera as a tool for monitoring the Danish population of European hare. This was achieved by testing multiple flight parameters along with different camera settings and recording methods. Based on the results of test flights, an appropriate method for identifying and counting hares with thermal image based drone surveys was suggested. The applied use of the suggested methodology was evaluated through a case survey with the aim of identifying and counting hare over a larger area of 206 ha. Two different sites with agricultural landscapes in Northern Jutland, Denmark were used to carry out multiple aerial surveys between March 21st, 2022 and April 20th, 2022. The drone used in this study was the DJI Mavic 2 Enterprise Advanced. Hare could be detected at flight altitudes up to 80 m with the drones thermal camera and it was possible to fly as low as 40 m without disturbing the animals. Thermal images taken at altitudes between 40 and 80 m provided enough detail to differentiate between species. Moreover, animal body size proved to be a good indicator of species, with with the species in this study varying significantly in size. The case survey confirmed the use of thermal image based drone surveys to identify hare and conduct population counts.

1. Introduction

Quantitative information on wildlife populations is necessary for understanding relations between species and their habitat requirements, thereby, providing information essential for nature management and conservation. To conduct wildlife population counts, traditional field surveys have been widely used in the past. Traditional population monitoring includes direct methods, such as, field observations of animals on foot or from a manned aircraft, images from fixed on–site locations captured using camera traps, fecal density counts, and sampling with mark–recapture methods, and indirect monitoring methods, e.g., yearly hunting harvest statistics [1–8]. However, over the past decade the use of unmanned aerial vehicles (drones) has emerged as a precise and noninvasive method for surveying wildlife populations [9–15]. Drones may be used in environments that are difficult to monitor by traditional methods [11,16]. Even in areas that are easily accessible, drone surveying has in many cases been proven to provide accurate population estimates [9,11,12,14,16,17]. Moreover, drones often reduce time and labor expended on ground surveys and are a cheaper alternative to manned aerial surveys [18].

Drones equipped with thermal cameras have recently become readily available [19]. This development has furthered the use of drones in wildlife research, broadening the possibilities with drone surveys. Thermal imaging relies on animals' body heat, i.e. an animal will appear as a bright object at thermal infrared wavelengths, if the surface temperature of an animal is warmer than the surface of its surroundings. Thus, making drone surveys with thermal imaging ideal for monitoring nocturnal and crepuscular species, e.g. kangaroos [20,21] and deer [18,22,23], along with forest dwelling species, e.g. koalas [24] and macaques [22], and species camouflaged by their cryptic fur or plumage [25].

The European hare (*Lepus europaeus*) is a nocturnal species with a cryptic fur making them difficult to detect. The European hare has been a species of interest in many European countries since the mid 1900s, where populations began declining all over Europe [26–28]. Moreover, the European hare has also received a lot of attention as a valued game species in many countries [26,29]. The status of the European hare is classified as least concern in Europe, despite populations continuing to decline [28,30]. Population declines have been linked to the intensification of agricultural practices, e.g. increased use of herbicides and homogeneous crop choices [26,31,32]. The danish population declined

more that 30% in the early 2000s, leading to the European hare being included on the Danish Red List as a vulnerable species in 2007 [28]. However, throughout the past decade this decline has been reduced to 10% and the European hare was reclassified as least concern in 2019 [33]. A national management plan was created in 2013, which has resulted in a steady development in the danish hare population [34,35]. These results are based on annual hunting game statistics and local population counts conducted by volunteers annually in the spring and fall.

Local population counts are completed with the spotlight method, where counts are performed 1–2 hours after sunset [36]. Spotlight counts are conducted from a car moving approximately 10–25 km/h along a transect line. Hand held spotlights are then used to illuminate 150 m to each side of the transect route. Observers detect hare based on their silhouette and the light reflection from the hare's eyes [36]. The quantity of reflected light that is returned to the observer's eye decreases with distance, e.g. if the distance between the hare and observer is doubled, the amount of light returned is reduced by 94% [32]. Counts are conducted by volunteers without any formal training, thus, results are likely biased based on observer experience and hare distance [37]. The spotlight method assumes that the population distribution in the illuminated area is representative of the distribution of the entire population. However, hare have been found to have an irregular spatial distribution [29,32]. Nonetheless, spotlighting is still considered to be the best method for studying large scale hare population trends with many study areas and volunteers [29]. Hunting game statistics is also used in many countries to provide an overall indication of population trends, however, game bag records may not provide reliable data for counting hares [4,26,29,38].

The limitations of spotlight counts and hunting game statistics could be overcome by relying on drone surveys with thermal imaging for population counts. However, the use of drone surveys with thermal imaging has yet to be demonstrated for identifying and counting hare. The value of drone surveys is dependent on a number of flight parameters, such as, flight altitude and speed. When determining flight altitude and speed there is a trade–off between the maximum ground area able to be covered in the available flight time and the minimum resolution required for species identification. It is, therefore, necessary to consider the size of the animals of interest and the aim of the survey when determining flight altitude.

Research demonstrating the use of drone surveys with thermal imaging for detecting and monitoring small mammals is limited, with the majority of previous studies focusing on larger mammals, such as, deer spp. (Cervidae), alpaca (*Vicugna pacos*), and long–tailed macaque (*Macaca fascicularis*) [19,22,23,39,40]. Thus, there is a need for studies assessing the use of drones equipped with thermal cameras as a monitoring tool for smaller mammals. Psiroukis *et al.* [41] recently demonstrated the use of aerial thermal imaging to monitor free–range rabbits, proving that mammals as small as rabbits can be identified and counted using drone surveys with thermal imaging. This study identified a flight altitude of 25 m as the optimal flight altitude that was low enough to capture images of sufficient resolution without disturbing the rabbits [41]. However, while this study proves the use of aerial thermal imaging for monitoring mammals smaller than hare, the the survey areas of the study were only 2 ha each [41]. Wildlife population counts often rely on the surveillance of much larger areas. It is, therefore, important to determine a flight methodology, including the optimal flight altitude suited for covering larger ground areas.

The aim of this study was, therefore, to investigate the potential use of a drone equipped with a thermal camera as a tool for monitoring the European hare (*Lepus europaeus*) population in Denmark. More specifically, this study tested multiple flight altitudes to find the appropriate flight altitude for identifying European hare. The maximum flight altitude was expected to be dependent on animal size. Furthermore, it was anticipated that animal body size could be used as a general indicator of species. Moreover, flight speed and method were tested along with camera angle and recording method, to identify the ideal parameters for conducting population surveys with drone based thermal imaging. Based on the results of these test flights, an appropriate method for identifying and counting hare with drone surveys using thermal imaging was suggested. The applied use of the suggested methodology was evaluated through a case survey with the aim of identifying and counting hare over a larger area of 206 ha.

2. Methods

Two different sites with agricultural landscapes in Northern Jutland, Denmark were used to carry out multiple aerial surveys. The first site had an area of 39 ha and was used to carry out test flights between March 21st, 2022 and April 13th, 2022. The second site had an area of 206 ha and was only used for the case survey that took place on April 20th, 2022. All flights took place before sunrise or after sunset with the ambient temperature ranging from 2.4°C to 8.5°C. The drone used in this study was the DJI Mavic 2 Enterprise Advanced (M2EA) equipped with low–noise propellers. The M2EA

had an integrated dual camera and gimbal system with a 640×514 px thermal camera that had a field of view (FOV) of $48° \times 38°$. The DJI Pilot App was used to conduct both manual flights and mission flights [42].

2.1. Flight parameters

In order to find the optimal method for identifying and counting hares with drone surveys, flight method, flight altitude, and flight speed were tested along with recording method and camera angle. To compared flight methods both manual and mission flights were conducted, and while manual flights were not well suited for conducting systematic surveys, they were ideal for quickly finding individuals and closing in on them. Manual flights were, therefore, used to test the animals' response to different flight altitudes. This was done by the drone hovering above an animal at an altitude of 80 m before slowly descending in altitude, briefly pausing every 10 m and stopping when the animal reacted to the presence of the drone.

To assess the trade–off between area covered and species identification a series of flights were conducted at 40 m, 60 m, or 80 m. These three flight altitudes were selected based on initial flights indicating that at flight altitudes greater than 80 m animal detection becomes challenging and at flight altitudes lower than 40 m animals began reacting to the presence of the drone, thus, altering their behavior, e.g. running away from the drone. Moreover, flights conducted at an altitude of 40 m should ensure well–resolved images for species identification. Burke *et al.* [43] suggested that the minimum resolution for accurate classification and temperature measurement is approximately 10 pixels. The optimal flight altitude can, therefore, be calculated based on camera specifications and the average size of the animal species in question using the following equations [43]. First, it is important to know the camera's angular pixel scale, ρ_a, as defined by the camera's horizontal field of view, θ, and the horizontal resolution of the camera, N_{pixels}:

$$\rho_a = \frac{\theta}{N_{pixels}} \tag{1}$$

It is also necessary to find the desired physical pixel scale, ρ_p, i.e. the desired length in meters each pixel should cover. Thus, determining the resolution, based on the length of the animal, l_a, and the desired resolution of the animal, n_{pixel}:

$$\rho_p = \frac{l_a}{n_p} \tag{2}$$

The body length of a European hare is approximately 50–70 cm [28], i.e. for optimal thermal detection a pixel scale of $\rho_p = 0.05$ m/pixel (5 cm per pixel) is required. Body width could also be used instead of body length, depending on which is larger. The optimal flight altitude, h, can then be calculated based on the desired physical pixel scale and the angular pixel scale of the camera:

$$h = \frac{\rho_p}{\tan(\rho_a)} \tag{3}$$

Therefore, to detect a hare with a body length of 60 cm the flight altitude should be approximately 46 m.

2.2. Case survey

A case survey was conducted with the aim of surveying the hare population over a larger area, where the flight route covered an area of 206 ha. The survey was conducted as a mission flight, meaning that, a flight plan was created prior to take off ensuring a systematic coverage of the entire area (Figure 1). This flight method was selected based on previous flights exploring both mission flights and manual flights, where it was determined that mission flights were ideal for conducting systematic population counts. The flight route was created with a 10% side overlap, meaning that, neighboring frames from parallel transect lines had a 10% overlap. Moreover, the case flight was conducted at an altitude of 60 m and a speed of 7 m/s based on previous flights comparing flight altitude (40 m, 60 m, and 80 m) and flight speed. Previous flights also determined video filming as the preferred recording method compared to taking systematic overlapping pictures throughout route. The camera was, therefore, set to record in video mode at an angle of 90°, i.e. the camera was pointing straight down towards the ground. This angle was selected as it enables the option of mapping the animals' position later on.

Figure 1. Example flight route mapped in DJI Pilot App [42]. The blue area indicates the ground area covered on the aerial images and the green lines show the flight route with distances between mapping points annotated along the route.

2.3. Data analysis

2.3.1. Species classification

Species were primarily classified from images and videos based on the size and shape of their heat signatures. Moreover, when analyzing videos the animals' movement style could also contribute to correctly identifying species. The size of each animal was calculated based on its pixels using Equation 3:

$$l_a = h \cdot \tan(\rho_a) \cdot n_p \tag{4}$$

A pairwise Mann Whitney U–test was conducted with R [44] to test if median body size, calculated based on the animal's thermal pixel size using Equation 4, was different between animal species.

2.3.2. Mapping observations

Observations from the case flight were mapped in ArcGIS Pro [45] using the Full Motion Video (FMV) player [46], which is an Image Analyst extension in ArcGIS. The FMV player requires videos to be combined with their associated metadata into a single geospatially aware video file [46]. Each video from the case flight was, therefore, combined with its associated metadata file to create FMV compliant video data using the Video Multiplexer tool. However, prior to this the original metadata files had to be converted from SRT files to CSV files, which was done in Python [47]. The FMV player was then used to play the resulting FMV compliant videos and map animal observations. A new point feature class was created for each animal group, and observations were annotated in the FMV player and added to their respective feature class when they occurred in the video.

3. Results

### 3.1. Flight altitude

Hare can be identified at flight altitudes up to 80 m (Figure 2). During test flights, animals initially identified as hare were further observed until they moved, where their unique posture during movement was used to confirm the species classification. Moreover, at flight altitudes below 40 m the animals reacted to the drone, moving away from the drone in 90% of the cases.

(a) Image of hare taken at 40 m.

(b) Image of hare taken at 60 m.

(c) Image of hare taken at 80 m.
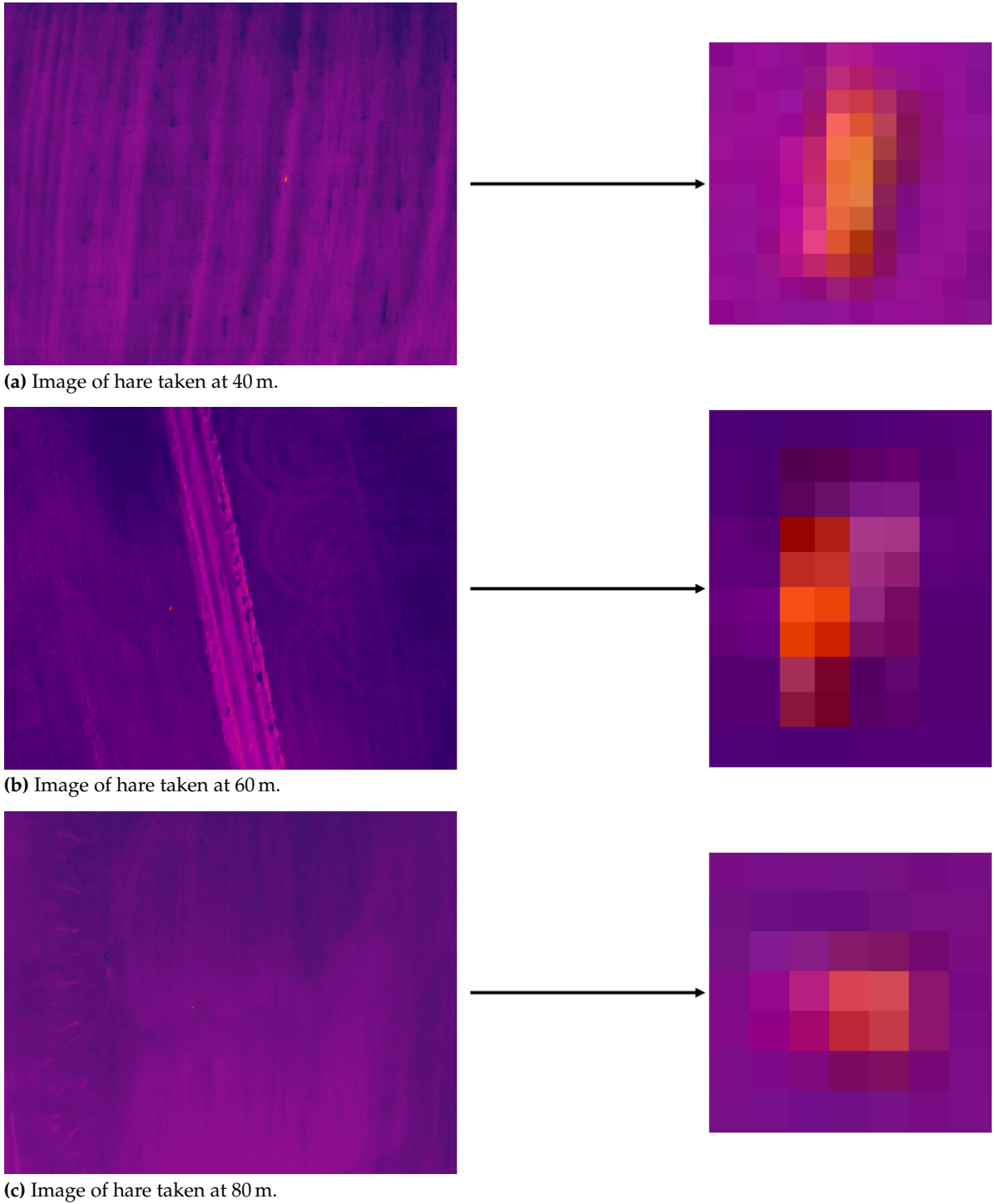
Figure 2. Thermal images of hare taken at an altitude of 40, 60, and 80 m, respectively.

3.2. Species classification

A total of 85 animals were recorded throughout all flights, including the case survey. Of these animals, 35 were classified as hare, 34 as roe deer (*Capreolus capreolus*), 15 were classified as smaller unidentifiable animals, and a single animal was classified as a red fox (*Vulpes vulpes*). Animals were mainly classified based on their size, however, the red fox was only possible to classify due to its unique posture during movement (Figure 3).

(a) European hare

(b) Four roe deer

(c) Small unidentified animals

(d) Red fox
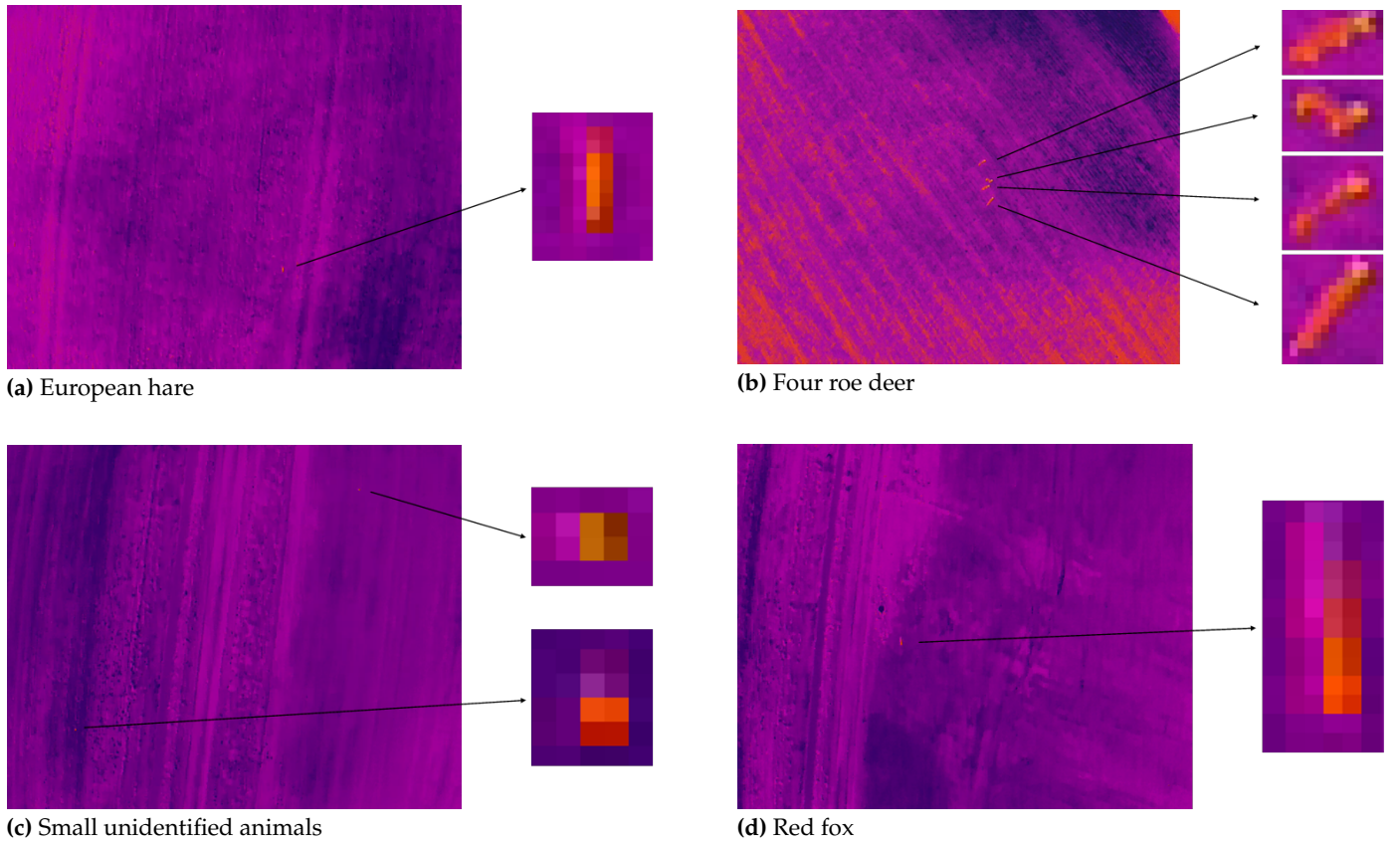
Figure 3. Thermal images of different animals taken at an altitude of 60 m.

There was a significant difference between body sizes of different animal species based on their thermal pixel size (Figure 4). The median body length of hare was 0.694 m ($IQR = 0.555 - 0.833$ m), which was significantly smaller ($p < 0.001$) than the body length of roe deer ($median = 1.11$ m, $IQR = 0.989 - 1.25$ m) and significantly larger ($p < 0.001$) than the body length of smaller unidentifiable animals ($median = 0.416$ m, $IQR = 0.416 - 0.416$ m). The body width of hare ($median = 0.416$ m, $IQR = 0.382 - 0.555$ m) was also significantly smaller ($p < 0.001$) than that of the roe deer ($median = 0.642$ m, $IQR = 0.446 - 0.833$ m). However, the hare's median body width was not significantly different from that of the smaller unidentifiable animals ($median = 0.416$ m, $IQR = 0.416 - 0.416$ m).
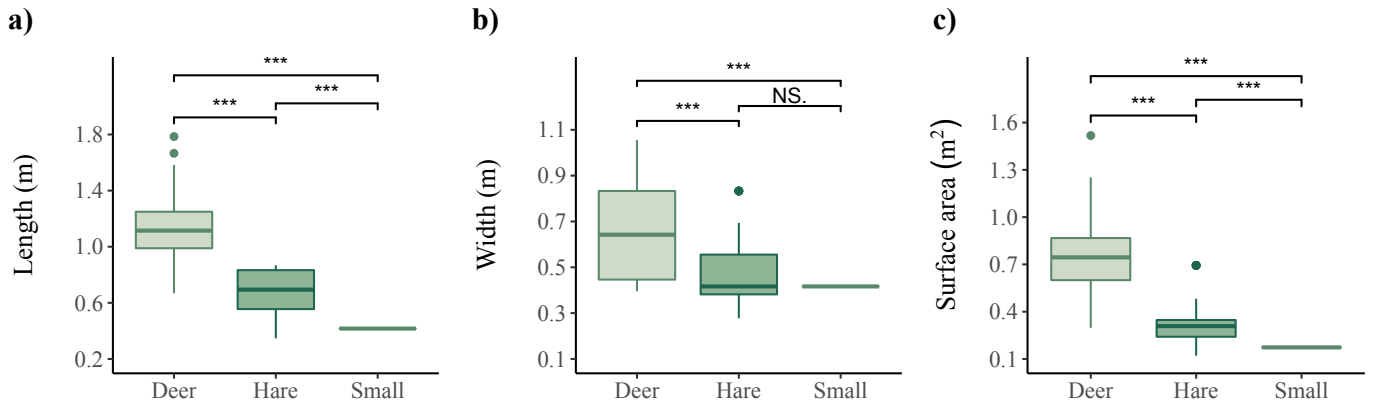

Figure 4. Body size of hare ($n = 35$), deer ($n = 34$), and smaller unidentifiable animals ($n = 15$). The body size was defined by **a)** body length, **b)** body width, and **c)** surface area visible from above. Significance differences between the respective animal groups are denoted above the box plots, with *** indicating a significance level of $p < 0.001$.

3.3. Case survey

The case survey, conducted at an altitude of 60 m, covered a total area of 206 ha. This yielded a flight route with a total distance of 60 719 m, which took approximately three hours, excluding additional time and distance required to change battery. Six batteries were needed to complete the aerial survey. If the case survey had been conducted at an altitude of 40 m the flight route would have been 82 393 m and taken approximately four hours to complete. The case flight resulted in the mapping of 55 animals in total, of which 17 were identified as hare, 22 were identified as roe deer, a single observation was identified as a red fox, and 15 were classified as unidentifiable animals smaller than hare (Figure 5).
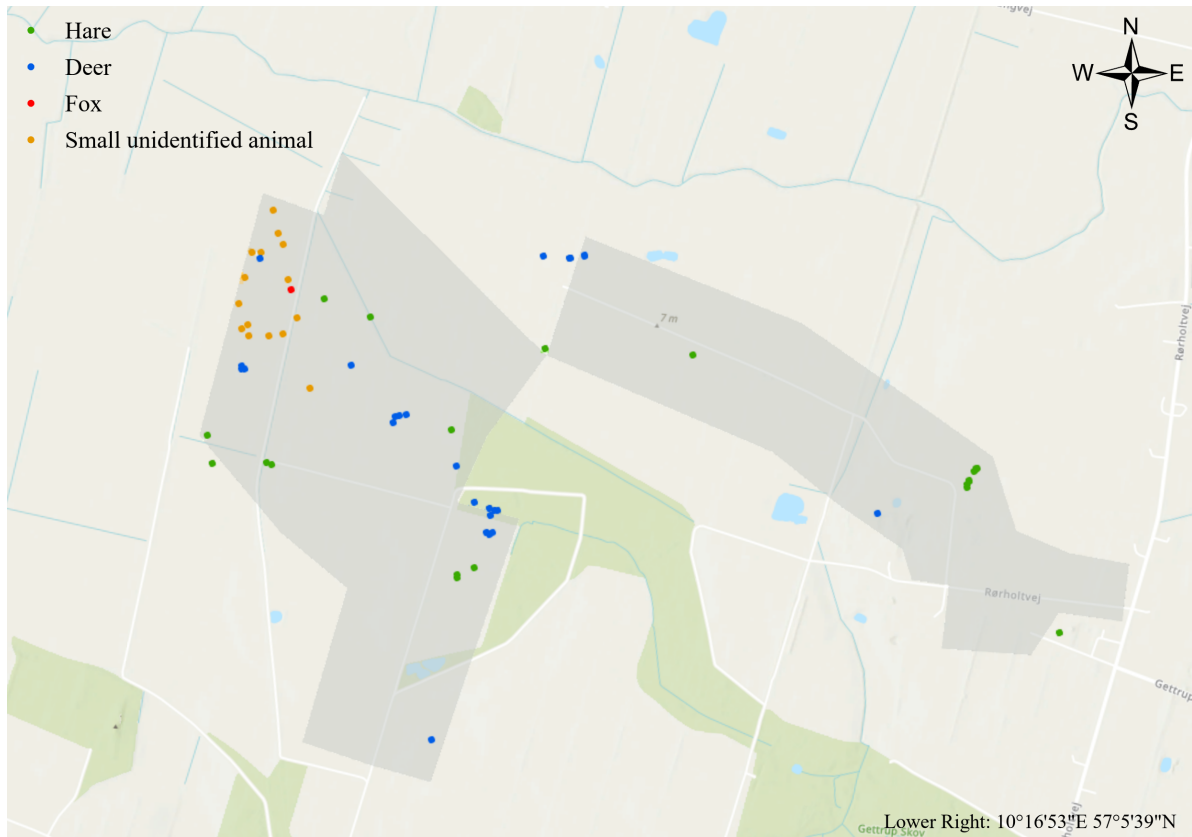
Figure 5. Animal observations recorded April 20th, 2022 during the case survey. The light gray area shows area surveyed. Note, this map only includes 133 ha of the entire survey area of 206 ha, as no animals were found for the rest of the survey area.

4. Discussion

4.1. Flight parameters

The flight route of the case study was set to have a 10% side overlap between parallel transect lines to reduce the probability of counting the same animal multiple times. [18] suggests a 100 m gap between parallel transect lines to minimize the chance of recapture. However, when mapping the video images and observations it was easy to identify stationary individuals that appear in the 10% overlap margin on parallel transects and thereby ensure these individuals are not counted twice. That being said, it is difficult to completely avoid the multiple observations of the same individual. For recapture to occur certain conditions must be met after first detection, first, the animal has to be moving, second, the direction of movement must be towards the remaining transects, and lastly, the speed of movement needs to be fast enough for the animal to arrive before the drone [18]. Hare have a home range of approximately 20–40 ha and can run up to 70 km/h [28]. Thus, the probability of recapture is relatively high but will also be dependent on transect length, with longer transect lines increasing the time before the drone surveys the next transect lines. However, as long as animal movement is random relative to the transect lines, which it will be if animals are not affect by the drone, then multiple detection of the same animals on different transects does not introduce bias [18]. Hence, flying at altitudes at which the

animals are affected by the presence of the drone will result in animal movement to no longer being random relative to transects and introducing bias.

Different flight altitudes each have their own advantages and disadvantages. Lower altitudes increase detection probability, however, flight distance and time are also increased when flying at lower altitudes. Thus, flying at lower altitudes may limit the survey area, depending on time frame and batteries available. When determining the size of the survey area it is important to consider the distribution of the animals in question. In theory, the size of the survey area will not bias the results for species with a completely homogeneous distribution. However, for most this is usually not the case, making it important to take the species distribution into account when deciding the survey area and analyzing the results. For species with a more heterogeneous distribution, a larger area is necessary to to provide an accurate estimation of the population size. In the case study the hare were irregularly distributed, supporting the findings of previous studies and emphasizing the importance of large scale population surveys [29,32]. Moreover, flying at low altitudes may also have a disturbance effect on the animals, depending on the species, wind factors, and drone used. In this study hare and deer were observed to react to the drone when flying at altitudes under 40 m, despite the M2EA being equipped with noise reducing propellers. Similarly, Rahman *et al.* [22] and Rahman and Setiawan [40] found that flying at altitudes below 50 m increased the risk of disturbing the animals.

The case study showed that a flight altitude of 60 m was sufficient to detect and classify species as small as hare. It was also possible to detect animals smaller than hare, however, it was not possible to determine the species of these small animals. The thermal signatures of all the small animals were 2×2 pixels and in all cases the small animals lied motionless, making it difficult to determine the species. Flying at a lower flight altitude would have increased the pixel size of these animals, providing their thermal signatures with more detail. There is a risk that the small unidentifiable animals were indeed hare responding to nearby predators, e.g. the red fox, or perceiving the drone as an avian predator. Hare are known to lay low and still in the vegetation to avoid predation [48]. To avoid detection they compress their surface area, e.g. by laying their ears back along their body, thus, decreasing their body length visible from above and eliminating shape features on the thermal signature that can be used to determine the species.

4.2. Species classification

Body size proved to be a good determiner of species, with the species in this study varying significantly in size. However, body size should not be the only criterion for species determination, as the size of some species may overlap. Prior to surveying an area it is important to not only consider the size of the target species, but to also consider the size of any other species in the area. Species overlapping in size, may be distinguishable based on shape and movement posture, i.e. a hare's jumping locomotion contrary to a fox trotting. Witczuk *et al.* [18] was able to differentiate between species overlapping in body length (red deer (*Cervus elaphus*) and wild boar (*Sus scrofa*)) based on the shape of their thermal signatures. The thermal signature of red deer was thinner with a distinctive head, where wild boar had a wider thermal signature without a distinctive head [18]. In the same study the thermal signatures of roe deer were described as small headless signatures [18]. Contrary to this, the roe deer recorded in the current study were easily classified due to their thermal signatures having distinctive heads. This difference in thermal signature shape can be explained by the difference in flight altitude. In Witczuk *et al.* [18] thermal signatures were recorded at an altitude of 150 m, whereas thermal signatures in this study were recorded at altitudes between 40 m and 80 m. Thus, increasing the resolution and allowing thermal signatures to include more detail.

Automatic detection and species identification may become available for thermal drone surveys of mammals with the collection of more data. With automatic detection it may be possible to identify smaller species that have too little detail for the human eye to classify [18]. Species recognition with machine learning techniques should not only be based on size and shape of thermal signatures, but can incorporate other variables, such as pixel temperature or distribution of pixel intensity, to distinguish between species [11,18]. Automatic recognition may also allow for species identification at higher altitudes, depending on the detail level required for recognition by machine learning techniques. Thus, potentially further reducing the time and labor required to conduct population counts. Recent advances in machine learning have already enabled automated identification and enumeration of wildlife [41,49]. Psiroukis *et al.* [41] demonstrated that using deep learning techniques to count the number of rabbits in single thermal drone images taken at an altitude of 25 m was comparable to manual counts. For automatic species identification to be reliable, an extensive reference library with a large variety of training data is required. Future research should, therefore, focus on creating such a reference library with not only a variety of species, but more importantly a variety of intra–specific observations, as intra–specific

observations can be highly variable based on the environmental conditions, camera angle, and animal posture. However, automatic detection with smaller data sets is possible using convolutional neural networks (CNNs) [50]. Pre–existing general purpose CNNs can be retrained to detect a target species in thermal drone images, i.e. only a few hundred images are necessary to train a CNN for automatic detection of a target species. Other machine–learning methods require hundreds of thousands of training images [50]. CNNs use the spectral value of each pixel along with the pixel's proximity to other pixels in the image matrix to identify unique features, e.g. the outline of an animal. These features are then used to classify the animal based on their similarities with features in training images. CNNs can recognize when an object in an image matches most but not all of the expected features and is able to correctly classify the object despite these differences [50]. Thus, enabling identification of wildlife in different contexts e.g. different backgrounds resulting in contrast between an animal and its background varying and intra–specific differences in size, shape, and temperature.

4.3. Limitations

The current European drone regulations state that the drone must always be in the pilot's line of sight. Thus, requiring the pilot to frequently relocate and limiting the survey areas to locations where the pilot is able to follow the drone as to not loose line of site when covering larger areas. However, it is possible to receive dispensation, particularly when flights are carried out in agreement with local authorities for research and conservation purposes. Another current limitation of drone surveys is the time associated with analyzing and mapping the large amounts of video and image data acquired. Hence, emphasizing the importance of developing robust software for automatic detection and species identification.

5. Conclusion

It was possible to identify hare and conduct population counts using drone surveys with thermal imaging. Hare could be detected at flight altitudes up to 80 m with the M2EA's thermal camera and it was possible to fly as low as 40 m without disturbing the animals. Images taken at flight altitudes between 40 and 80 m provided enough detail to differentiate between species, with animal body size proving to be a good indicator of species. Future research should focus on advancing automatic detection, species identification, and creating a shared reference library with robust data gathered from a variety of species in different contexts.

References

1. Webbon, C.C.; Baker, P.J.; Harris, S. Faecal Density Counts for Monitoring Changes in Red Fox Numbers in Rural Britain. *Journal of Applied Ecology* **2004**, *41*, 768–779.
2. Aebischer, N.J.; Baines, D. Evaluating the Use of Drones Equipped with Thermal Sensors as an Effective Method for Estimating Wildlife. *Revista Catalana d'Ornitologia* **2008**, *24*, 30–43.
3. Begon, M.; Howarth, R.; Townsend, C. *Essentials of Ecology*, 4 ed.; Wiley, 2014.
4. Kahlert, J.; Fox, A.D.; Heldbjerg, H.; Asferg, T.; Sunde, P. Functional Responses of Human Hunters to Their Prey — Why Harvest Statistics may not Always Reflect Changes in Prey Population Abundance. *Wildlife Biology* **2015**, *21*, 294–302. doi:10.2981/wlb.00106.
5. Nakashima, Y.; Fukasawa, K.; Samejima, H. Estimating Animal Density Without Individual Recognition Using Information Derivable Exclusively from Camera Traps. *Journal of Applied Ecology* **2018**, *55*, 735–744. doi:10.1111/1365-2664.13059.
6. Hyun, C.U.; Park, M.; Lee, W.Y. Remotely Piloted Aircraft System (RPAS)-Based Wildlife Detection: A Review and Case Studies in Maritime Antarctica. *Animals* **2020**, *10*, 2387. doi:10.3390/ani10122387.
7. Ramos, P.L.; Sousa, I.; Santana, R.; Morgan, W.H.; Gordon, K.; Crewe, J.; Rocha-Sousa, A.; Macedo, A.F. A Review of Capture-recapture Methods and Its Possibilities in Ophthalmology and Vision Sciences. *Ophthalmic Epidemiology* **2020**, *27*, 310–324. doi:10.1080/09286586.2020.1749286.

8. Delisle, Z.J.; Flaherty, E.A.; Nobbe, M.R.; Wzientek, C.M.; Swihart, R.K. Next-Generation Camera Trapping: Systematic Review of Historic Trends Suggests Keys to Expanded Research Applications in Ecology and Conservation. *Frontiers in Ecology and Evolution* **2021**, *9*. doi:10.3389/fevo.2021.617996.

9. Sweeney, K.L.; Helker, V.T.; Perryman, W.L.; LeRoi, D.J.; Fritz, L.W.; Gelatt, T.S.; Angliss, R.P. Flying Beneath the Clouds at the Edge of the World: Using a Hexacopter to Supplement Abundance Surveys of Steller Sea Lions (*Eumetopias Jubatus*) in Alaska. *Journal of Unmanned Vehicle Systems* **2016**, *4*, 70–81. doi:10.1139/juvs-2015-0010.

10. Bech-Hansen, M.; M. Kallehauge, R.; Bruhn, D.; H. Funder Castenschiold, J.; Beltoft Gehrlein, J.; Laubek, B.; F. Jensen, L.; Pertoldi, C. Effect of Landscape Elements on the Symmetry and Variance of the Spatial Distribution of Individual Birds within Foraging Flocks of Geese. *Symmetry* **2019**, *11*. doi:10.3390/sym11091103.

11. Rahman, D.A.; Sitorus, A.B.Y.; Condro, A.A. From Coastal to Montane Forest Ecosystems, Using Drones for Multi-Species Research in the Tropics. *Drones* **2021**, *6*, 6. doi:10.3390/drones6010006.

12. Wen, D.; Su, L.; Hu, Y.; Xiong, Z.; Liu, M.; Long, Y. Surveys of Large Waterfowl and Their Habitats Using an Unmanned Aerial Vehicle: A Case Study on the Siberian Crane. *Drones* **2021**, *5*, 102. doi:10.3390/drones5040102.

13. Castenschiold, J.H.F.; Bregnballe, T.; Bruhn, D.; Pertoldi, C. Unmanned Aircraft Systems as a Powerful Tool to Detect Fine-Scale Spatial Positioning and Interactions between Waterbirds at High-Tide Roosts. *Animals* **2022**, *12*. doi:10.3390/ani12080947.

14. Fettermann, T.; Fiori, L.; Gillman, L.; Stockin, K.A.; Bollard, B. Drone Surveys Are More Accurate Than Boat-Based Surveys of Bottlenose Dolphins (*Tursiops Truncatus*). *Drones* **2022**, *6*, 82. doi:10.3390/drones6040082.

15. Setyawan, E.; Stevenson, B.C.; Izuan, M.; Constantine, R.; Erdmann, M.V. How Big Is That Manta Ray? A Novel and Non-Invasive Method for Measuring Reef Manta Rays Using Small Drones. *Drones* **2022**, *6*, 63. doi:10.3390/drones6030063.

16. Dronova, I.; Kislik, C.; Dinh, Z.; Kelly, M. A Review of Unoccupied Aerial Vehicle Use in Wetland Applications: Emerging Opportunities in Approach, Technology, and Data. *Drones* **2021**, *5*, 45. doi:10.3390/drones5020045.

17. Wich, S.; Dellatore, D.; Houghton, M.; Ardi, R.; Koh, L.P. A Preliminary Assessment of Using Conservation Drones for Sumatran Orangutan (*Pongo abelii*) Distribution and Density. *Journal of Unmanned Vehicle Systems* **2016**, *4*, 45–52. doi:10.1139/juvs-2015-0015.

18. Witczuk, J.; Pagacz, S.; Zmarz, A.; Cypel, M. Exploring the Feasibility of Unmanned Aerial Vehicles and Thermal Imaging for Ungulate Surveys in Forests - Preliminary Results. *International Journal of Remote Sensing* **2018**, *39*, 5504–5521. doi:10.1080/01431161.2017.1390621.

19. Lee, S.; Song, Y.; Kil, S.H. Feasibility Analyses of Real-Time Detection of Wildlife Using UAV-Derived Thermal and RGB Images. *Remote Sensing* **2021**, *13*, 2169. doi:10.3390/rs13112169.

20. Brunton, E.A.; Leon, J.X.; Burnett, S.E. Evaluating the Efficacy and Optimal Deployment of Thermal Infrared and True-Colour Imaging When Using Drones for Monitoring Kangaroos. *Drones* **2020**, *4*, 20. doi:10.3390/drones4020020.

21. Lethbridge, M.; Stead, M.; Wells, C. Estimating Kangaroo Density by Aerial Survey: A Comparison of Thermal Cameras with Human Observers. *Wildlife Research* **2019**, *46*, 639. doi:10.1071/WR18122.

22. Rahman, D.A.; Setiawan, Y.; Wijayanto, A.K.; Rahman, A.A.A.F.; Martiyani, T.R. An Experimental Approach to Exploring the Feasibility of Unmanned Aerial Vehicle and Thermal Imaging in Terrestrial and Arboreal Mammals Research. *E3S Web of Conferences* **2020**, *211*, 02010. doi:10.1051/e3sconf/202021102010.

23. Obermoller, T.R.; Norton, A.S.; Michel, E.S.; Haroldson, B.S. Use of Drones with Thermal Infrared to Locate White-tailed Deer Neonates for Capture. *Wildlife Society Bulletin* **2021**, *45*, 682–689. doi:10.1002/wsb.1242.

24. Howell, L.G.; Clulow, J.; Jordan, N.R.; Beranek, C.T.; Ryan, S.A.; Roff, A.; Witt, R.R. Drone Thermal Imaging Technology Provides a Cost-Effective Tool for Landscape-Scale Monitoring of a Cryptic Forest-Dwelling Species across All Population Densities. *Wildlife Research* **2021**, *49*, 66–78. doi:10.1071/WR21034.

25. Shewring, M.P.; Vafidis, J.O. Using UAV-mounted Thermal Cameras to Detect the Presence of Nesting Nightjar in Upland Clear-fell: A Case Study in South Wales, UK. *Ecological Solutions and Evidence* **2021**, *2*, e12052. doi:10.1002/2688-8319.12052.

26. Schmidt, N.M.; Asferg, T.; Forchhammer, M.C. Long-term Patterns in European Brown Hare Population Dynamics in Denmark: Effects of Agriculture, Predation, and Climate. *BMC Ecology* **2004**, *4*, 1–7. doi:10.1186/1472-6785-4-15.

27. Misiorowska, M.; Wasilewski, M. Survival and Causes of Death Among Released Brown Hares (*Lepus europaeus* Pallas, 1778) in Central Poland. *Acta Theriologica* **2012**, *57*, 305–312. doi:10.1007/s13364-012-0081-1.

28. Nationalt Center for Miljø og Energi, A.U. *Forvaltningsplan for hare*, 2013.

29. Sliwinski, K.; Strauß, E.; Jung, K.; Siebert, U. Comparison of Spotlighting Monitoring Data of European Brown Hare (Lepus europaeus) Relative Population Densities with Infrared Thermography in Agricultural Landscapes in Northern Germany. *PLOS ONE* **2021**, *16*, 1–16. doi:10.1371/journal.pone.0254084.

30. Hacklander, K.; Schai-Braun, S. *Lepus europaeus. The IUCN Red List of Threatened Species 2019* **2019**. doi:10.2305/IUCN.UK.2019-1.RLTS.T41280A45187424.en.

31. Pépin, D.; Angibault, J.M. Selection of Resting Sites by the European Hare as Related to Habitat Characteristics During Agricultural Changes. *European Journal of Wildlife Research* **2007**, *53*, 183–189. doi:10.1007/s10344-007-0087-1.

32. Jensen, T.W. *Identifying causes for population decline of the brown hare (Lepus europaeus) in agricultural landscapes in Denmark. PhD Thesis*, 2009.

33. Moeslund, J.; Nygaard, B.; Ejrnæs, R.; Bell, N.; Bruun, L.; Bygebjerg, R.; Carl, H.; Damgaard, J.; Dylmer, E.; Elmeros, M.; Flensted, K.; Fog, K.; Goldberg, I.; Gønget, H.; Helsing, F.; Holmen, M.; Jørum, P.; Lissner, J.; Læssøe, T.; Madsen, H.; Misser, J.; Møller, P.; Nielsen, O.; Olsen, K.; Sterup, J.; Søchting, U.; Wiberg-Larsen, P.; Wind, P. *Den danske Rødliste*, 2019.

34. Asferg, T.; Clausen, P.; Christensen, T.K.; Bregnballe, R.; Clausen, K.K.; Elmeros, M.; Fox, A.D.; Haugaard, L.; Holm, T.E.; Laursen, K.; Madsen, J.; Nielsen, R.D.; Sunde, P.; Therkildsen, O. *Vildtbestand og jagttider i Danmark: Det biologiske grundlag for jagttidsrevisionen 2018*, 2016. http://dce2.au.dk/pub/SR195.pdf.

35. Sørensen, I.H.; Midtgaard, L. *Notat vedr. markvildtindsatsens resultater 2013-2020*, 2021.

36. Jægerforbund, D. *Vejledning: pattedyrstællinger*, 2022.

37. Sunde, P.; Jessen, L. It Counts Who Counts: An Experimental Evaluation of the Importance of Observer Effects on Spotlight Count Estimates. *European Journal of Wildlife Research* **2013**, *59*, 645–653. doi:10.1007/s10344-013-0717-8.

38. Smith, R.K.; Jennings, N.V.; Harris, S. A Quantitative Analysis of the Abundance and Demography of European Hares *Lepus europaeus* in Relation to Habitat Type, Intensity of Agriculture and Climate. *Mammal Review* **2005**, *35*, 1–24.

39. Chrétien, L.P.; Théau, J.; Ménard, P. Visible and Thermal Infrared Remote Sensing for the Detection of White-tailed Deer Using an Unmanned Aerial System. *Wildlife Society Bulletin* **2016**, *40*, 181–191. doi:10.1002/wsb.629.

40. Rahman, D.A.; Setiawan, Y. Possibility of Applying Unmanned Aerial Vehicle and Thermal Imaging in Several Canopy Cover Class for Wildlife Monitoring – Preliminary Results. *E3S Web of Conferences* **2020**, *211*, 04007. doi:10.1051/e3sconf/202021104007.

41. Psiroukis, V.; Malounas, I.; Mylonas, N.; Grivakis, K.E.; Fountas, S.; Hadjigeorgiou, I. Monitoring of Free-Range Rabbits Using Aerial Thermal Imaging. *Smart Agricultural Technology* **2021**, *1*, 100002. doi:10.1016/j.atech.2021.100002.

42. DJI. *DJI Pilot Android v2.5.1.3*, 2021. https://www.dji.com/downloads/djiapp/dji-pilot.

43. Burke, C.; Rashman, M.; Wich, S.; Symons, A.; Theron, C.; Longmore, S. Optimizing Observing Strategies for Monitoring Animals Using Drone-Mounted Thermal Infrared Cameras. *International Journal of Remote Sensing* **2019**, *40*, 439–467. doi:10.1080/01431161.2018.1558372.

44. R Core Team. *R version 4.0.3*. R Foundation for Statistical Computing, Vienna, Austria, 2020. https://www.R-project.org/.

45. Esri. *ArcGIS Pro 2.9.2*, 2021. http://www.esri.com/.

46. Esri. *Using the ArcGIS Full Motion Video 1.4 Add-In*, 2020. http://www.esri.com/fmv.

47. Foundation, P.S. *Python 3.9.12*, 2022. https://www.python.org/.

48. Steen, K.A.; Villa-Henriksen, A.; Therkildsen, O.R.; Green, O. Automatic Detection of Animals in Mowing Operations Using Thermal Cameras. *Sensors* **2012**, *12*, 7587–7597. doi:10.3390/s120607587.

49. Seymour, A.C.; Dale, J.; Hammill, M.; Halpin, P.N.; Johnston, D.W. Automated Detection and Enumeration of Marine Wildlife Using Unmanned Aircraft Systems (UAS) and Thermal Imagery. *Scientific Reports* **2017**, *7*, 45127. doi:10.1038/srep45127.

50. Corcoran, E.; Winsen, M.; Sudholz, A.; Hamilton, G. Automated Detection of Wildlife Using Drones: Synthesis, Opportunities and Constraints. *Methods in Ecology and Evolution* **2021**, *12*, 1103–1114. doi:10.1111/2041-210X.13581.

Quantifying Raptors' Flight Behavior to Assess Collision Risk and Avoidance Behavior to Wind Turbines

Anne Cathrine Linder [1]*

1   Department of Chemistry and Bioscience — Section of Biology and Environmental Science, Aalborg University, Fredrik Bajers Vej 7, 9220 Aalborg, Denmark

Simple Summary: An increasing amount of wind turbines installed worldwide has in turn lead to an increase in bird fatality due to collisions. This conservation threat has led to the development of automated camera–based monitoring systems, that have recently been installed on some wind energy sites to mitigate the impact of wind turbines on protected raptors. This study describes a new quantitative framework to assess birds' flight behavior in proximity to wind turbines based on data from these camera–based monitoring systems. It is demonstrated how this novel method for describing flight behavior can be used to identify risk prone behavior, which is a crucial step towards quantifying collision risk with wind turbines.

Abstract: Some wind farms have implemented automated camera–based monitoring systems e.g. IdentiFlight to mitigate the impact of wind turbines on protected raptors. These systems have effectuated the collection of large amounts of unique data that can be used to describe flight behavior in a novel way. The aim of this study was to evaluate how this unique data could be used to create a robust quantitative behavioral analysis, that could be used to identify risk prone flight behavior and avoidance behavior and thereby, used to assess collision risk in the future. This was attained through a case study at a wind farm on the Swedish island Gotland, where golden eagles (*Aquila chrysaetos*), white–tailed eagles (*Haliaeetus albicilla*), and red kites (*Milvus milvus*), were chosen as the selected bird species. These three species are generally rare breeders in Europe and have also been shown to be particularly vulnerable to collisions with wind turbines. The results demonstrate that data from the IdentiFlight system can be used to identify risk prone flight behaviors, e.g., tortuous flight and foraging behavior. Moreover, it was found that these flight behaviors were affected by both weather conditions, but also distance to the nearest wind turbine. This data can, thus, be used to evaluate collision risk and avoidance behavior. This study presents a promising framework for future research, demonstrating how data from camera–based monitoring systems can be utilized to quantitatively describe risk prone behavior and thereby assess collision risk and avoidance behavior.

Keywords: IdentiFlight, avoidance response, golden eagle, white-tailed eagle, red kite, wind turbine curtailment, flight types

1. Introduction

Wind energy production has over the past decades undergone a rapid development, due to the increasing demand for green energy. This has in turn led to a green on green predicament, due to the adverse effects of turbines on many avian species [1–9]. These adverse effects of wind turbines on birds result primarily from direct fatalities due to collisions and secondarily through habitat alteration and loss [9]. Loss *et al.* [7] estimated that bird fatality increases proportionally with increasing turbine height. The exact number of avian collisions with wind turbines is uncertain. Nonetheless, even relatively few fatalities can have detrimental effects on slow maturing species with low reproduction rates, e.g., raptors, especially when considering the cumulative effect of multiple wind farms. This is particularly an issue for species of conservation concern when considering regional and national populations [1,7]. Collision related mortality is unevenly spread among species, with few species often accounting for a large proportion of collision victims [10]. Large soaring raptors are known to be specifically vulnerable for collision with turbines [2,3,9,11]. Species-specific differences, such as, differences in size and wingspan can, thus, attribute to some species groups being more prone to collisions with turbines. However, mortality cannot, as such, be compared across species, as some birds have a longer longevity, fewer nestlings, and are generally rare. The loss of such individuals is worse, compared to common birds, e.g., the chiffchaff or mallard. In Europe some raptors have been described as vulnerable species, such as, golden eagles (*Aquila chrysaetos*), white–tailed eagles (*Haliaeetus albicilla*), and red kites (*Milvus milvus*) [12].

Collision risk is assumed to be dependent on multiple factors, e.g., flight altitude, behavior, and morphology. In regard to flight behavior, some types of behavior, e.g., flying at altitudes within turbine rotor zone and tortuous flight paths, have been described as more risk prone than others [6]. Another suggested predictor of collision risk is whether birds are migrating or engaging in local activities, e.g., foraging, as foraging individuals are expected to be less vigilant in regard to their flight direction and more focused on searching for prey on the ground [1,6,13,14]. Local individuals may also have a higher risk of collision, as they may have to move through the wind farm between their foraging grounds and

nesting sites multiple times throughout a single day, thus, possibly increasing their collision risk. Moreover, flight type is another behavioral factor suggested to affect collision risk. Large raptors such as golden eagles, depend upon soaring flight to retain energy, this flight type may however increase their risk of colliding with turbines, especially under less favorable conditions for gaining altitude [15–18]. Barrios and Rodríguez [15] found an increased collision rate when birds were forced to gain altitude using thermal soaring, i.e. slow circle–soaring flight on thermals, which often took place in airspace overlapping with turbines. Hence, flight type and thereby also collision risk are suggested to be affected by environmental factors such as weather (e.g. wind speed and direction, temperature, cloud coverage, and visibility) and topography [15,19]. Furthermore, the risk of collision is presumably also strongly affected by avoidance behavior [14].

Avoidance behavior is generally observed as changes in flight behavior and trajectories in response to wind turbines, this avoidance response can be found at different scales i.e. micro–scale (last second) and meso–scale (within wind farm) avoidance responses to single turbines within a wind farm and macro–scale avoidance responses, avoiding the entire wind farm [18,20]. Garvin *et al.* [14] defined avoidance as changes in flight height or flight direction deviating away from turbines and found that raptors showing no response to turbines were individuals passing through the wind farm on a straight flight path. It has been suggested that raptors are more vulnerable to turbines due to lower avoidance compared to the avoidance of migratory species e.g. geese [21]. Dahl *et al.* [19] showed that white–tailed eagles displayed high risk flight behavior i.e. no flight response and lack of avoidance close to turbines, which was also associated with high collision rates. However, multiple other studies have also found implications of raptors adjusting their flight trajectories to avoid wind turbines [22,23]. Whitfield and Madders [22] showed that red kites displayed avoidance rates between 98 and 100%. These contradicting findings indicate that avoidance behavior is both site–and species–specific [3,14,24]. It is therefore necessary to gain an understanding of which variables affect flight behavior in general for specific species and sites to gain a more thorough understanding of avoidance behavior.

Regardless of avoidance behavior, some protected raptor species have been suggested to be more vulnerable to wind turbines and the impact of wind turbines on such species may, therefore, be mitigated by turbine curtailment [25]. Some wind farms, particularly in the United States, have implemented an automated camera–based monitoring system e.g. IdentiFlight, to detect birds in flight and determine whether they are protected species e.g. eagles. If a bird, that is detected as one of the protected species, has a calculated trajectory on course to a turbine or is within a specified radius of a wind turbine, the system will issue a curtailment recommendation resulting in curtailment of the wind turbine before a collision would occur [26]. However, the actual collision risk between raptors and wind turbines is presumably determined by the vigilance of individuals i.e. their avoidance behavior, which is suggested to be dependent on multiple factors, e.g. weather conditions [8,14,19,20]. Knowledge on the avoidance behavior of protected raptors, such as eagles and the red kite, and how this behavior can be affected by environmental factors is therefore crucial to improving curtailment decisions. Curtailing wind turbines is expensive and energy companies would, therefore, benefit from the development of behavior specific curtailment models. Furthermore, the IdentiFlight camera system can provide a useful service to avian biologists, as it enables the collection of large amounts of data including not only flight trajectories based on spatial coordinates, but also images of individual birds throughout their flight trajectories, thus giving the unique opportunity of assessing flight behavior based on both flight trajectories and behavioral observations i.e. flight orientation.

The development of camera–based monitoring systems at wind farms has effectuated the collection of large amounts of data that can be used to describe the behavior of selected bird species, thus, enabling the possibility of creating quantitative behavioral analyses, which may be used to assess collision risk and avoidance behavior, potentially providing avian biologists with new imperative knowledge. Therefore, this study will investigate how the behavior of raptors can be quantified by using unique data from the IdentiFlight system, demonstrating how this type of data can be used to assess general flight behavior and investigate site and species–specific avoidance behavior. This was achieved through a case study investigating the behavior of golden eagles (*Aquila chrysaetos*), white–tailed eagles (*Haliaeetus albicilla*), and red kites (*Milvus milvus*) at a wind farm on the Swedish island Gotland.

It was a prerequisite that the flight behavior of these species could be described by flight altitude, flight type, active flight, and flight vigilance. It was expected that these variables describing flight behavior could be used to assess risk prone behavior and thereby utilized as an indicator of collision risk. Flight behavior was also expected to be affected by weather variables, e.g., temperature, wind speed, and cloud coverage. Furthermore, it was expected that the birds' distance to the nearest turbine would impact their flight behavior, i.e., the individuals were expected to exhibit avoidance behavior. Thus, proving that avoidance behavior could be detected through the new quantitative assessment of flight behavior in proximity to wind turbines.

2. Methods

2.1. Study Site

The study site is situated on Näsudden, a peninsula on Gotland's southwest coast. The terrain is generally flat and the highest peak of the island is only 135 meters above sea level [27]. The peninsula is mainly covered by open fields, often utilized as foraging sites by the island's raptors. Gotland is home to breeding populations of approximately 55 pairs of the golden eagle, 45 pairs of the white–tailed eagle and at least 15 pairs of the red kite [28,29]. The island is not directly part of any migratory routes for these species and these species are, therefore, mainly represented by local individuals [30]. The wind farm consists of 55 turbines, ranging from 45–145 meters in total height. The first turbines were constructed in 1979. The area The observational area of the wind farm was defined by a radius of 400 meters around the IdentiFlight (IDF) camera tower and included nine turbines (Figure 1). The remaining turbines on the wind farm were not covered by the IDF system, as a single IDF camera tower has a maximum range of one kilometer.

Figure 1. The IDF Tower (red drop) and the 400 meters zone (orange circle) around the tower, i.e., the observational zone. The wind turbines that the birds within the 400 meters zone flew closest to (orange crosses) and other turbines (grey crosses) within the wind farm.

2.2. Data Collection

Observations of the selected species were collected using the IdentiFlight system over a period of 10 months in 2020, spanning from the middle of February to the end of November. These observations may include both local and non-local individuals of the three species, however, the majority of observations are expected to be local breeders. Throughout this period of time, the system was periodically out of operation and the study is therefore based on a total of 231 days over the course of these 10 months (Appendix A). Out of the 231 days, raptors of the species golden eagle, white–tailed eagle or red kite were only observed within the observational area (up to 400 meters away from the camera tower) of the wind farm on 153 of these days. During the study period the IdentiFlight system was only collecting simulated curtailment data for the nine turbines, hence, the system was not actively curtailing turbines.

2.2.1. IdentiFlight System

The IdentiFlight system was developed to detect eagles at risk of collision with a rotating wind turbine. The system can detect a bird up to one kilometer away from the camera tower and in real time classify whether it is a protected species or not. This species identification is based on IdentiFlight's machine vision algorithms that use a catalog of rules developed by pattern recognition technology. Size, plumage, color, wing shapes and flight profiles are some of the variables used to classify a bird. If a bird is identifies as a protected species the system will then determine if a specific turbine or turbines should be shut down to prevent collision, based on a set of site–specific criteria (curtailment prescription) [26]. In the curtailment prescription an outer and inner cylinder is determined for each turbine, based on the turbine height and rotor diameter. The system will issue a curtailment order resulting in a curtailment of a turbine if a bird, classified as a protected species, flies into the inner cylinder. If the bird is flying between the outer and inner

cylinder the system will only issue a curtailment order if certain criteria are met, e.g., the bird is flying toward a turbine with a flight speed above a certain value. However, the system will never issue a curtailment order if the bird is flying outside of the outer cylinder (Appendix B.1).

The camera system consists of a ring of eight fixed wide field of view cameras and a high resolution stereo camera mounted on top of a six meter high tower (Appendix B.2). The eight wide field of view cameras use image sensor arrays to detect moving objects in the environment and begin to track them. These cameras collect 10 images per second and detect moving objects by comparing the placement of an object relative to the background between images. When a moving object is detected, the movable high resolution stereo camera is directed at the object and uses high magnification stereoscopic sensors to determine the distance to the object. Furthermore, the high resolution stereo camera collects approximately one image per second and gathers the necessary information to classify the object.
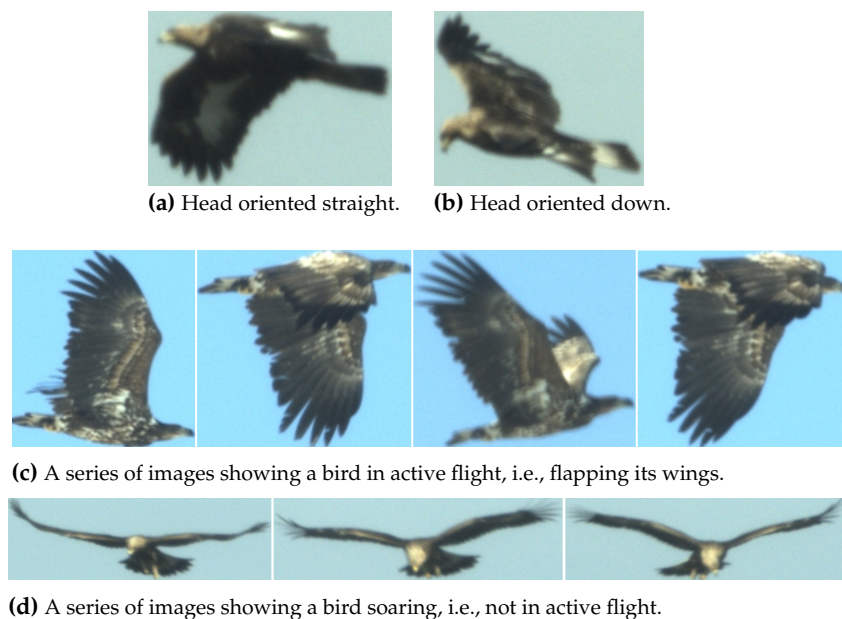
The IdentiFlight system provides a data set with a large variety of variables, including bird images, describing each observation and giving each track a unique Track ID (Appendix C). Furthermore, flight trajectories for each track are saved as Keyhole Markup Language (KML: a file format used to display geographic data) files, which can be imported into ArcGIS Pro [31]. Thus, resulting in a data set with multiple observations of each track, i.e., the flight trajectory of a bird's flight path illustrating its observed flight activity. Hereafter, when referring to observations it is a reference to all observations (multiple observation for each track) and when referring to tracks it is a reference to flight trajectories, i.e., all observations summarized for each track. It should be noted that the automated data collection by the IdentiFlight system may be biased, as the tracks may be incomplete, as the system may stop tracking birds for multiple reasons, one being the system identifying the target bird as not at risk of colliding with a turbine, e.g. due to the flight direction and position of the bird. The system also stops tracking birds if it mistakenly reclassifies the bird as a non-protected species, thus, losing interest in the bird.

2.2.2. Weather Data

Temperature, wind speed and wind direction, provided by Vattenfall, was collected at 10 minute intervals by weather stations on the turbines at a height of 80 meters, hence portraying the weather conditions near the rotor zone of the turbines. Cloud coverage was measured at hourly intervals at a weather station in the southern part of Gotland approximately 34 meters above sea level. This data was downloaded from the Swedish Meteorological and Hydrological Institute [32].

2.3. Data Preparation

Observations from the data collected were filtered based on the species classified by the system in order to obtain a subset with the species golden eagle, white–tailed eagle, and red kite. The bird images were used to classify the head

(a) Head oriented straight. **(b)** Head oriented down.

(c) A series of images showing a bird in active flight, i.e., flapping its wings.

(d) A series of images showing a bird soaring, i.e., not in active flight.

Figure 2. Examples of how behavior was scored based on bird images, a single image was used to classify head position and a series of images had to be used to classify active flight in order to evaluate wing movement between images.

position of the raptors, as either oriented straight forward or down and whether or not the raptor was engaging in active flight (Figure 2). These classifications were done for each observation. Only observations within 400 meters of the camera system were used, as it was difficult to classify the head position for images taken at further distances. Furthermore, only tracks longer than 100 meters were used, as shorter tracks were not considered to be fully descriptive of a bird's behavior within the area. This resulted in a data set of 564 different tracks of the three selected species (Appendix D).

ArcGIS Pro [31] was used to analyze the flight trajectories (KML files). The flight trajectories were used to classify flight type, i.e., each track was assigned one of four different flight types based on a qualitative assessment of flight trajectories (Figure 3). The flight type straight describes raptors flying in a linear path with only minor directional deviations. Raptors flying in the same general direction, but with slightly larger directional deviations than those depicted as straight were classified as the flight type curvy. These two flight types presumably represent birds passing through the study site on route to another location, e.g., birds traveling from roosting sites to foraging sites. The flight type spiral represents raptors presumed to be using thermal soaring, i.e., soaring in updrafts using thermal convection, thus directional changes were mainly in the same direction, creating loops while increasing altitude. When a raptor's flight path had no general flight direction and many large directional changes in all directions, the flight type was categorized as chaotic. This chaotic flight type may be attributed to local birds foraging within the study site.
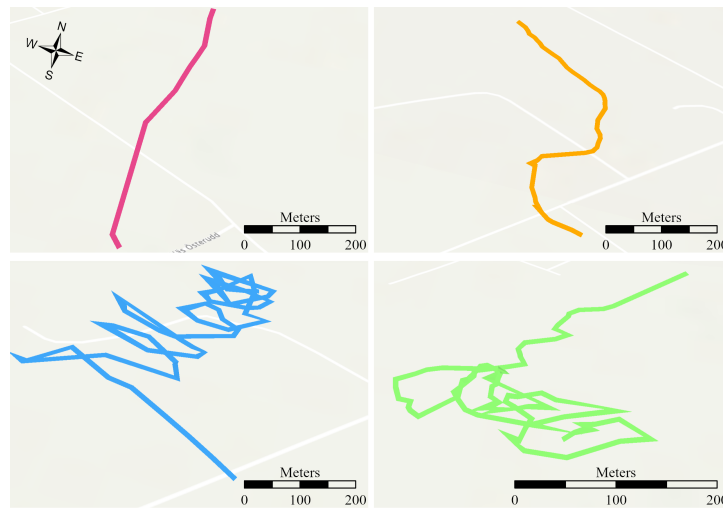
Figure 3. Examples of the four different track types: straight (pink), curvy (orange), spiral (blue), and chaotic (green). The images are based on three–dimensional tracks, i.e., multiple points with x, y and z coordinates.

The flight trajectories were also assessed by calculating the track symmetry and tortuosity, which was done using the ArcPy package in Esri [31] (Appendix E.1 & E.2). Track symmetry was determined by calculating the angles of directional changes throughout the track. These angles ranged from $-180°$ to $180°$, distinguishing between left and right turns. The signed track angles, i.e., directional changes were then summed for each track, resulting in a measure of flight symmetry (Appendix E.2). Track tortuosity was determined by the ratio between direct track length, i.e., the shortest distance between a track's start point and its end point, and actual track length (Appendix E.1). Track symmetry and track tortuosity were used to assess the qualitative classification of track types.

2.4. Data Analysis

The data analyses were carried out for all observations, but also for subsets of observations based on track type, flight type, flight direction, flight altitude and distance to turbine (Appendix D). For analyses involving flight vigilance or active flight only individuals with more than three observations (bird images) were used. All tracks were divided into four subsets based on track type. Another subset was created only including tracks with individuals engaging in active flight. All observations were divided into two subsets based on flight direction, i.e., flying towards the wind turbine or away from the wind turbine, this was based on whether the distance to the nearest turbine was decreasing or increasing, meaning that most individuals are present in both subsets, as throughout their track they both fly towards and away from a turbine. Furthermore, three subsets were created dividing observations based on flight altitude into the categories: below, in or above the rotor zone of the nearest turbine, i.e., each individual could be represented in multiple subsets (see Appendix B.1 for rotor zone definitions). Lastly, two subsets were created by dividing all observations based on the distance to the nearest turbine into the categories: close proximity to turbine (<150 m) and distant to turbine

(>150 m), i.e., each individual could be represented in multiple subsets. This distance of 150 meters was based on initial observations indicating changes in behavior at this distance. The statistical analyses were conducted in R version 4.1.1 [33].

2.4.1. Flight Behavior Classifications

To assess how the general flight behavior of raptors can be quantified and how it is affected by the weather, associations both among the different variables describing flight behavior and between these variables and weather variables were tested with the χ^2 contingency test and Spearman's rank correlation (r_s) [34] (Table 1). Bonferroni's correction for multiple comparisons was applied, as the same variables are included in multiple tests [34]. For the χ^2 contingency test, continuous variables such as % time spent looking down, % time spent on active flight, distance to nearest turbine, and weather variables were described as categorical variables, e.g., temperature was categorized as low (0–10 °C), medium (10–20 °C) or high (20–30 °C).

Table 1: Overview of all univariate tests. The χ^2 contingency test is annotated by χ^2 and Spearman's rank correlation is annotated by r_s.

	Response variable				
Independent variable	Proportion of tracks	Flight vigilance	Flight altitude	Track symmetry	Track tortuosity
Flight vigilance	χ^2			r_s	r_s
Active flight	χ^2	r_s		r_s	r_s
Flight altitude	χ^2	r_s		r_s	r_s
Track symmetry	χ^2	r_s			
Track tortuosity	χ^2	r_s			
Turbine distance	χ^2	r_s	r_s	r_s	r_s
Cloud coverage	χ^2	r_s	r_s	r_s	r_s
Temperature	χ^2	r_s	r_s	r_s	r_s
Wind speed	χ^2	r_s	r_s	r_s	r_s

In order to evaluate the applicability of track symmetry and track tortuosity, as indicators of the overall track type, a box plot of each variable was created, describing median and interquartile range (25%–75%) for each track type. Furthermore, associations between track type as the response variable and flight behavior and weather variables, described as categorical covariates, were assessed using the χ^2 contingency test using the number of tracks in each mutually exclusive combination, along with bar plots depicting the proportions. To assess the respective univariate relationships between different response variables describing flight behavior (% time spent looking down, flight altitude, track symmetry and track tortuosity) and various explanatory weather variables (temperature, wind speed and cloud coverage), correlation coefficients were calculated and the relationships between these variables were visualized with linear regressions. The univariate relationships between the aforementioned variables describing flight behavior were also visualized with linear regression and their respective correlation coefficients were calculated as well. All regressions were based on grouped medians of the dependent variable, that were determined by class intervals of independent variables, with horizontal bars representing the interquartile range (IQR) to illustrate the variation around the medians. This was done for all subsets.

2.4.2. Avoidance Behavior

To assess avoidance behavior, i.e., behavioral changes, such as changes in flight altitude, in proximity to wind turbines, flight altitude was assessed as the response variable in relation to distance to nearest turbine as the explanatory variable. This was achieved by calculating the correlation coefficient and the relationship was also visualized with a linear regression based on grouped medians. This was also done for all subsets. It was assumed that avoidance behavior would only be observed within a certain radius of a wind turbine. Therefore, the cumulative regression between distance to nearest turbine and flight altitude was calculated with increasing turbine distance, to find the distance at which the relationship weakened. This distance was hereafter used as an upper limit for the analysis of avoidance behavior. This was done for all subsets used in this analysis and the upper limit varied across subsets. Furthermore, the relationship between flight vigilance as the response variable and flight altitude as the explanatory variable for the the subset with observations in close proximity to the nearest turbine was compared to that of the subset with observation distant to the nearest turbine.

2.4.3. Collision risk

In an attempt to quantify collision risk generalized linear models were created to determine which variables affect flight behaviors influencing collision risk, i.e., flight vigilance, flight altitude, track tortuosity, and track symmetry. To assess collinearity between explanatory variables, Spearman's correlation coefficient (r) was calculated among the covariates and pairwise scatter-plots were created to detect obvious correlations among the covariates (Appendix F). The possible explanatory variables included distance to nearest turbine, wind speed, cloud coverage, and temperature, but depended on the flight behavior being assessed and the other flight behaviors were also often included as possible explanatory variables. Automated model selection (glmulti) was then used to find the best regression model based on prediction error using the Akaike information criterion (AIC). The automated model selection builds all possible unique models from a list of explanatory variables, i.e., all models are compared (it is not iterative) [35]. The automated model selection was carried out for models both with and without pairwise interactions and the final models were then selected using an anova χ^2 test comparing the models with and without interactions [36].

3. Results

3.1. Flight Behavior Classification

There was a difference in track symmetry and track tortuosity between the different track types (Appendix G.1). Furthermore, there was an association between flight vigilance (% time spent looking down) and flight type ($\chi^2_9 = 55.8^{***}$). When flying in straight or curvy flight patterns raptors spent less time looking down and when flying in a chaotic or spiraling pattern they spent more time looking down (Figure 4a). There was also an association between time spent on active flight and flight type ($\chi^2_9 = 65.3^{***}$).
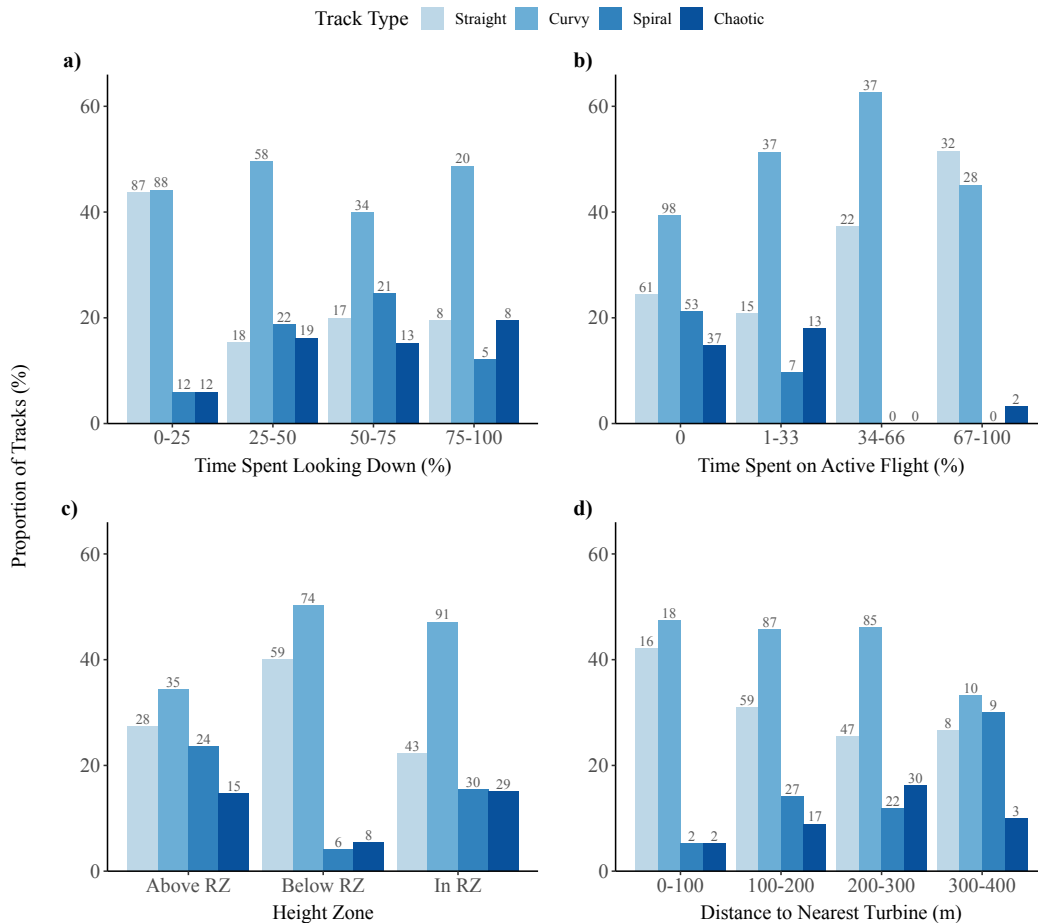
Figure 4. Proportion of occurrences of each track type in relation to **(a)** the proportion of time the birds spent looking down, **(b)** the proportion of time spent on active flight, **(c)** flight altitude divided into groups based on the rotor zone (RZ) of the nearest turbine and **(d)** the distance of the nearest turbine. The number of tracks is annotated above each bar.

Individuals flying in chaotic or spiraling patterns generally spent a small proportion of time ($< 33\%$) on active flight (Figure 4b). Furthermore, flight type was dependent on the height zone at which flight activity took place ($\chi^2_6 = 38.2^{***}$). Most of the individuals flying below the rotor zone were flying in straight (40.1%) or curvy (50.3%) patterns (Figure 4c). For individuals flying above the rotor zone there was a larger variation between the flight patterns utilized. A large proportion of the individuals flying in curvy (45.5%) or chaotic (55.8%) patterns were flying in the rotor zone. Flight type was also associated with distance to the nearest turbine ($\chi^2_9 = 18.6^*$), where most of the individuals flying near turbines were flying in straight or curvy patterns. The proportion of individuals flying in curvy or chaotic patterns increased with distance to the nearest turbine (Figure 4d). Moreover, flight type was also associated with temperature ($\chi^2_6 = 40.8^{***}$) and wind speed ($\chi^2_6 = 56.9^{***}$) (Appendix G.2).
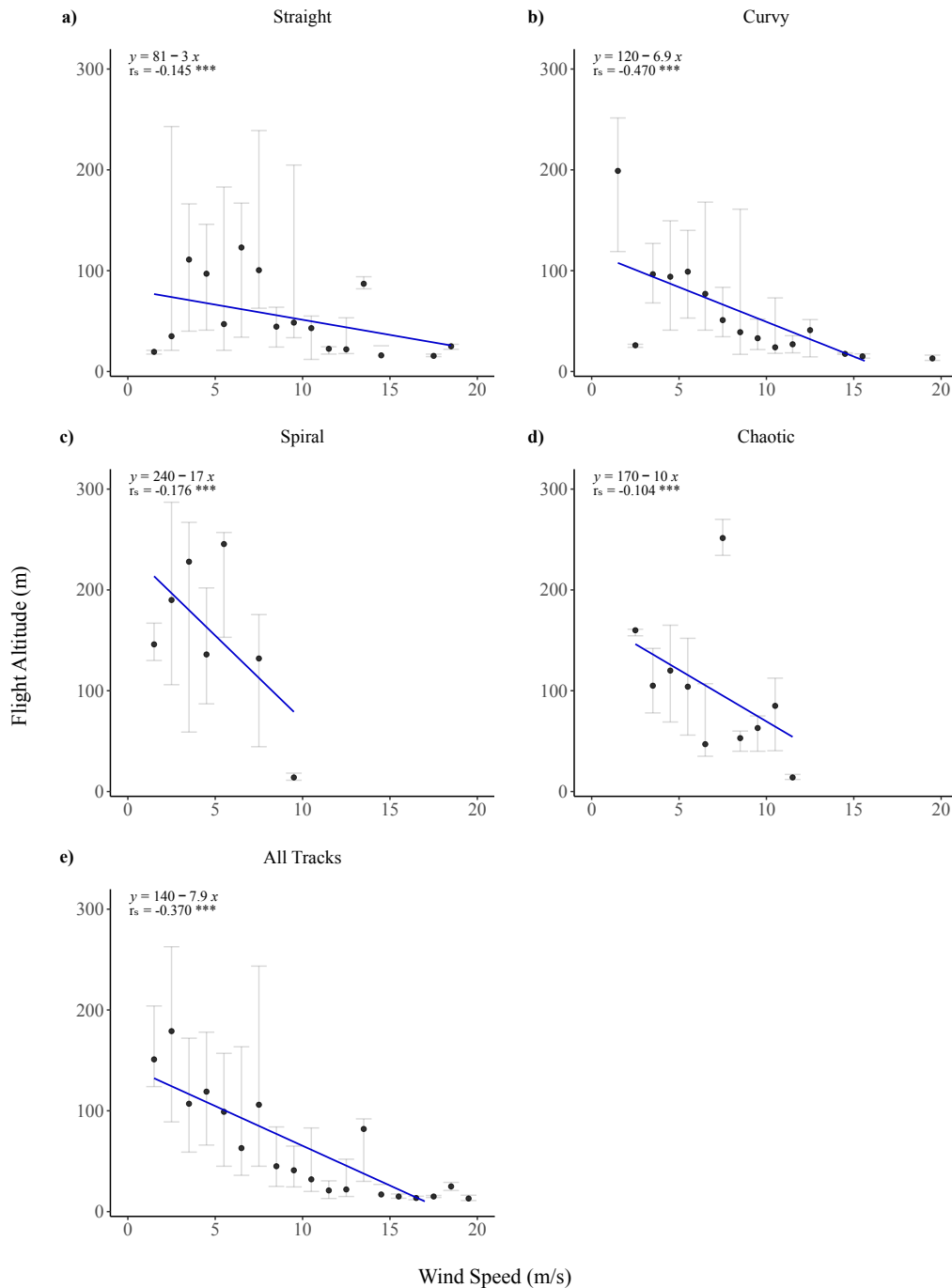
Figure 5. Linear regression of flight altitude above ground level in relation to wind speed, **(a–d)** grouped by track type and for **(e)** all track types collectively. For each regression, the median flight altitude was used for wind speed at each m/s. The regression equation and correlation coefficient (r_s) is given for each plot. The horizontal bars represent the variance around each median (IQR).

Flight altitude was negatively correlated with wind speed ($r_s = -0.370^{***}$) and raptors flew at lower altitudes with increasing wind speeds (Figure 5). When assessing this correlation for each track type individually, this association was strongest for individuals flying in curvy patterns ($r_s = -0.470^{***}$). There was also a correlation between flight altitude and cloud coverage ($r_s = 0.0349^{**}$) and between flight altitude and temperature ($r_s = 0.0833^{***}$), however these correlations were weaker than that of wind speed (Appendix G.3).

There was a significant positive correlation ($r_s = 0.309^{***}$) between general flight vigilance (time spent looking down) and track asymmetry (sum of directional changes) (Appendix G.4). Showing the more asymmetrical a raptor's flight path was, the less vigilant they were. Furthermore, for individuals in active flight, the relationship between general flight vigilance and flight asymmetry was more positively correlated ($r_s = 0.426^{***}$) (Appendix G.5). General flight vigilance was negatively correlated ($r_s = -0.310^{***}$) with track tortuosity, indicating that raptors with more direct paths also were the most vigilant in their flight direction (Appendix G.4). General flight vigilance was also negatively correlated ($r_s = -0.427^{***}$) with time spent on active flight, meaning that raptors actively flying were more vigilant in their flight direction (Appendix G.4). There was also a significant positive correlation between general flight vigilance and flight altitude ($r_s = 0.135^{***}$). However, when looking at this relationship for each track type individually, it was only straight tracks that also showed a significant positive correlation ($r_s = 0.208^{***}$). For chaotic tracks this correlation was negative ($r_s = 0. - 149^*$) and no significant correlation occurred for the two other track types (Appendix G.6).

3.2. Avoidance Behavior

There was a weak correlation between distance to nearest turbine and flight altitude for all track types ($r_s = 0.0658^{***}$) (Appendix G.7). When grouping the tracks by type a slightly larger positive correlation occurred for the track types curvy ($r_s = 0.110^{***}$), and spiral ($r_s = 0.134^{***}$), whereas for chaotic tracks this correlation was negative ($r_s = -0.0854^{**}$) and for straight tracks this correlation was not significant ($p > 0.05$). When comparing the relationship between flight altitude and time spent looking down for raptors in close proximity to a turbine with those distant to a turbine, positive correlations occurred at both distances (close: $r_s = 0.219^{***}$; distant: $r_s = 0.177^{***}$), but the slope of the regression trend line for raptors in close proximity was a fivefold larger than that of distant raptors (Figure 6). Hence, individuals in close proximity to the nearest wind turbine clearly flew at higher altitudes if spending a larger amount of time looking down.
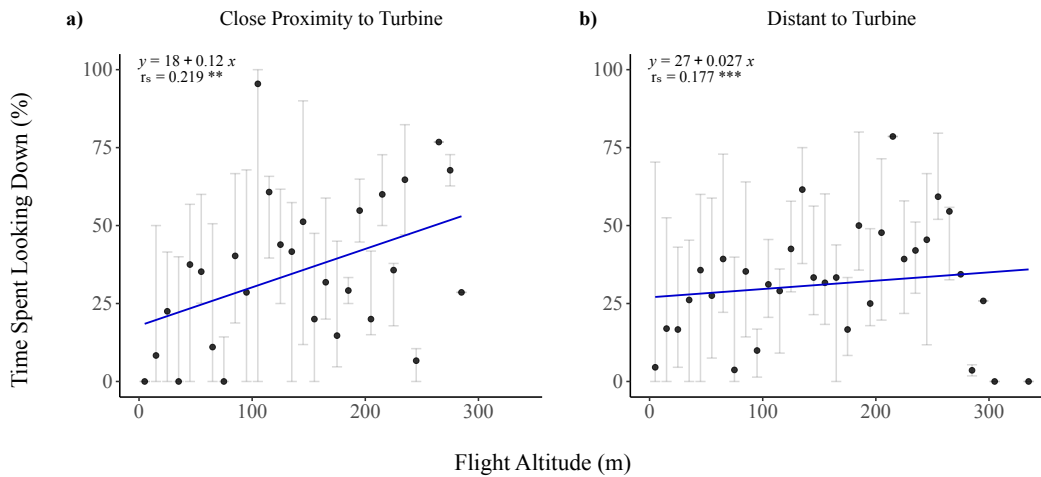

Figure 6. Linear regression of flight vigilance i.e. proportion of time each individual spent looking down in relation to flight altitude above ground level, grouped by distance to nearest turbine **(a)** close: <150 m and **(b)** distant: >150 m. For each regression, the median proportion of time spent looking down was used for every 10 m. The regression equation and correlation coefficient (r_s) is given for each plot. The horizontal bars represent the variance around each median (IQR).

For raptors in close proximity to the nearest turbine (<150 m) there was a significant positive correlation between distance to the nearest turbine and flight altitude when raptors were flying towards the nearest turbine ($r_s = 0.158^{***}$) and the correlation was slightly stronger when raptors were flying away from the nearest turbine ($r_s = 0.209^{***}$) (Figure 7). When raptors were flying towards a turbine, there was a positive correlation between distance to nearest turbine and flight vigilance for all three altitude zones separately (above: $r_s = 0.126^{***}$; below: $r_s = 0.147^{***}$; in: $r_s = 0.0789^*$) (Figure 8).
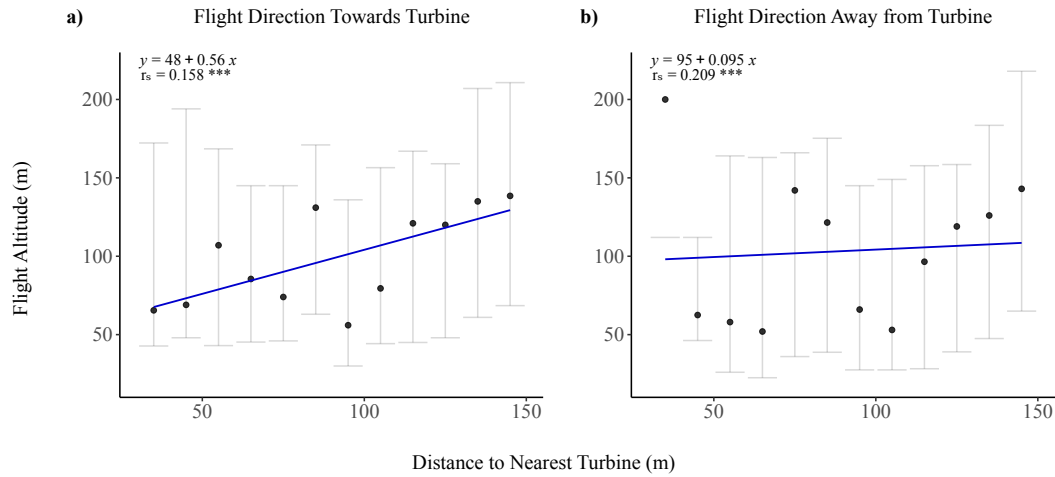
Figure 7. Linear regression of distance to the nearest turbine (<150 m) in relation to flight altitude above ground level grouped by flight direction **(a)** flying towards the nearest turbine and **(b)** flying away from the nearest turbine. For each regression, the median flight altitude (m) was used for every 10 m. The regression equation and correlation coefficient (r_s) is given for each plot. The horizontal bars represent the variance around each median (IQR).
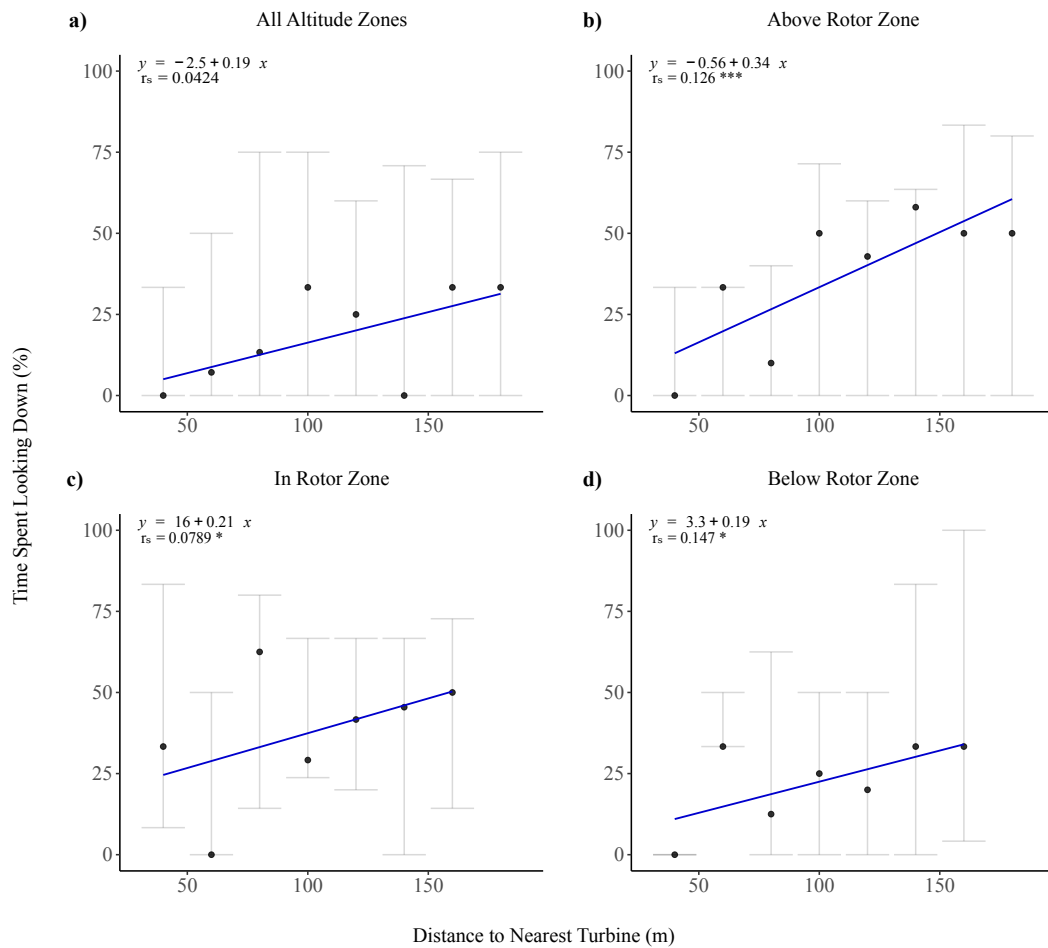
Figure 8. Linear regression, for individuals flying towards a turbine, of the proportion of time the birds spent looking down for each track (median values for turbine distance groups per 20 m) in relation to distance of the nearest turbine. The linear regression models were also made for tracks divided into groups based on the rotor zone of the nearest turbine. The regression equation and correlation coefficient (r_s) is given for each plot. The horizontal bars represent the variance around each median (IQR).

3.3. Collision risk

The comparison of models with and without interactions, indicated the simpler of the two models, i.e. the model without interactions, to be the better choice when assessing track tortuosity as the response variable, as adding interaction terms did not significantly improve the model. When assessing the other response variables, i.e., flight vigilance, flight altitude, and track symmetry, respectively, the addition of interaction terms significantly improved the model's goodness of fit (Appendix H).
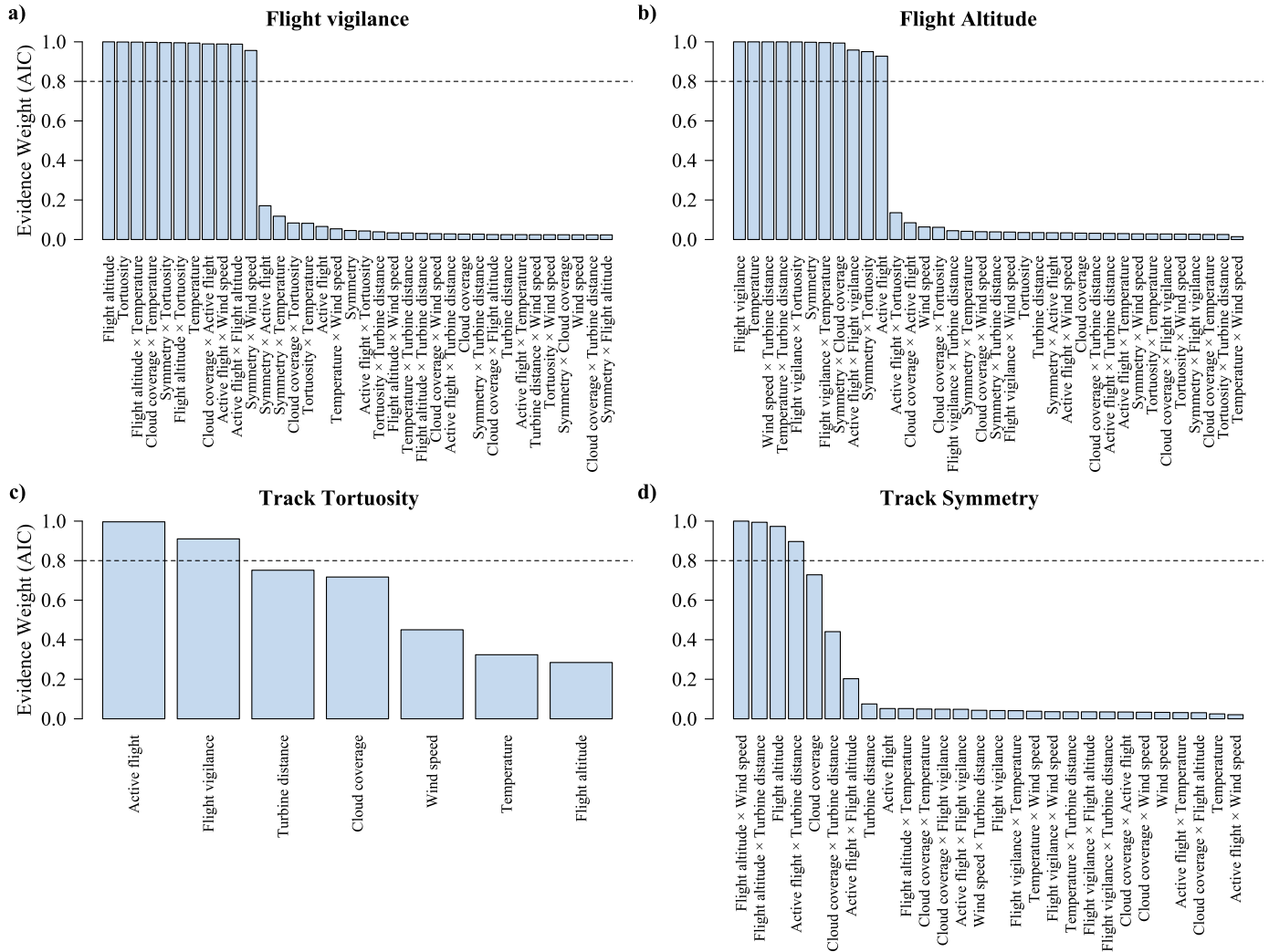
Figure 9. Relative importance of each model term when assessing **a)** flight vigilance as the response variable with interactions, **b)** flight altitude as the response variable with interactions, **c)** track tortuosity as the response variable without interactions, and **d)** track symmetry as the response variable with interactions. Each term's relative importance was estimated with the automated model selection as the sum of Akaike evidence weights of all models in which the term appears.

When assessing flight vigilance as the response variable, the automated model selection indicated that flight altitude (evidence weight = 1.00) and track tortuosity (evidence weight = 0.999) were the two most important model terms (Figure 9a). However, all covariates, with the exception of turbine distance, significantly contributed to explaining the variation of flight vigilance. The automated model selection assessing flight altitude, as the response variable, indicated that flight vigilance (evidence weight = 1.00) and temperature (evidence weight = 1.00) were the two most important model terms, but all other covariates also significantly contributed to explaining the variation in flight altitude (Figure 9b). When assessing the response variable track tortuosity, the evidence weights highlighted active flight (evidence weight = 0.996) and flight vigilance (evidence weight = 0.910) as the only covariates significantly contributing to the variation in track tortuosity (Figure 9c). When assessing track symmetry as the response variable, flight altitude was included in three out of the four model terms with an evidence weight over the threshold of 0.8 (Figure 9d). It should be emphasized

that the absolute results from the automated model selections should only be interpreted as indications and should not be taken literally.

4. Discussion

The negative effects of wind turbines on birds result primarily from collision related fatalities and secondarily through displacement effects resulting in habitat loss [9,37]. The precise number of collision related fatalities is uncertain. Nonetheless, large soaring raptors are known to be specifically vulnerable for collision with turbines [2,3,9,11]. Furthermore, some wind farms are located close to the nesting sites of these species, thus, the risk of wind farms having a significant impact on both local and migrating raptors is likely high. Such a negative impact can have detrimental effects on slow maturing species with low reproduction rates, particularly for species of conservation concern when considering regional and national populations [1,7]. This research takes an important step in understanding the effects of wind farms on raptors.

4.1. Flight Behavior as a Predictor of Collision Risk

The results of the case study demonstrate how flight trajectories can be used to describe flight behavior by classifying track type. Moreover, track symmetry and tortuosity can be used to quantitatively assess risk prone behavior. Previous studies have often described tortuosity as an indicator for collision risk, hypothesizing birds with a more tortuous flight path to be at higher risk for collision [6,38,39]. The inference of these studies is based on the expectation that a more tortuous flight path is associated with a larger amount of time flying and when flying there will always be a collision risk. Furthermore, the associations between flight vigilance and flight tortuosity, respectively, found in this study, indicate that individuals with a more tortuous flight behavior are less vigilant, hence supporting the hypothesis that birds with a tortuous flight path are at increased risk for collision. This is further supported by the multivariate analysis, which also indicated that flight vigilance was dependent on track tortuosity.

Another presumable predictor of collision risk is flight altitude in relation to the rotor zone i.e. flight in the rotor zone is associated with a higher collision risk [6,14,38–40]. Flight altitude has previously been found to be determined by movement type e.g. migratory or local movement [6]. Katzner *et al.* [6] and Bergen *et al.* [39] found that migratory birds flying in a linear fashion flew at higher altitudes. Contrary to this, the results in this study show that most individuals flying in straight (or curvy) patterns flew at altitudes in or below the rotor zone. These contradicting results are, however, likely to be due to the raptors on Gotland mainly consisting of breeding populations, as the island is not directly part of any migratory routes for these species [30]. The raptors in this study are therefore assumed to be mainly local birds, however, some of the studied raptors may be migratory. However, other factors, such as, weather conditions and distance to nearest wind turbine may further explain this behavior. Similar to the findings in this study, Dahl *et al.* [19] found that occurrences below the rotor zone were mainly individuals engaging in directional flight and some engaging in social behavior. Moreover, distance to wind turbines is an obvious predictor of collision risk. In this study it was found that most of the raptors flying near turbines had the flight type straight or curvy and that the proportion of raptors flying in a spiral or chaotic pattern increased with distance to the nearest turbine. This is in agreement with previous studies showing that soaring birds change their flight trajectories to avoid wind turbines [3,15,18].

4.1.1. Effect of Weather on Flight Behavior

Understanding how weather affects flight behavior is important for developing risk assessment models. In this study the raptors flew at lower altitudes with increasing wind speeds. In accordance with these findings previous studies also found that eagles were more likely to fly at altitudes under 150 meters at higher wind speeds [40,41]. Kuehn *et al.* [40] suggests that these results reflect an increasing collision risk at higher wind speeds. Contrary to this, we suggest that, while moderate wind speeds (5–10 m/s) result in an increased collision risk, due to the resulting flight altitudes being within the rotor zone, high wind speeds (>10 m/s) generally result in flight altitudes below the rotor zone and the risk of collision with moving rotor blades is therefore negligible.

4.2. Avoidance Behavior

The findings of the case study prove the use of variables describing flight behavior and thereby camera–based monitoring systems such as IdentiFlight for evaluating avoidance behavior, as the results indicate that golden eagles, white–tailed eagles and red kites exhibit some degree of meso–avoidance to the turbines within the wind farm on Gotland. However, the correlations describing avoidance behavior are generally weak, and should, therefore, only be interpreted as general indications. These weak correlations may be due to avoidance behavior being highly species-specific [3].

Moreover, previous studies show that raptors exhibit avoidance behavior by increasing flight altitude in proximity to turbines [8,14,16,20,23]. In this study the species studied decreased flight altitude in proximity to turbines. This response is also an indication of avoidance behavior, as it can be argued that avoidance also can take place under the rotor zone. This avoidance response became more evident when dividing the track types according to flight direction. This avoidance response may be explained as when nearing a turbine the use various flight methods to increase altitude is reduced.

Furthermore, it was found that individuals in close proximity to the nearest wind turbine flew at higher altitudes if spending a larger amount of time looking down. Thus, individuals foraging increase their altitude to increase time spent looking down to forage, indicating even foraging individuals, which are expected to be less vigilant, display avoidance behavior to turbines. Moreover, when comparing the avoidance behavior of individuals oriented towards the nearest turbine when flying either above, below or in the rotor zone, a positive correlation was found, between distance to nearest turbine and time spent looking down, for all three altitude zones. While this correlation was largely similar for individuals flying at altitudes above or below the rotor zone, the correlation was weaker for individuals flying towards the turbine at altitudes within the rotor zone. This could indicate that individuals flying at altitudes within the rotor zone exhibit a lower avoidance behavior and are at a larger risk for colliding with the turbine. Similarly, Garvin *et al.* [14] found the individuals flying in close proximity to the turbines generally demonstrated high risk behaviors, displaying no signs of avoidance.

5. Conclusion

This study provides a framework for future research, using data from camera–based monitoring systems, demonstrating how flight trajectories and bird images can be utilized to describe risk prone behavior and thereby assess collision risk and avoidance behavior. Thus, providing a crucial step towards quantifying collision risk to be used in future predictive models. However, this study is only based on assumptions that behaviors decreasing flight vigilance, e.g. foraging, and tortuous flight are more prone to collision. It is therefore necessary to assess the behavior of individuals hit by turbines prior to the collision. The use of camera–based monitoring systems along with a collision detecting system such as the WT–Bird system, that can detect collisions through the use of acoustic sensors on turbine blades [42] would enable the necessary data to be collected. Future studies should also focus on the foraging behavior of the birds and more specifically investigate the effect of carrion located under the rotor. This could be done by eliminating carrion under the rotors of the wind turbines and comparing the raptors' flight behavior in the two different situations, with and without carrion. This study provides a quantitative method that can be utilized to analyze such data and factually determine which behaviors lead to an increased collision risk.

Appendix A. Operational Days

Table A.1. Number of days where the camera system were operational, number of days with sightings of the selected raptor species (red kite, golden eagle, and white–tailed eagle), and number of tracks for each month.

Month	Operational days	Days with raptors	Number of tracks
February	20	14	53
March	31	25	153
April	30	23	91
May	31	20	69
June	12	8	8
July	11	6	20
August	18	16	87
September	30	23	140
October	26	13	39
November	22	5	12
Total	**231**	**153**	**672**

Appendix B. IdentiFlight System

Appendix B.1. Curtailment Prescription

Table B.1. Model type, number of turbines, rotor diameter, hub height, rotor zone, radius of outer and inner cylinder, and height of outer and inner cylinder for covered and partially covered wind turbines.

Model	Number of turbines	Rotor diameter (m)	Hub height (m)	Rotor zone (m above ground level)	Radius of outer cylinder (m)	Radius of inner cylinder (m)	Height of outer cylinder (m)	Height of inner cylinder (m)
Covered								
Vestas V27	1	27	31	15.5–46.5	700	250	300	200
Vestas V29	1	29	31	14.5–47.5	700	250	300	200
Vestas V90	1	90	80	33–127	700	400	400	250
Partially covered								
Kenersys 2500 100	1	100	85	33–137	600	300	400	250
Vestas V47	2	47	45	19.5–70.5	600	300	300	200
Vestas V90	2	90	80	33–127	700	300	400	250
Vestas V100	1	95	100	50.5–149.5	700	400	400	250
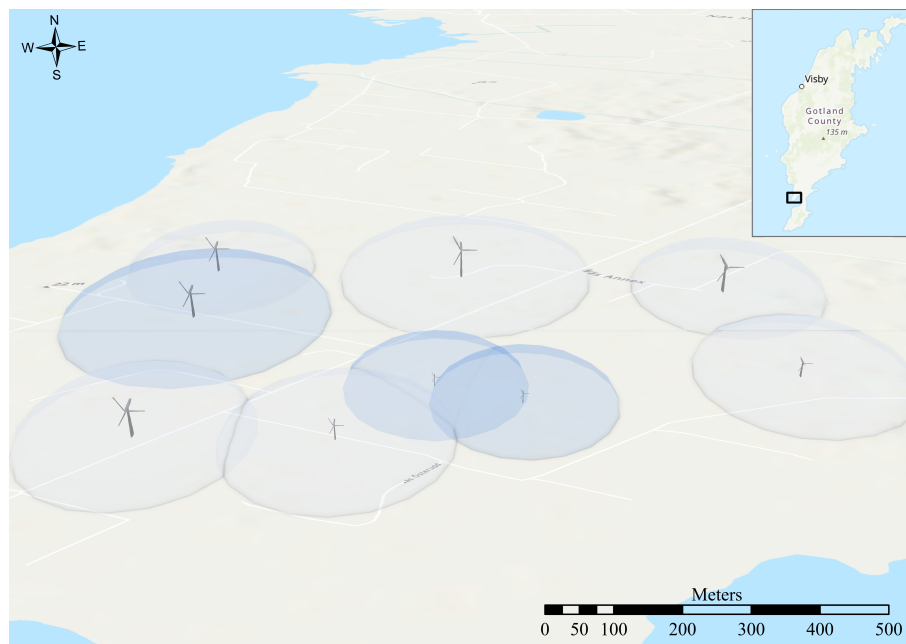
Figure B.1. Fully covered (dark blue) and partially covered (light blue) wind turbines by the IDF tower. The horizontal curtailment zone (radius of inner cylinder) is shown around each turbine.

Appendix B.2. IdentiFlight Camera System

Figure B.2. IdentiFlight tower at study site.
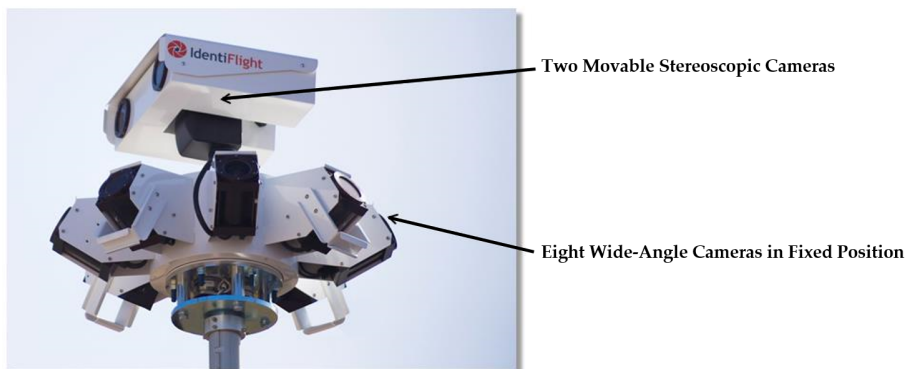
Figure B.3. Imaging head components of the IdentiFlight tower. The bottom part consist of eight fixed cameras that can detect eagle sized objects and separate important from unimportant motion of birds. When important motion is detected the top part tracks that bird as it consist of two movable cameras, that also measure the distance of the the bird it is tracking.

Appendix C. IdentiFlight Data

The IDF system registers a large variety of variables for each observation of each track (Figure C.1). Whenever a bird of interest is detected it is assigned an unique track ID that is used for all observations of that bird. For each observation a image is taken of the bird at that specific time, as the system notes the time and date. Furthermore, the longitude and latitude as well as the height above ground level is registered, which gives multiple coordinates of each bird i.e. tracks. Horizontal distance between the bird and camera tower as well as the distance between the bird and nearest turbine is also registered for each observation. Moreover, the system determines the species of each bird and gives a confidence level of the species classification. The system can classify a bird in the following categories: eagle, white–tailed eagle, golden eagle, non eagle, red kite, red or black kite, buzzard, gull, and other avian species.

**Figure C.1.** Example of data output given by the IdentiFlight system.

Appendix D. Subsets

Table D.1. Number of observations and tracks for each data set and each subset based on track type, distance to turbine and altitude zone, respectively. For analyses containing all tracks and the variables, % time looking down and active flight, the data set ≥ 100 m & ≥ 4 images was used. Otherwise the dataset the ≥ 100 m was used for analyses with all tracks. Tracks with odd deviations were removed from all data sets. For the subset dividing observations by altitude zone only observations within 180 meters of the nearest turbine were used.

	Observations	Tracks
All tracks		
≥ 100 m	8036	564
≥ 100 m & ≥ 4 images	7796	442
Divided by track type		
Straight	1418	130
Curvy	3190	200
Spiral	1892	60
Chaotic	1296	52
Divided by distance to turbine		
Close	2215	148
Distant	5826	348
Divided by altitude zone		
Above rotor zone	1311	256
Below rotor zone	820	236
In rotor zone	1580	320

Appendix E. Calculations

*Appendix E.1. Track Length Ratios*
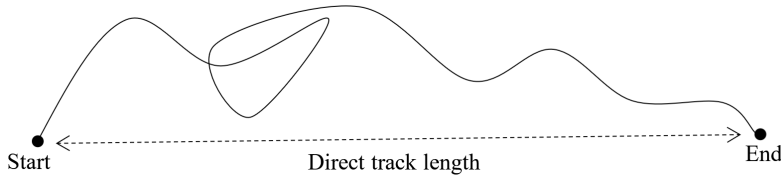
Figure E.1. Model of a track, showing the direct track length (the dotted arrow) in comparison to the actual track length.

The track length ratio was calculated for each track as shown in Equation A1, where the direct track length is the shortest distance from a track's start point to the track's end point (Figure E.1). This resulted in a measure of deviations from the most direct path, where a value of 1 represents a flight path with no deviations. The smaller the value the more deviations from the direct flight path.

$$Track\ length\ ratio = \frac{Direct\ track\ length}{Actual\ track\ length} \tag{A1}$$

Appendix E.2. Track Angles

A track is based on the observations of a single individual i.e. multiple points that are connected in a chronological order. When an individual turns it will be seen as an angle in the connected points. Left turns and right turns were distinguish as the track angles ranged from $-180°$ to $180°$ (figure E.2).
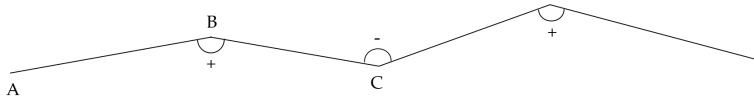
Figure E.2. Model of a track. Right turns ranged from 0 to $180°$ and left turns from -180 to $0°$, which are annotated with $+$ and $-$, respectively. Trigonometry was used to calculate the angles therefore three points were used to calculate each angle e.g. when calculating the angle for the point B the points A and C was used as well.

To calculate the angles of the track the inverse trigonometric function of cosine (arccos) was used as shown in Equation A2. A, B and C represents points as shown in Figure E.2, where AB is the distance from point A to point B, and BC is the distance between point B and C and so on.

$$\angle B = arccos\left(\frac{AB^2 + BC^2 - AC^2}{2 \cdot AB \cdot BC}\right) \tag{A2}$$

The absolute sum of track angles was calculated for each track as shown in Equation A3. This resulted in a measure of flight symmetry, where a value of 0 represents a perfectly symmetrical track in terms of the number of turns and the size of them to the left and to the right. The larger the value the more asymmetrical the track in relation to turns to either the left or the right.

$$Absolute\ Sum\ of\ \angle = \left|\sum_{i=1}^{n} \angle_i\right| \tag{A3}$$

Appendix F. Testing for Collinearity

To assess collinearity Spearman's correlation coefficient was calculated among the covariates and pairwise scatterplots were created to detect obvious correlations among the covariates.
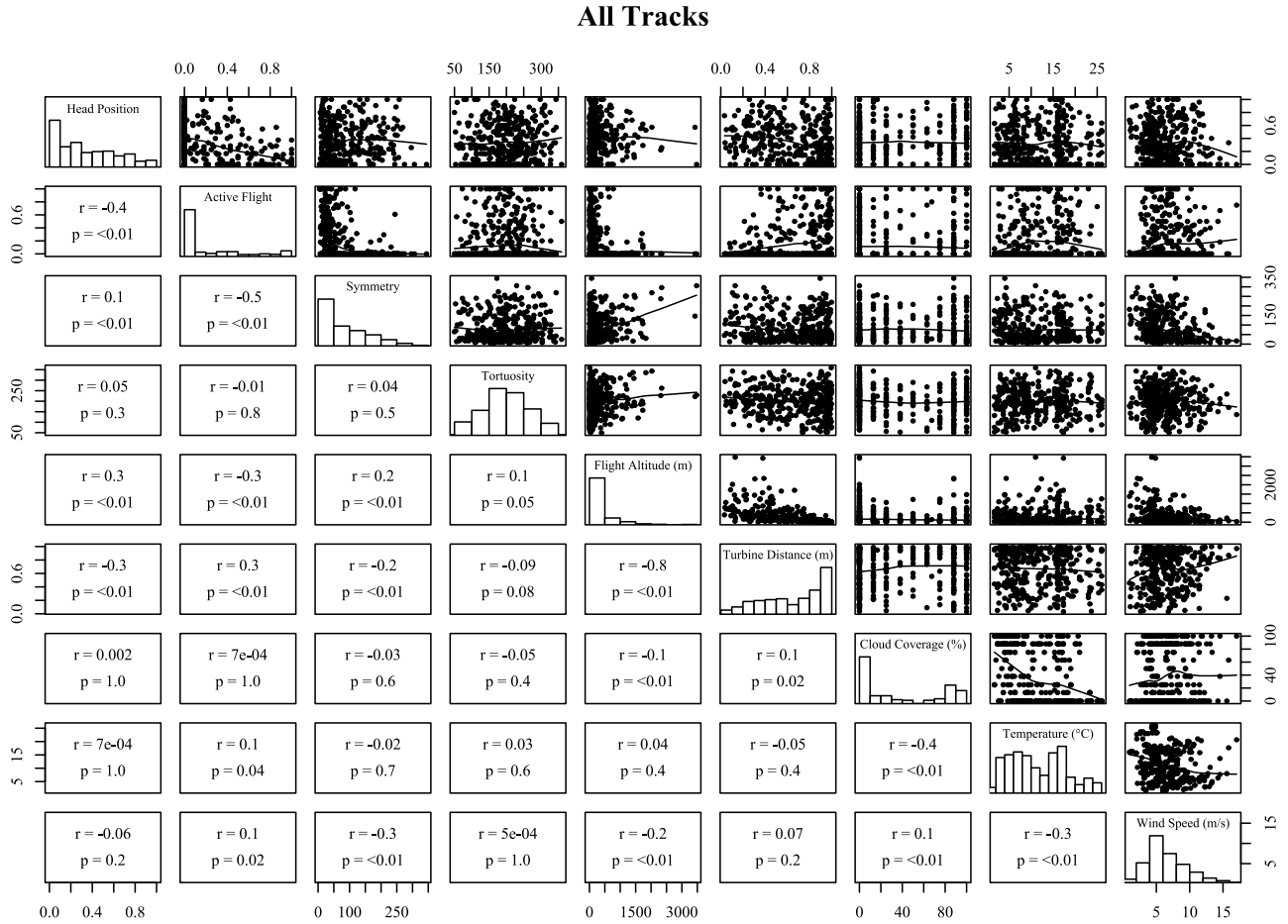

Figure F.1. Correlation between the different continuous predictor variables.

Appendix G. Supplementary Results

*Appendix G.1. Flight Behavior Classification*
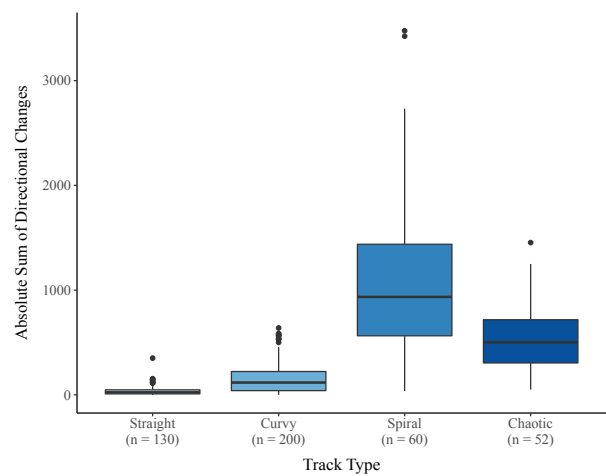
Figure G.1.1. Track symmetry quantified by the absolute sum of directional changes (measured as angles) grouped by track type. Note that the larger the value the more asymmetrical the track is. The number of tracks each subset is based on is annotated under each track type.
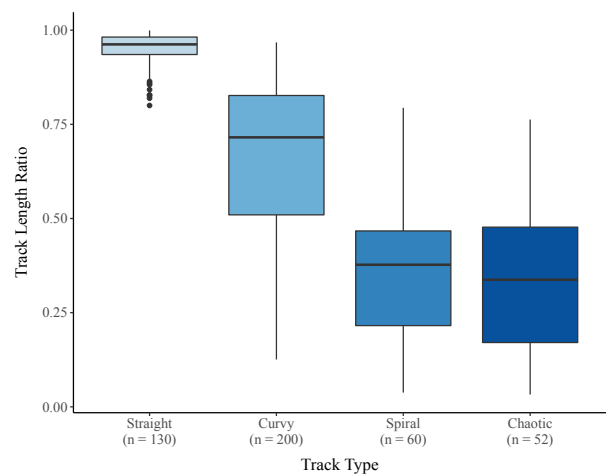
Figure G.1.2. The ratio between the shortest path from a track's start to end point and the actual track length, grouped by track type. The number of tracks each subset is based on is annotated under each track type.
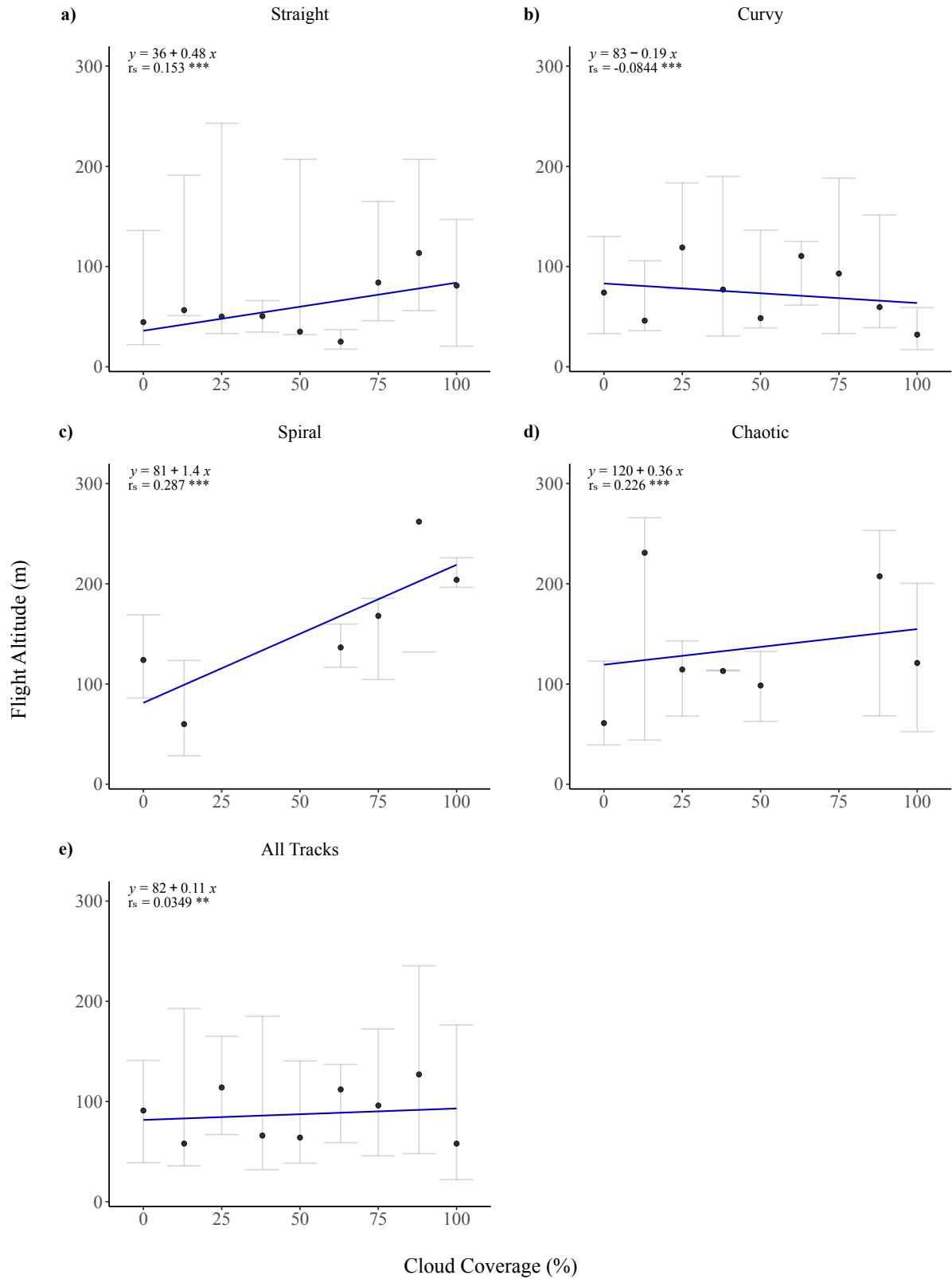
*Appendix G.2. Track Types in Relation to Weather*
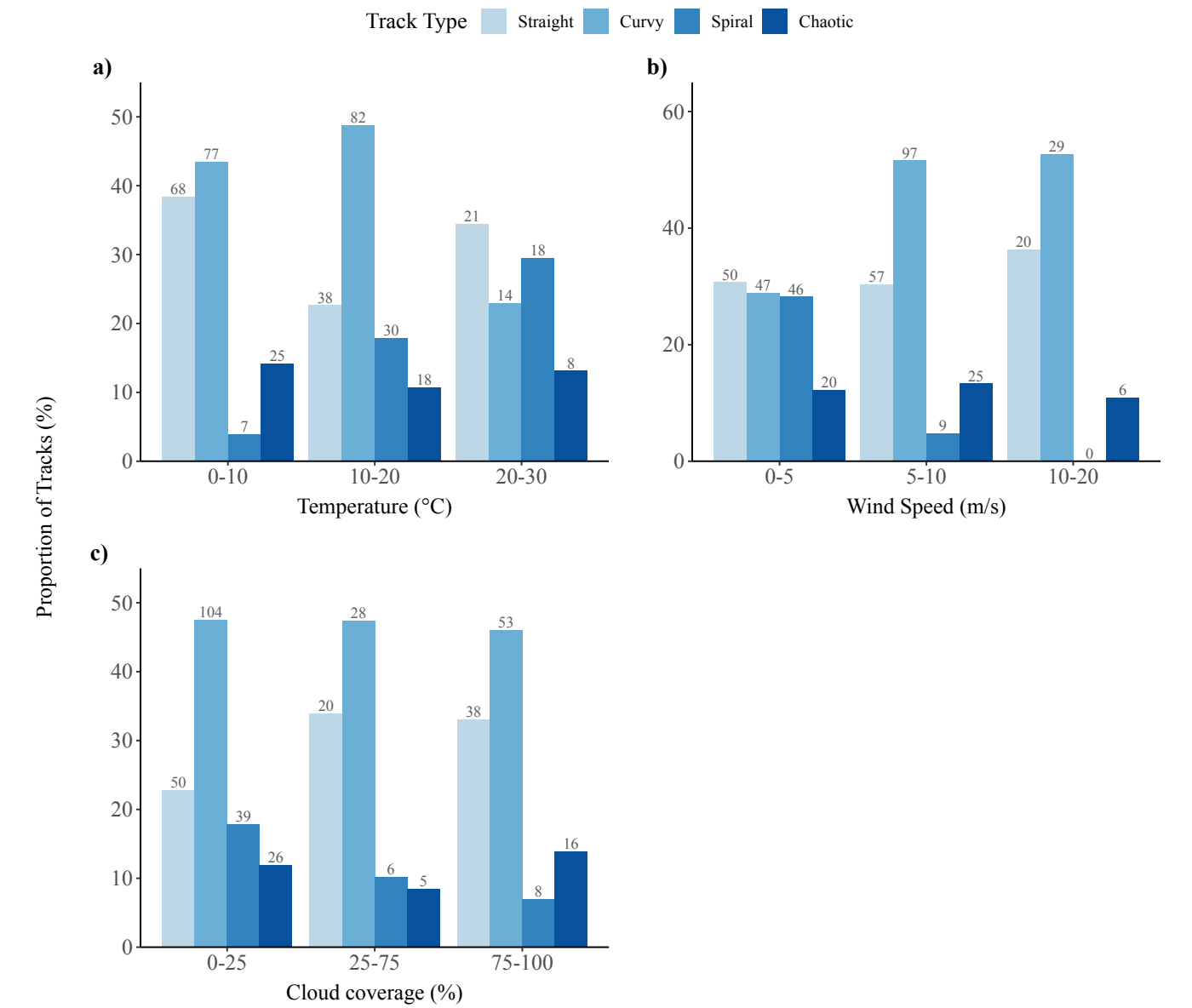
Figure G.2.1. Proportion of occurrences of each track type in relation to wind speed, temperature, and cloud coverage, respectively. The number of tracks is annotated above each bar.

Appendix G.3. Flight Altitude in Relation to Weather

Figure G.3.1. Linear regression of flight altitude above ground level in relation to cloud coverage, **(a–d)** grouped by track type and for **(e)** all track types collectively. For each regression, the median flight altitude was used for each % cloud coverage. The regression equation and correlation coefficient (r_s) is given for each plot. The horizontal bars represent the variance around each median (IQR).
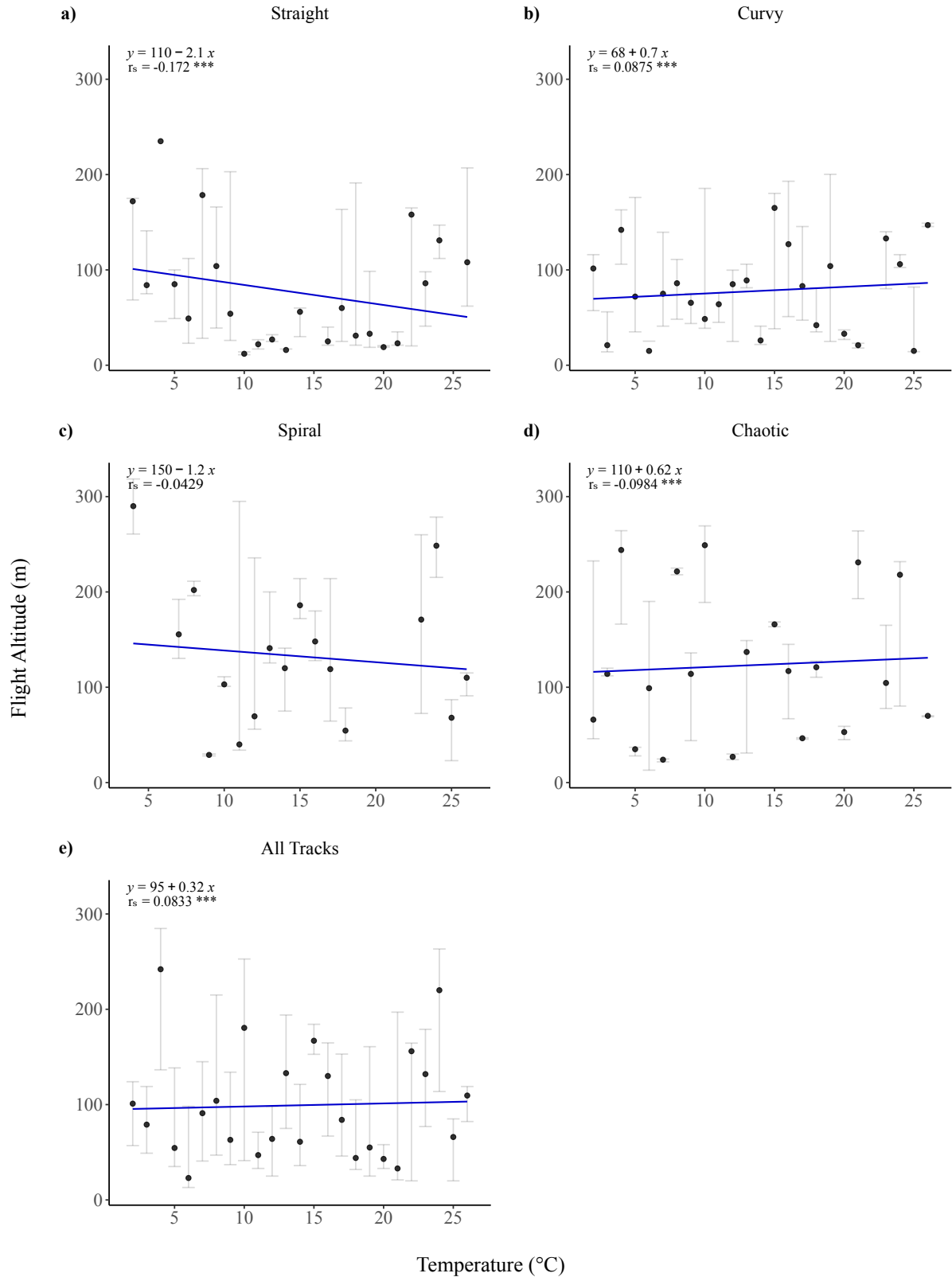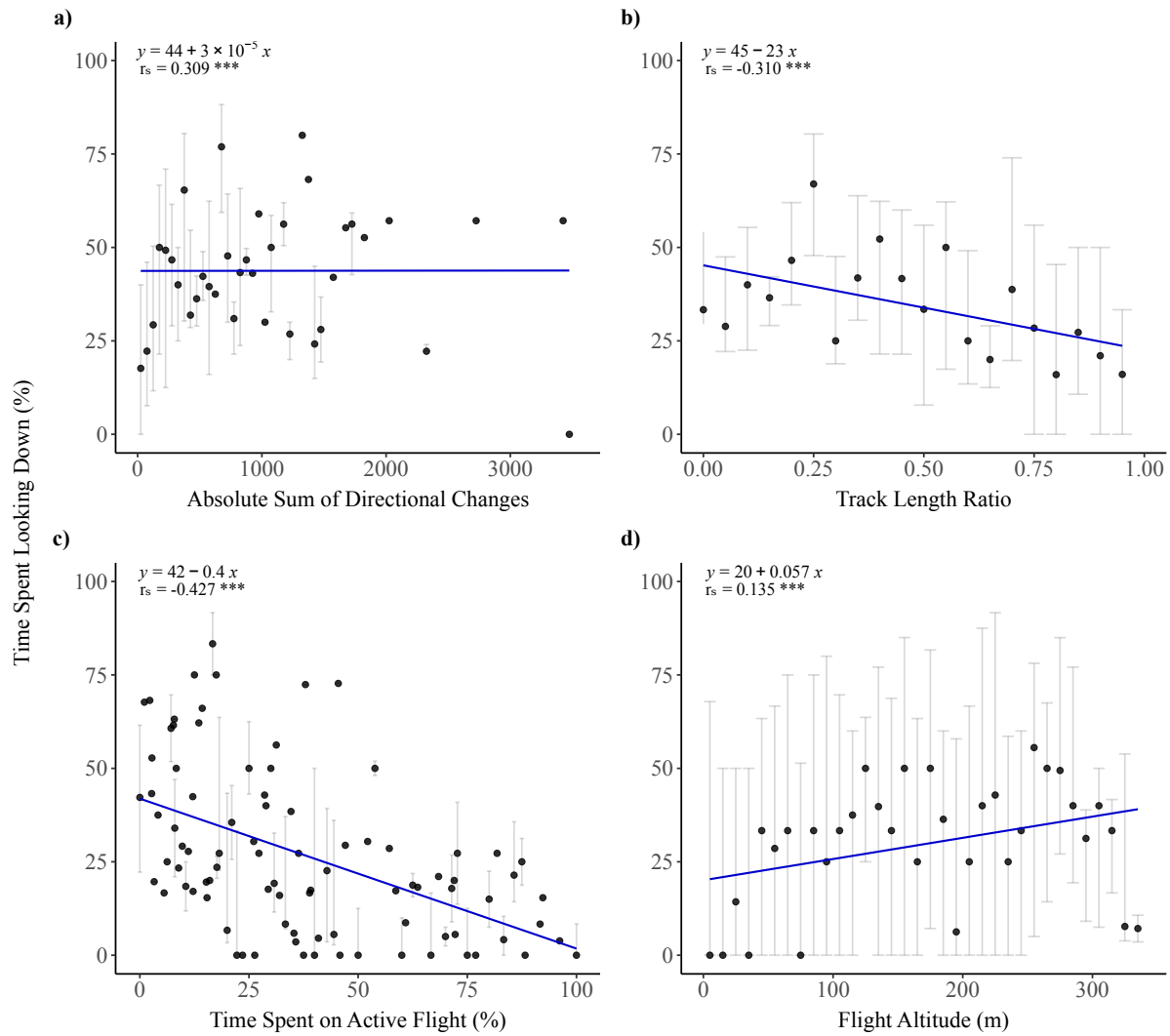
Figure G.3.2. Linear regression of flight altitude above ground level in relation to temperature, **(a–d)** grouped by track type and for **(e)** all track types collectively. For each regression, the median flight altitude was used for each °C. The regression equation and correlation coefficient (r_s) is given for each plot. The horizontal bars represent the variance around each median (IQR).

Appendix G.4. Flight behavior in relation to vigilance

Figure G.4.1. Linear regression of flight vigilance quantified by % time each individual spent looking down in relation to **(a)** track symmetry (sum of directional changes), **(b)** track tortuosity (track length ratio), **(c)** proportion of time spent on active flight, and **(d)** flight altitude. For each regression, the median proportion of time spent looking down was used for each corresponding variable (every 50 sum of directional changes; each 0.05 ratio value; each % for active flight; and every 10 m). The regression equation and correlation coefficient (r_s) is given for each plot. The horizontal bars represent the variance around each median (IQR).
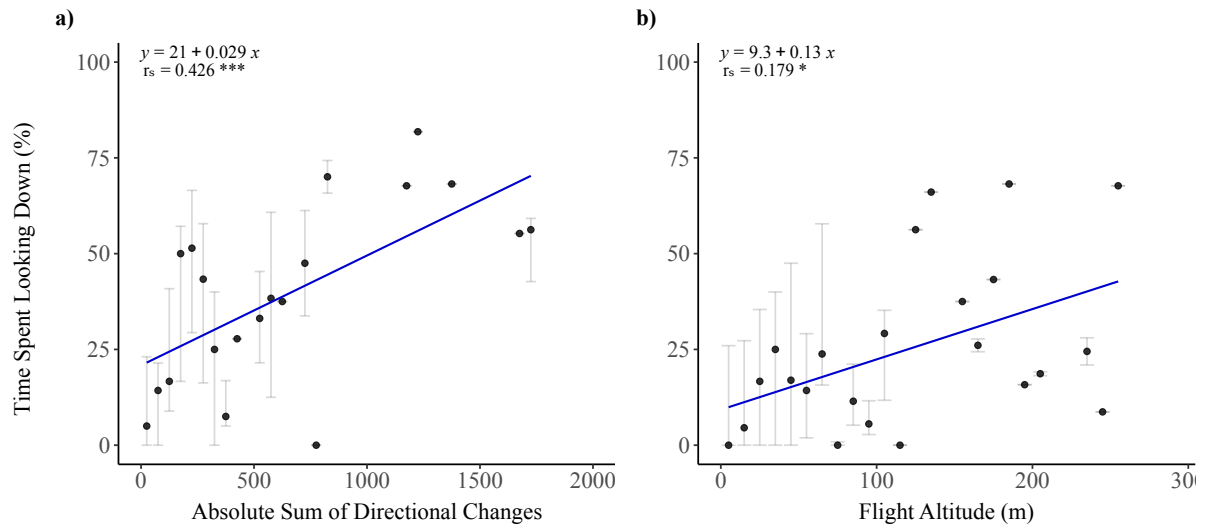
Appendix G.5. Flight Behavior of Birds in Active Flight

a)
$y = 21 + 0.029\,x$
$r_s = 0.426$ ***

b)
$y = 9.3 + 0.13\,x$
$r_s = 0.179$ *

Figure G.5.1. Linear regression, for individuals in active flight, of the proportion of time each individual spent looking down in relation to **(a)** the sum of directional changes, and **(b)** flight altitude above ground level. For each regression, the median proportion of time spent looking down was used for each corresponding variable (every 200 sum of directional changes; and every 10 m for flight altitude). The regression equation and correlation coefficient (r_s) is given for each plot. The horizontal bars represent the variance around each median (IQR).

Appendix G.6. Vigilance
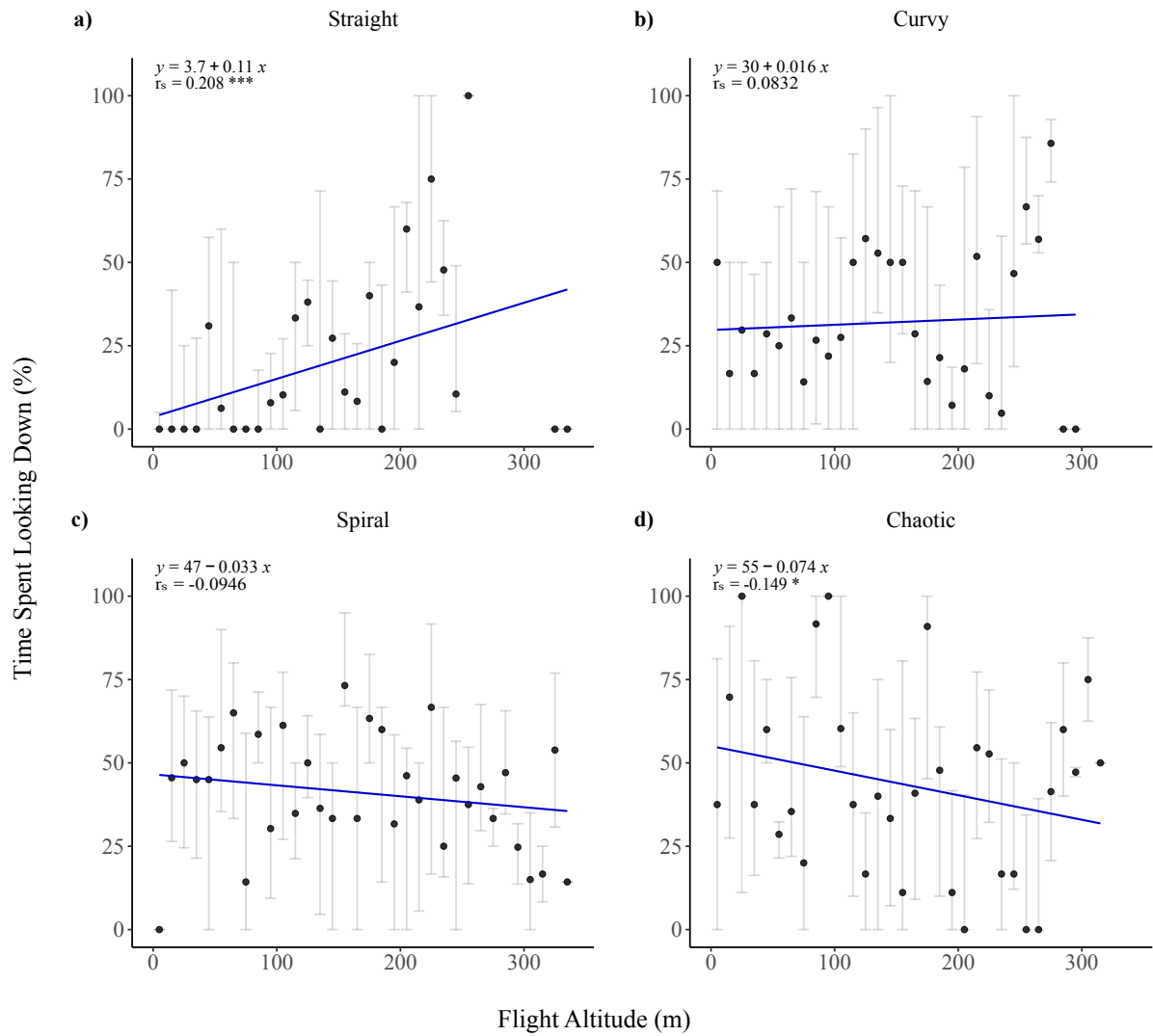
Figure G.6.1. Linear regression of the proportion of time each individual spent looking down in relation to flight altitude above ground level, grouped by track type. For each regression, the median proportion of time spent looking down was used for every 10 m. The regression equation and correlation coefficient (r_s) is given for each plot. The horizontal bars represent the variance around each median (IQR).

Appendix G.7. Avoidance Behavior

Figure G.7.1. Linear regression of distance to the nearest turbine in relation to flight altitude above ground level, **(a–d)** grouped by track type and for **(e)** all track types collectively. For each regression, the median flight altitude was used for every 20 m. The regression equation and correlation coefficient (r_s) is given for each plot. The horizontal bars represent the variance around each median (IQR).
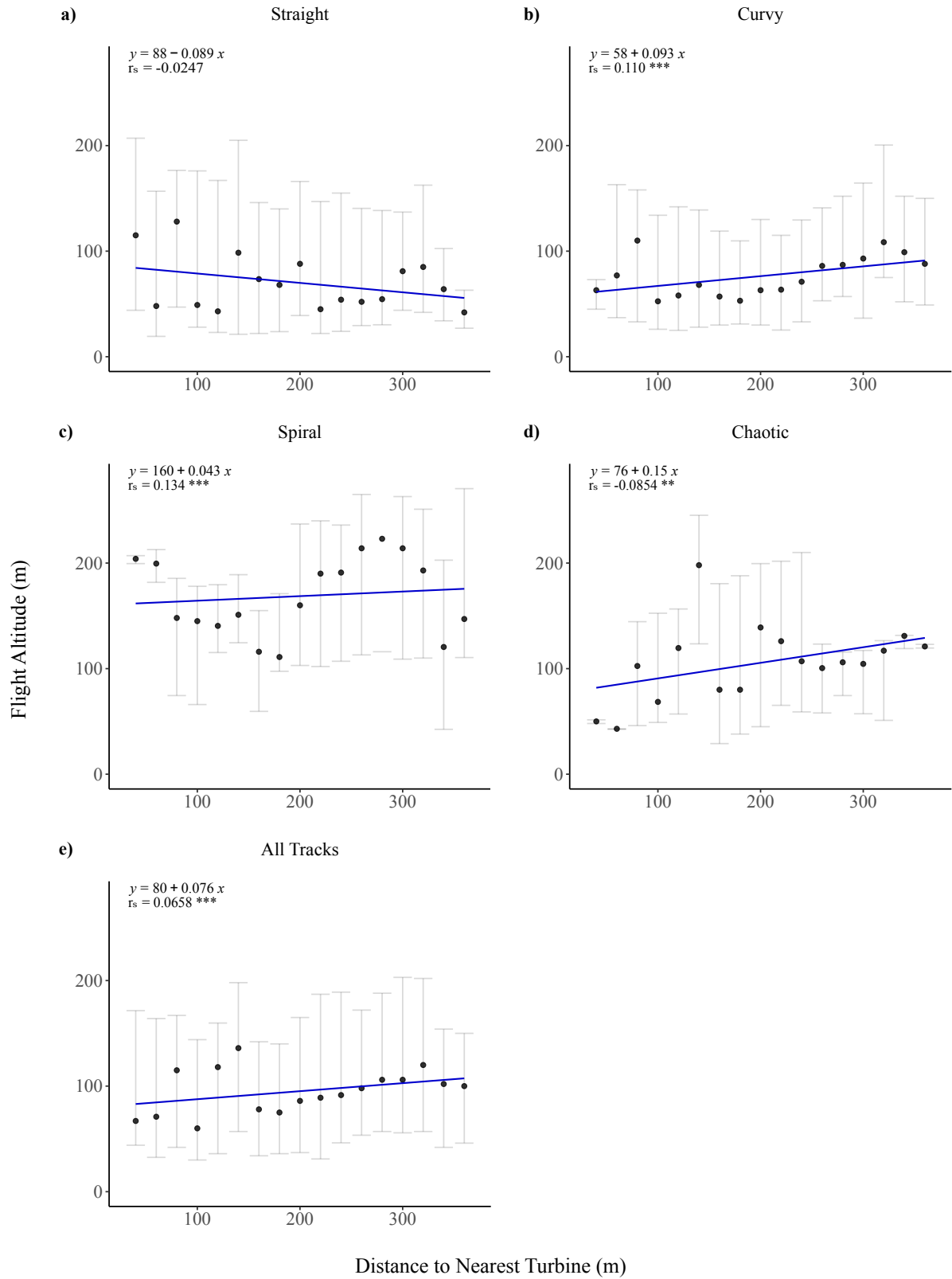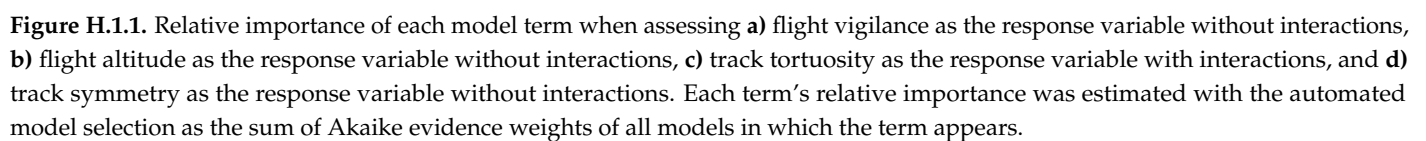
Appendix H. Model selection

The automated model selection was carried out for models both with and without interactions for flight vigilance, flight altitude, track tortuosity, and track symmetry. For each response variable the models with and without interactions were compared based on their respective AIC values. Moreover, an Anova test using the χ^2 test statistic was also used to assess the goodness of fit of the nested regression models, i.e. the models with and without interactions [36]. The model with interactions was selected as the best model if the addition of interaction terms significantly increased the model's goodness of fit, if not the simpler of the two models, i.e. the model without interactions, was selected. The models that were not selected as the best models are presented below.

Table H.1. Details of the automated model selection completed with *glmulti*. The * annotation indicates that the addition of interaction terms significantly improved the model's goodness of fit.

Name	No. of covariates	No. of generations	Best AIC
Flight vigilance*			
Without interactions	8	250	48.1
With interactions	8	490	36.3
Flight altitude*			
Without interactions	8	250	4000
With interactions	8	380	3982
Track tortuosity			
Without interactions	7	250	78.4
With interactions	7	500	70.7
Track symmetry*			
Without interactions	7	250	5419
With interactions	7	520	5400

Appendix H.1. Importance of model terms

Figure H.1.1. Relative importance of each model term when assessing **a)** flight vigilance as the response variable without interactions, **b)** flight altitude as the response variable without interactions, **c)** track tortuosity as the response variable with interactions, and **d)** track symmetry as the response variable without interactions. Each term's relative importance was estimated with the automated model selection as the sum of Akaike evidence weights of all models in which the term appears.

References

1. Drewitt, A.L.; Langston, R.H.W. Assessing the Impacts of Wind Farms on Birds. *Ibis* **2006**, *148*, 29–42. doi:10.1111/j.1474-919X.2006.00516.x.
2. Madders, M.; Whitfield, D.P. Upland Raptors and the Assessment of Wind Farm Impacts. *Ibis* **2006**, *148*, 43–56. doi:10.1111/j.1474-919X.2006.00506.x.
3. de Lucas, M.; Janss, G.F.E.; Whitfield, D.P.; Ferrer, M. Collision Fatality of Raptors in Wind Farms does not Depend on Raptor Abundance. *Journal of Applied Ecology* **2008**, *45*, 1695–1703. doi:10.1111/j.1365-2664.2008.01549.x.
4. Smallwood, K.S.; Thelander, C. Bird Mortality in the Altamont Pass Wind Resource Area, California. *The Journal of Wildlife Management* **2008**, *72*, 215–223. doi:10.2193/2007-032.
5. Bevanger, K.; Berntsen, F.; Clausen, S.; Dahl, E.L.; Flagstad, Ø.; Follestad, A.; Halley, D.; Hanssen, F.; Johnsen, L.; Kvaløy, P.; et al. *Pre- and Post-construction Studies of Conflicts Between Birds and Wind Turbines in Coastal Norway (Bird-Wind). Report on Findings 2007-2010*, 2010.
6. Katzner, T.E.; Brandes, D.; Miller, T.; Lanzone, M.; Maisonneuve, C.; Tremblay, J.A.; Mulvihill, R.; Jr, G.T.M. Topography Drives Migratory Flight Altitude of Golden Eagles: Implications for On-Shore Wind Energy Development. *Journal of Applied Ecology* **2012**, *49*, 1178–1186. doi:10.1111/j.1365-2664.2012.02185.x.
7. Loss, S.R.; Will, T.; Marra, P.P. Estimates of Bird Collision Mortality at Wind Facilities in the Contiguous United States. *Biological Conservation* **2013**, *168*, 201–209. doi:10.1016/j.biocon.2013.10.007.

8. Marques, A.T.; Batalha, H.; Rodrigues, S.; Costa, H.; Pereira, M.J.R.; Fonseca, C.; Mascarenhas, M.; Bernardino, J. Understanding Bird Collisions at Wind Farms: An Updated Review on the Causes and Possible Mitigation Strategies. *Biological Conservation* **2014**, *179*, 40–52. doi:10.1016/j.biocon.2014.08.017.

9. Watson, R.T.; Kolar, P.S.; Ferrer, M.; Nygård, T.; Johnston, N.; Hunt, W.G.; Smit-Robinson, H.A.; Farmer, C.J.; Huso, M.; Katzner, T.E. Raptor Interactions with Wind Energy: Case Studies from Around the World. *The Journal of Raptor Research* **2018**, *52*, 1–18.

10. Perold, V.; Ralston-Paton, S.; Ryan, P. On a Collision Course? The Large Diversity of Birds Killed by Wind Turbines in South Africa. *Journal of African Ornithology* **2020**, *91*, 228–239. doi:10.2989/00306525.2020.1770889.

11. Powlesland, R.G. Impacts of Wind Farms on Birds: A Review. *Science for Conservation* **2009**, *289*.

12. Directorate-General for Environment (European Commision). *Guidance Document: Wind Energy Development and Natura 2000*, 2010.

13. May, R.; Hoel, P.L.; Langston, R.; Dahl, E.L.; Bevanger, K.; Reitan, O.; Nygård, T.; Pedersen, H.C.; Røskaft, E.; Stokke, B.G. Collision Risk in White-tailed Eagles. Modelling Collision Risk using Vantage Point Observations in Smøla Wind-power Plant. *Norwegian Institute for Nature Research* **2010**, *Report 639*.

14. Garvin, J.C.; Jennelle, C.S.; Drake, D.; Grodsky, S.M. Response of Raptors to a Wind farm. *Journal of Applied Ecology* **2011**, *48*, 199–209. doi:365-2664.2010.01912.X.

15. Barrios, L.; Rodríguez, A. Behavioural and Environmental Correlates of Soaring-bird Mortality at On-shore Wind Turbines. *Journal of Applied Ecology* **2004**, *41*, 72–81. doi:10.1111/j.1365-2664.2004.00876.x.

16. Johnston, N.N.; Bradley, J.E.; Otter, K.A. Increased Flight Altitudes Among Migrating Golden Eagles Suggest Turbine Avoidance at a Rocky Mountain Wind Installation. *PloS one* **2014**, *9*, e93030. doi:10.1371/journal.pone.0093030.

17. Murgatroyd, M.; Photopoulou, T.; Underhill, L.G.; Bouten, W.; Amar, A. Where Eagles Soar: Fine-Resolution Tracking Reveals the Spatiotemporal Use of Differential Soaring Modes in a Large Raptor. *Ecology and Evolution* **2018**, *8*, 6788–6799. doi:10.1002/ece3.4189.

18. Marques, A.T.; Santos, C.D.; Hanssen, F.; Muñoz, A.; Onrubia, A.; Wikelski, M.; Moreira, F.; Palmeirim, J.M.; Silva, J.P. Wind Turbines Cause Functional Habitat Loss for Migratory Soaring Birds. *Journal of Animal Ecology* **2019**, *89*, 93–103. doi:10.1111/1365-2656.12961.

19. Dahl, E.L.; May, R.; Hoel, P.L.; Bevanger, K.; Pedersen, H.C.; Røskaft, E.; Stokke, B.G. White-Tailed Eagles (*Haliaeetus albicilla*) at the Smøla Wind-Power plant, Central Norway, Lack Behavioral Flight Responses to Wind Turbines. *Wildlife Society Bulletin* **2013**, *37*, 66–74. doi:10.1002/wsb.258.

20. Cook, A.S.C.P.; Humphreys, E.M.; Masden, E.A.; Burton, N.H.K. The Avoidance Rates of Collision Between Birds and Offshore Turbines - BTO Research Report No. 656. *Scottish Marine and Freshwater Science* **2014**, *5*.

21. Rydell, J.; Ottvall, R.; Pettersson, S.; Green, M. *Report 6791 The Effects of Wind Power on Birds and Bats*, 2017.

22. Whitfield, D.P.; Madders, M. *Deriving Collision Avoidance Rates for Red Kites Milvus milvus*; Natural Research Information Note 3, Natural Research Ltd: Banchory, UK, 2006.

23. Cabrera-Cruz, S.A.; Villegas-Patraca, R. Response of Migrating Raptors to an Increasing Number of Wind Farms. *Journal of Applied Ecology* **2016**, *53*, 1667–1675. doi:10.1111/1365-2664.12673.

24. Mojica, E.K.; Watts, B.D.; Turrin, C.L. Utilization Probability Map for Migrating Bald Eagles in Northeastern North America: A Tool for Siting Wind Energy Facilities and Other Flight Hazards. *PloS one* **2016**, *11*, e0157807. doi:10.1371/journal.pone.0157807.

25. Smallwood, K.S.; Bell, D.A. Effects of Wind Turbine Curtailment on Bird and Bat Fatalities. *The Journal of Wildlife Management* **2020**, *84*, 685–696. doi:10.1002/jwmg.21844.

26. McClure, C.J.W.; Martinson, L.; Allison, T.D. Automated Monitoring for Birds in Flight: Proof of Concept with Eagles at a Wind Power Facility. *Biological Conservation* **2018**, *224*, 26–33. doi:10.1016/j.biocon.2018.04.041.

27. Esri.; HERE.; Garmin.; FAO.; NOAA.; USGS. *World Topographic Map*, 2020. http://www.esri.com/.

28. Wirdheim, A.; Corell, M. *Fågelrapport*, 2015.

29. Aldén, L.; Ottvall, R.; Soares, J.P.D.S.; Klein, J.; Liljenfeldt, J. *Rapport: Samexistens Örnar och Vindkraft på Gotland*, 2017.

30. Jensen, B.B. *Efterårets Rovfugletræk*. Fuglehåndbogen på Nettet, 2015.

31. Esri. *ArcGIS Pro 2.5.0*, 2020. http://www.esri.com/.

32. SMHI, S.M.; Institute, H. *SMHI, Swedish Meteorological and Hydrological Institute*. Norrköping, 2020. www.smhi.se.

33. R Core Team. *R: A Language and Environment for Statistical Computing*. R Foundation for Statistical Computing, Vienna, Austria, 2020.

34. Whitlock, M.C.; Schluter, D. *The Analysis of Biological Data*, 2 ed.; W. H. Freeman and Company: New York, NY, 2015.

35. Calcagno, V.; de Mazancourt, C. glmulti: An R Package for Easy Automated Model Selection with (Generalized) Linear Models. *Journal of Statistical Software* **2010**, *34*.

36. Zuur, A.F.; Ieno, E.N.; Walker, N.J.; Saveliev, A.A.; Smith, G.M. *Mixed Effects Models and Extensions in Ecology with R*; Statistics for Biology and Health, Springer New York: New York, NY, 1009.

37. Walker, A.; Mcgrady, M.; Mccluskie, A.; Madders, M.; Mcleod, D.R.A. Resident Golden Eagle Ranging Behaviour Before and After Construction of a Windfarm in Argyll. *Scottish Birds* **2005**, *25*, 24–40.

38. Miller, T.; Lockhart, M.; Braham, M.; Smith, B.; Katzner, T. *Flight Behavior of Golden Eagles in Wyoming: Implications for Wind Power*. American Wind Wildlife Institute: Wind Wildlife Research Meeting, 2020.

39. Bergen, S.; Huso, M.; Braham, M.; Duerr, A.; Katzner, T.; Miller, T.; Schmuecker, S. *Improved Behavioral Classification of Flight Behavior Informs Risk Modeling of Bald Eagles at Wind Facilities in Iowa*. American Wind Wildlife Institute: Wind Wildlife Research Meeting, 2020.

40. Kuehn, M.; Merrill, L.; Bloom, P.; Riley, E. *Temporal, Topographic, and Meteorological Correlates of Golden Eagle Flight Behavior in California's Tehachapi Wind Resource Area*. American Wind Wildlife Institute: Wind Wildlife Research Meeting, 2020.

41. Lanzone, M.J.; Miller, T.A.; Turk, P.; Brandes, D.; Halverson, C.; Maisonneuve, C.; Tremblay, J.; Cooper, J.; O'Malley, K.; Brooks, R.P.; et al. Flight Responses by a Migratory Soaring Raptor to Changing Meteorological Conditions. *Animal Behaviour* **2012**, *8*, 710–713. doi:10.1098/rsbl.2012.0359.

42. Wiggelinkhuizen, E.; den Boon, J. Monitoring of Bird Collisions in Wind Farm Under Offshore-like Conditions Using WT-BIRD System. *Energy Research Centre of the Netherlands* **2010**.

Modeling Species-Specific Collision Risk of Birds with Wind Turbines: A Behavioral Approach

Anne Cathrine Linder [1]*

1   Department of Chemistry and Bioscience — Section of Biology and Environmental Science, Aalborg University, Fredrik Bajers Vej 7, 9220 Aalborg, Denmark

Abstract: The increasing number of wind energy sites developed globally, has consequently resulted in a green on green predicament, due to an increase in avian mortality caused by collisions with wind turbines. The proportion of collision related fatalities is not evenly distributed across species, indicating that some species groups are more prone to turbine collision. Such differences between species have been proposed to be affiliated with species-specific foraging and flight behavior. The aim of this study is to investigate how the flight behavioral traits; head position, active flight, track symmetry, and track tortuosity can be used to model collision risk along with other influencing factors i.e. weather variables (temperature, wind speed and cloud coverage) and temporal variables (time of day and time of year). The study also sought to investigate the species-specificity of the four traits in relation to the phylogenetic relatedness of the study species. This was achieved through a case study at a wind farm on the Swedish island Gotland in which the behavior of birds from 11 different genera was studied. The flight behavior of these species was assessed using data collected by the IdentiFlight system, e.g. flight trajectories and images of the birds throughout their flight track. The results confirm the species-specificity of the four flight behaviors and indicated that all four traits can be used to predict collision risk along with species as a categorical factor. The framework provided in this study along with results of the case study can be used to identify risk prone species based on phylogenetic relatedness and flight behavior.

Keywords: Collision risk, IdentiFlight, wind turbine curtailment, phylogenetic signal, flight behavior

1. Introduction

The growing demand for green energy has resulted in the rapid development of wind energy production, yielding an increasing number of wind turbines globally. This has in turn led to a green on green predicament, due to the adverse effects of turbines on many avian species [1–9]. These adverse effects of wind turbines on birds result primarily from direct fatalities due to collisions and secondarily through habitat alteration and loss [9]. The precise number of avian collisions with wind turbines is uncertain, but even relatively few fatalities can have detrimental effects on slow maturing species with low reproduction rates, particularly for species of conservation concern when considering regional and national populations [1,7]. Collision related mortality is unevenly spread among species, with a few species often accounting for a large proportion of collision victims [10]. Large soaring raptors are known to be specifically vulnerable for collision with turbines [2,3,9,11]. Other species groups prone to collision fatalities at wind farms include herons, geese, and gulls [10,11].

Differences between species in regard to their susceptibility to turbine collisions are suggested to be associated with species-specific foraging behavior, flight behavior, and morphology [1,3,12]. In some species, e.g. raptors and cranes, particularly vulnerable to collisions, their visual field is such that even a small (25°–35°) forward pitch head movement will leave them blind directly ahead [13]. Thus, the foraging behavior of many raptors may explain why these species are more prone to turbine collisions. Many raptor species forage from the air, by bending their heads and looking downwards to search for prey or carrion on the ground [14]. Raptors that hunt terrestrial prey have a large blind spot above their head, which functions to avoid sun dazzling, thus, allowing for better prey detection. However, this blind spot also renders these raptors blind in their travel direction whilst foraging [13,14].

Morphological differences between species have also been proposed to attribute to species-specific differences in collision fatalities, where birds with high wing loading, i.e. the ratio between a bird's total mass and wing area, and relatively large bodies, e.g. cranes (*Grus* spp.), are suggested to be to be more vulnerable to turbine collision due to reduced maneuverability and rapid flight speeds [15–17]. Morphological differences between species may also impact how different species are affected by various weather conditions. It has been suggested that herons (*Ardea* spp.) and other species with a slow and ponderous flight can more easily be buffeted off course during strong head winds, thus, making them vulnerable to turbine collision when flying between roosts and foraging sites [18]. Furthermore, many large raptors utilize thermal soaring, i.e. slow circle–soaring flight on thermals. This flight strategy is highly dependent on weather conditions, e.g. temperature and cloud coverage and under less favorable conditions for gaining altitude thermal soaring

may impact turbine collision risk [12,19–21]. Turbine collision risk has also been found to differ throughout the day and throughout the year [20,22].

Species-specific differences in flight behavior and collision risk may also be correlated with phylogenetic relatedness of species. This correlation can be quantified by the phylogenetic signal of each trait. Phylogenetic signal can be defined as the tendency for closely related species to resemble one another more than species drawn at random from the phylogenetic tree [23]. A phylogenetic signal will occur if traits evolve in a Brownian motion-like manner, i.e. relatively small changes occur randomly in any given direction over time independent of the former state of the trait. This pattern evolution can arise from genetic drift or natural selection [24,25]. Hence, the phenotypic difference can be expected to be smaller between species who shared a common ancestor more recently [24,26]. For a trait that changes gradually over time, the covariance between species' trait values is expected to be proportional to the shared evolutionary history between species, i.e. the sum of the species' shared branch length in a phylogenetic tree. Furthermore, the variance of a trait value for a given species is expected to be proportional to the total length of the tree for that species, i.e. the summed branch length from the root to the tip [25].

Herrera-Alsina *et al.* [27] used a similar phylogenetic approach to study species-specific collision risk in relation to the species' morphological differences and phylogenetic relationship, finding a correlation between wing loading and likelihood of flight in the risk zone. However, it is more difficult to assess species-specific differences in flight behavior associated with collision risk, as flight behavior can be difficult to observe and quantify, particularly in relation to flight in close proximity to wind turbines (within a 100 meter radius from the nearest turbine's rotor tip), i.e. in collision risk zones [28]. The relationship between species-specific behavioral traits and turbine collision risk is, therefore, often based on assumptions. However, the development of automated camera-based monitoring systems, e.g. IdentiFlight, have effectuated the collection of large amounts of behavioral data within wind farms [29,30]. The IdentiFlight system was developed to mitigate the impact of wind turbines on species of conservation concern, by detecting birds in flight and curtailing turbines if a protected species is at collision risk [29,30]. The utilization of bird images and flight trajectories collected by the IdentiFlight system, to assess flight behavior, has recently been demonstrated and the quantitative flight behavioral traits head position, active flight, track tortuosity and track symmetry described by Linder *et al.* [28] can possibly be used to model collision risk.

The aim of this study was, therefore, to investigate how the flight behavioral traits; head position, active flight, track tortuosity, and track symmetry can be used to model collision risk along with other influencing factors, i.e. the weather variables; temperature, wind speed and cloud coverage, and the temporal variables; time of day, and time of year. This was achieved through a case study investigating the behavior of birds from 11 different genera (*Anser, Ardea, Aquila, Buteo, Corcus, Grus, Haliaeetus, Milvus, Larus, Pandion,* and *Phalacrocorax*) at a wind farm located on the Swedish island Gotland. The flight behavior of these species was assessed using data collected by the IdentiFlight system, e.g. flight trajectories and images of the birds throughout their track. It was expected that collision risk could be predicted by species, flight behavior, weather variables, and temporal variables. More specifically, collision risk was expected to increase with time spent looking down and an increase in tortuosity. Moreover, an increased utilization of active flight was expected to decrease collision risk. This study will also investigate whether the four flight behavioral traits and thereby collision risk are species-specific and if such species-specificity is due to random effects (lack of evolutionary signal) or shared evolutionary history (significant evolutionary signal). This was achieved by assessing the phylogenetic signal, i.e. the tendency of related species to resemble each other more than species randomly drawn from the same phylogenetic tree, for the four behavioral traits (head position, active flight, track symmetry and track tortuosity). It was expected The behavioral trait head position was expected to be species-specific in relation to the species' foraging ecology and active flight was expected to be species-specific in relation to the species' morphological differences. Track symmetry and tortuosity were expected to be species specific as a result of both foraging ecology and morphology. These expected species-specific differences in behavioral traits were expected to be correlated with phylogenetic relatedness.

2. Materials and Methods

2.1. Study Site

The study site is located on Näsudden, a peninsula on Gotland's southwest coast where the terrain is generally flat [31]. The entire wind farm consists of 55 turbines, with differing heights from 45–145 meters [28]. The observational area of the study site was defined by a 400 meter radius around the IdentiFlight camera tower, including nine wind turbines (Appendix A).

2.2. Study species

Gotland is home to a large number of bird species and is also visited by various migrating species. Some of the species living on Gotland include breeding populations of approximately 55 golden eagle (*Aquila chrysaetos*) pairs, 45 white-tailed eagle (*Haliaeetus albicilla*) pairs and 15 red kite (*Milvus milvus*) pairs [32,33]. Other avian species on Gotland include grey heron (*Ardea cinerea*), western osprey (*Pandion haliaetus*), black kite (*Milvus migrans*), common crane (*Grus grus*), great cormorant (*Phalacrocorax carbo*), common buzzard (*Buteo buteo*), as well as several goose (*Anser*), gull (*Larus*) and crow (*Corvus*) species. The only goose species included in this investigation is graylag goose (*Anser anser*) as there was not enough observations of other goose species. Furthermore, the genera crow and gull each consist of multiple species, as the image quality made it difficult to distinguish between the different species within each genus. The study species represent eight different families. The general term raptors is in this study used in reference to the order Accipitriformes, which includes the following species: golden eagle, white-tailed eagle, western osprey, red kite, black kite, and common buzzard.

2.3. Data Collection

Observations of the selected study species were collected by the IdentiFlight camera system [30] over a 13 month period from the middle of February, 2020 to the end of March, 2021. The camera system is developed to initiate turbine curtailment when individuals of the species; golden eagle, white-tailed eagle, or red kite, are within a predefined distance of one of the nine turbines covered by the system (Appendix B). However, at the time of the study, the system was still being trained. This resulted in a large number of false positives, i.e. other bird species wrongfully classified as golden eagle, white-tailed eagle, or red kite, which effectuated the collection of data for multiple other bird species. During the study period the IdentiFlight system was only collecting simulated curtailment data for the nine turbines, hence, the system was not actively curtailing turbines. Throughout this period of time, the system was periodically out of operation and the study is therefore based on a total of 375 days over the course of these months with bird sightings within the observational zone on only 296 of these days (Appendix C).
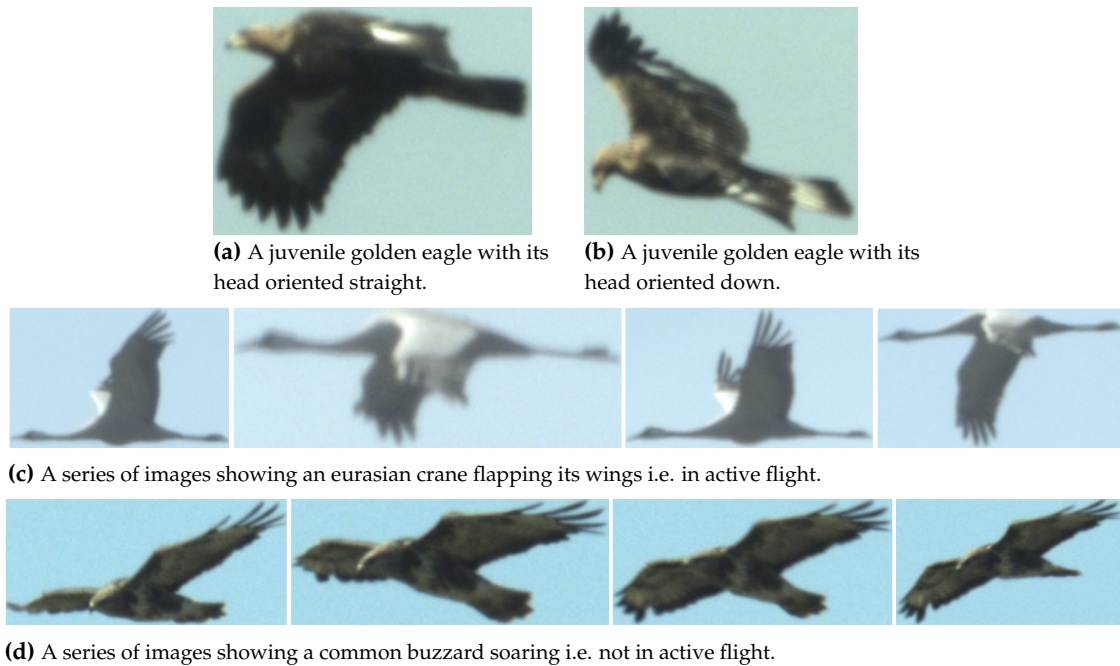
2.3.1. IdentiFlight System

The IdentiFlight system consists of eight wide field of view cameras fixed in a ring, and a single high resolution stereo camera mounted on top of a six meter tower (Appendix B). The eight wide field of view cameras use image sensor arrays to detect moving objects in the environment and begin to track them [28]. These cameras collect ten images per second. Upon detecting a moving object the movable high resolution stereo camera is directed at the object. This camera collects approximately one image per second and uses high magnification stereoscopic sensors to determine the distance to the object and gather the necessary information to classify the object. IdentiFlight's computer vision algorithms use a catalog of rules to analyze the images obtained by the high resolution stereo camera [28]. The IdentiFlight system collects a large variety of variables along with an image of the bird for each observation. A unique track ID is assigned to each track and annotated for each observations throughout the track. For each observation the time, date, and bird's geographical position are collected [28]. Furthermore, flight trajectories for each track are saved as Keyhole Markup Language (KML: a file format used to display geographic data) files, that can be imported into ArcGIS Pro for further analysis [34].

2.3.2. Weather Data

Temperature, wind speed, and cloud coverage were measured in hourly intervals by the Swedish Meteorological and Hydrological Institute at a weather station near the study site approximately 34 meters above sea level [35].

2.4. Data Preparation

The species of each track was determined manually, by the two authors, based on the bird images. The bird images were also used to classify the head position of each bird, i.e. oriented straight forward or down towards the ground, and whether the bird was utilizing active flight, i.e. flapping its wings, throughout its track (Figure 1). Classifications of head position and active flight were completed for each observation within 400 meters of the camera tower, as it was difficult to classify the head orientation of the bird for images taken at further distances. This resulted in a data set of 887 different tracks of the various species based on 30007 observations (Appendix D).

(a) A juvenile golden eagle with its head oriented straight.

(b) A juvenile golden eagle with its head oriented down.

(c) A series of images showing an eurasian crane flapping its wings i.e. in active flight.

**(d)** A series of images showing a common buzzard soaring i.e. not in active flight.

Figure 1. Examples of how the birds behavior was scored based on images. Head position was classified from a single image while active flight had to be classified from a series of images in order to evaluate the birds wing movement between images.

The flight trajectories (KML files) were analyzed using ArcGIS Pro [34]. For each flight trajectory the track symmetry, i.e. the summed angles of directional changes, and tortuosity, i.e. the ratio between the direct track length and the actual track length, were calculated using the ArcPy package in Esri [34] (Appendix E). The track angles distinguished between left and right turns, thus, ranging from $-180°$ to $180°$.

2.5. Data Analysis

Collision risk was quantified as the proportion of time an individual spent in the defined risk zone (Figure 2). The collision risk zone was defined as a sphere where the radius was the length of the rotor blade plus 100 meters around each wind turbine meaning the collision risk zone depended on turbine size.
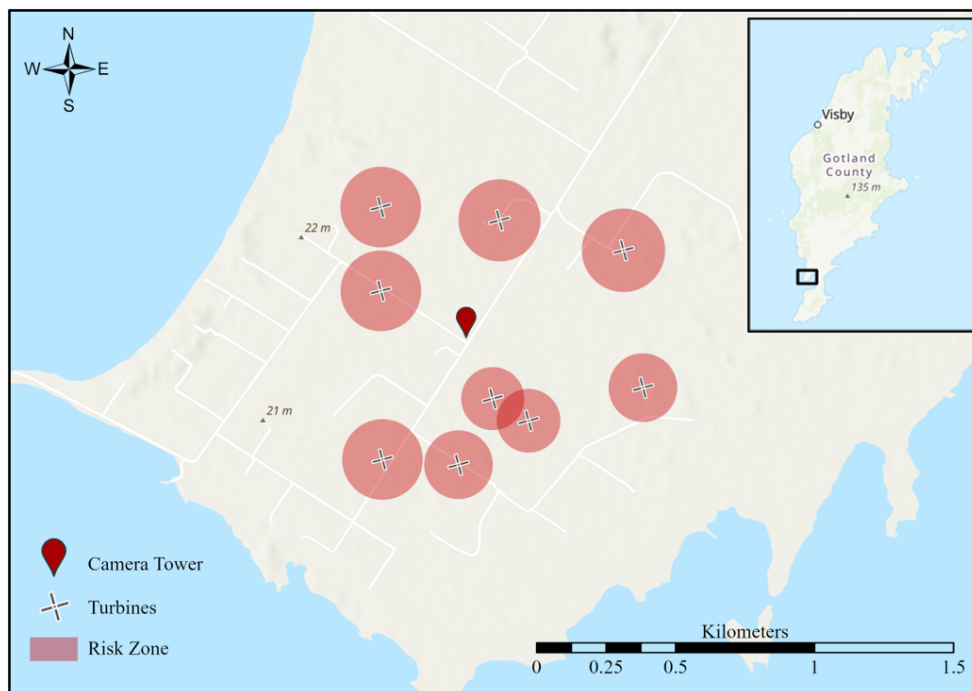
Figure 2. Risk zone around the turbines (Appendix F).

Both univariate and multivariate analyses were conducted to describe the relationship between the possible explanatory variables and collision risk as the response variable (Table 1). Furthermore, phylogenetic signals were calculated to determine if closely related species exhibited similar flight traits regarding flight symmetry and flight tortuosity as well as head position during flight and proportion of time spent on active flight. All statistical analyses were conducted in R version 4.0.3 [36].

Table 1: Variables used in the data analysis.

Variable	Description	Type
Risk proportion	Proportion of time spent in collision risk zone	Response variable
Species	Bird species	Categorical covariate
Head position	Proportion of observations looking down	Continuous covariate
Active flight	Proportion of observations spent on active flight	Continuous covariate
Track symmetry	Absolute sum of track angles	Continuous covariate
Track tortuosity	Track length ratio (proportion between 0 and 1)	Continuous covariate
Cloud coverage	Cloud cover as a percentage	Continuous covariate
Temperature	Temperature in °C	Continuous covariate
Wind speed	Wind speed in m/s	Continuous covariate
Time of year	Month (mo) from February to August	Continuous covariate
Time of day	Time (h)	Continuous covariate

2.5.1. Univariate predictions of collision risk

General species-specific differences in flight behavior and collision risk, were investigated by summarizing species grouped data. Graphs were created for the covariates; head position, active flight, track symmetry, and track tortuosity and also for the response variable to depict the median and interquartile range (25%–75%) for each species. The relationship between the response variable and each covariate was assessed individually in a simple regression analysis and quantified by the coefficient of determination (R^2). This analysis was conducted with all species pooled, raptor species pooled, and each species individually. Furthermore, subsets termed risk tracks were created including only tracks with a proportion of time spent in the risk zone greater than zero, due to the large number of zeros in the data set. The individual relationships between the response variable and covariates were then assessed for all tracks in the risk zone (all risk tracks), raptors in the risk zone (raptor risk tracks), and each species' tracks in the risk zone, individually (species risk tracks).

2.5.2. Modeling collision risk

A preliminary data exploration was used to select the explanatory variables for the multivariate analysis [37]. To assess collinearity Spearman's correlation coefficient (r) was calculated among the covariates and pairwise scatter-plots were created to detect obvious correlations among the covariates (Appendix G.2). Furthermore, a variance inflation factor (VIF) analysis was performed to identify collinearity (Appendix G.1). In this analysis VIF values higher than 2 meant that the predictor with the highest VIF was sequentially dropped and VIF values were recalculated [37]. This analysis resulted in the variables temperature and flight symmetry being excluded from the multivariate analysis due to collinearity. Thus, the possible explanatory variables used in the model selection were head position, active flight, flight symmetry, species, wind speed, cloud coverage, time of year, and time of day. Automated multivariate model selection, using the R package *glmulti* [38] was used to assess the importance of each covariate. In the automated model selection all possible models were fitted and the best model was selected according to prediction error using the Akaike information criterion (AIC) [37]. The automated model selection was carried out for models both with and without interactions for all tracks, raptor tracks, all risk tracks, and raptor risk tracks. For each subset the models with and without interactions were compared based on their respective AIC values. Moreover, an Anova test using the χ^2 test statistic was also used to assess the goodness of fit of the nested regression models, i.e. the models with and without interactions [39]. The model with interactions was selected as the best model if the addition of interaction terms significantly increased the model's goodness of fit, if not the simpler of the two models, i.e. the model without interactions, was selected. Furthermore, the estimated importance of model terms was estimated using the sum of Akaike evidence weights of all models in which the term appears. The relative importance of model terms, ranging between 0 and 1, can be used to identify covariates that significantly contribute to explaining the variation of the response variable, using a threshold of 0.8. This threshold is based on type I and II statistical risks, i.e. the probability of retaining a non-important term (type I error) and the probability of disregarding an important term (type II error) [38].

2.5.3. Phylogenetic signal

Evolutionary analyses were conducted in MEGA X (Molecular Evolutionary Genetics Analysis across computing platforms) [40]. The phylogenetic tree were created using the Maximum Likelihood method and the Tamura-Nei model [41]. The reliability of the tree was tested by bootstrapping the tree ten thousand times. Branches with bootstrap values above 70% are expected to define a true clade within the tree whereas branches with values under 30% are expected to show an incorrect clade [42]. The evolutionary history between the selected bird species was based on the mitochondrial gene cytochrome c oxidase I (COX1) as it is the mitocondrial gene with least variation among aves orders and at the same time have the lowest amount of heterogeneity across lineages, i.e. different mutations in the gene can cause highly different phenotypes [43]. The sequences were downloaded from GenBank [44] and aligned by Multiple Sequence Comparison by Log-Expectation (MUSCLE) in MEGA X. MUSCLE implements a progressive algorithm that re-optimizes alignments during the whole alignment process, making it possible to correct wrong alignments made in the beginning of the process [45]. Phylogenetic signal can be defined as the degree to which variations in species' trait values are predicted by the relatedness among species. The phylogenetic signal was evaluated by calculating Blomberg's K statistic [23,46]. The behavioral traits; proportion frames spent looking down, proportion frames spent on active flight, flight symmetry, and flight tortuosity were selected for this analysis.

3. Results

3.1. General flight behavior of each species
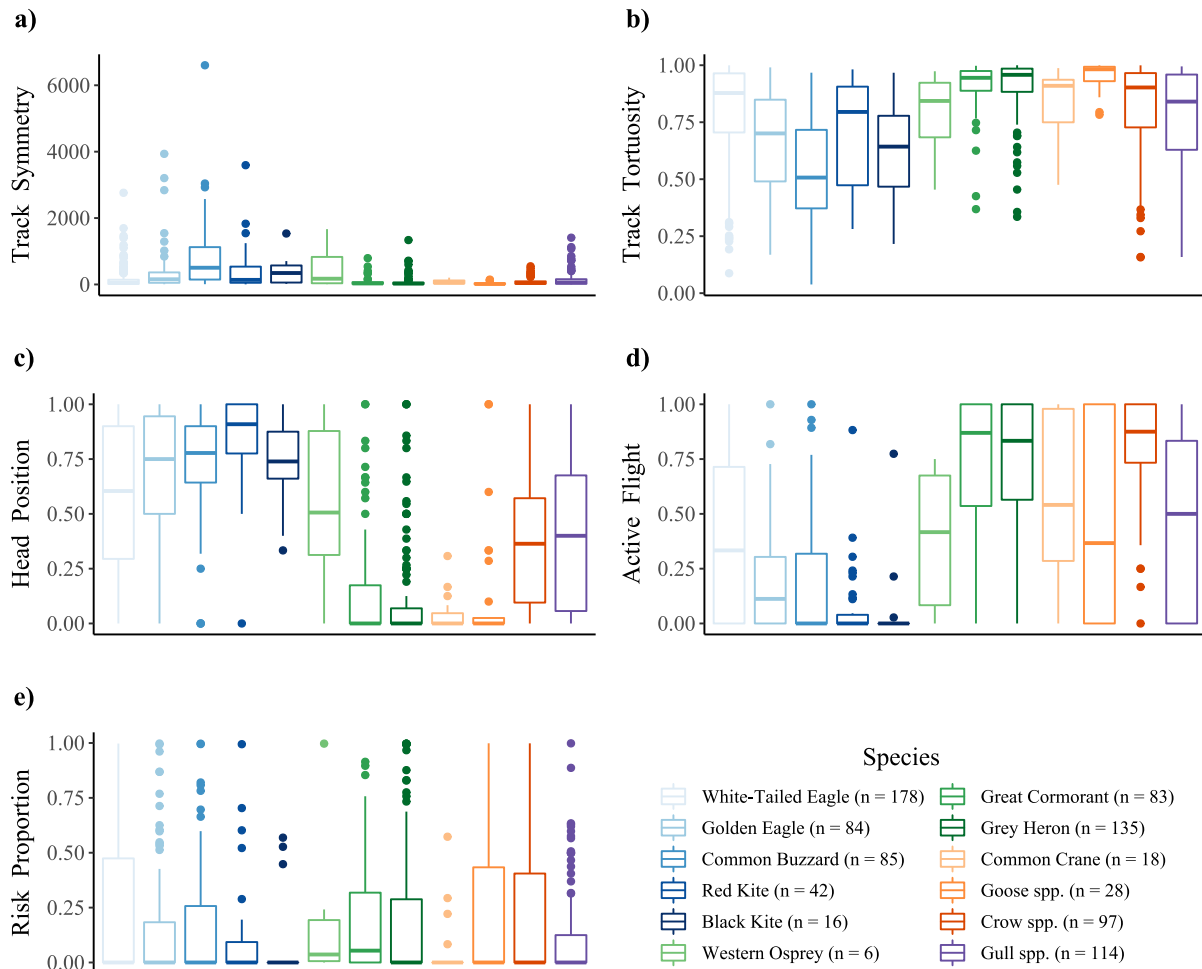
Figure 3. Distribution of each variable grouped by species. The number of tracks for each species is annotated in the legend beside the species' name. **a)** Track symmetry i.e. the absolute sum of directional changes where a value of zero indicates a completely symmetrical track. **b)** Track tortuosity as the ratio between the shortest distance from a track's start to end point and the actual track length i.e. a lower ratio represents a more tortuous track. **c)** Head position as the proportion of frames spent looking down throughout a track. **d)** Active flight as the proportion of frames spent on active flight throughout a track. **e)** Risk proportion i.e. the proportion of time spent in the defined collision risk zone throughout a track.

Raptors in general had more asymmetric and tortuous tracks than the other bird species (3a, b). It was clear that buzzards had the most asymmetric ($median = 503$, $IQR = 148 - 1124$) and tortuous ($median = 0.507$, $IQR = 0.372 - 0.717$) tracks. Furthermore, raptors generally had a large variation (IQR) within the single species in both track symmetry and tortuosity, compared to that of the other bird species. Raptors also spent a relatively large proportion of frames looking down ($median > 0.5$), where red kite was the species that spent the largest proportion of frames looking down ($median = 0.909$, $IQR = 0.776 - 1.00$) (Figure 3c). White-tailed eagles ($median = 0.333$, $IQR = 0.00 - 0.714$), western osprey ($median = 0.417$, $IQR = 0.0833 - 0.675$), and golden eagles ($median = 0.112$, $IQR = 0.00 - 0.304$) were the only raptors generally engaging in active flight i.e. all other raptors spent less than 15% of frames on active flight ($median < 0.12$) (Figure 3d). The birds generally spent little time in the defined collision risk zone, i.e. no species had a median risk proportion above 0.0540 (Figure 3e). Nonetheless, a large proportion the birds intersected the risk zone at one point or another throughout their track, particularly white-tailed eagles (48.3% of all tracks) (Figure 4).
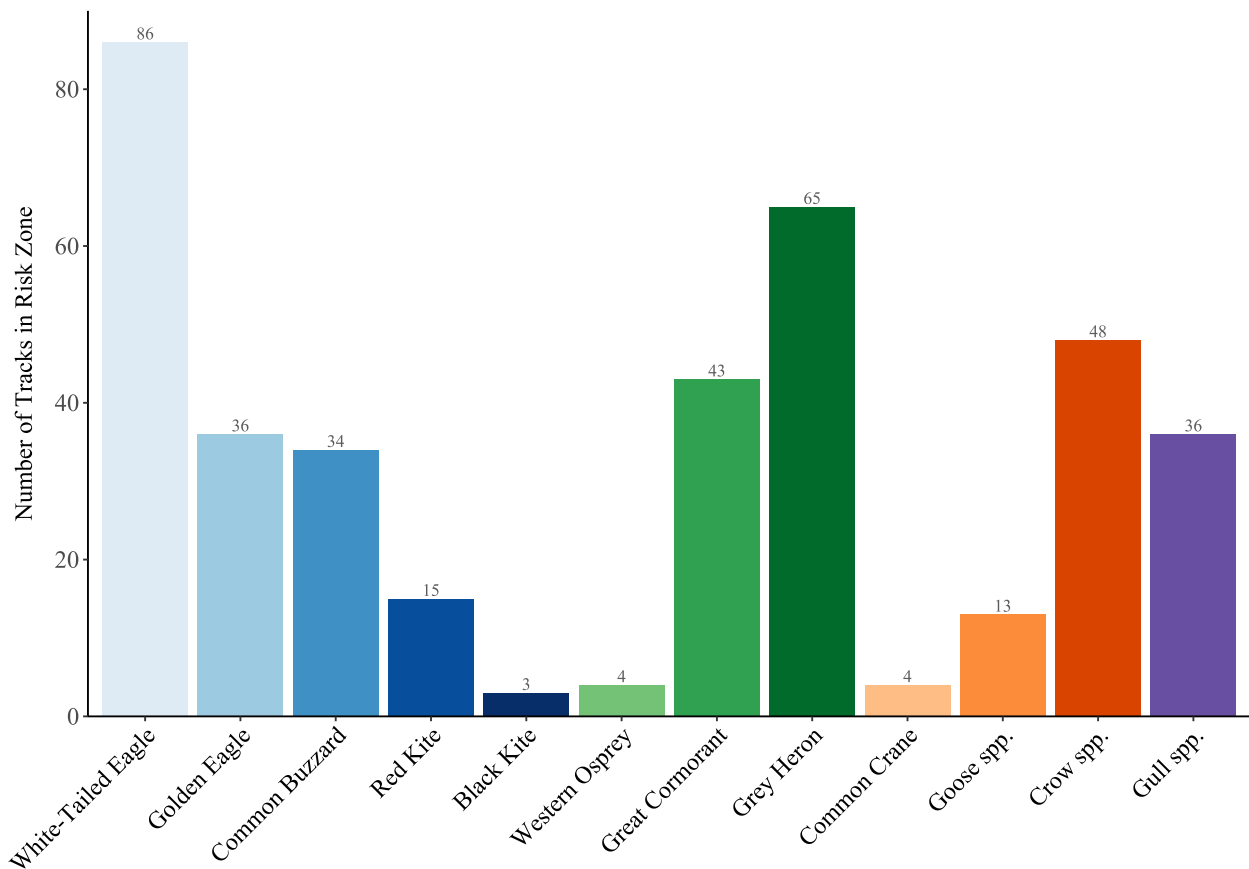
Figure 4. Number of tracks for each species that at some point enter the risk zone. The number of tracks is annotated above each bar.

3.2. Predicting collision risk

When assessing all tracks collectively, there were no significant relationships between the response variable, proportion time spent in the risk zone, and the individual covariates (Appendix H). This was also the case when assessing the relationship for each individual species' tracks, with the exception of white-tailed eagle tracks and gull spp. tracks. For white-tailed eagle tracks there was a significant but weak negative relationship between head position and the collision risk ($R^2 = 0.0220$, $p < 0.05$) and between temperature and collision risk ($R^2 = 0.0428$, $p < 0.01$) (Appendix H). For all raptor tracks there was a significant relationship between collision risk and the respective covariates, head position ($R^2 = 0.0181$, $p < 0.01$) and temperature ($R^2 = 0.0163$, $p < 0.01$). When assessing only tracks in the risk zone the relationship between the response variable and some of the covariates was more apparent, particularly when focusing on the raptor species. A significant but weak relationship was found for between collision risk and the respective covariates, track symmetry ($R^2 = 0.0217$, $p < 0.05$), track tortuosity ($R^2 = 0.02785$, $p < 0.001$), and time of day ($R^2 = 0.0119$, $p < 0.05$) (Figure 5).
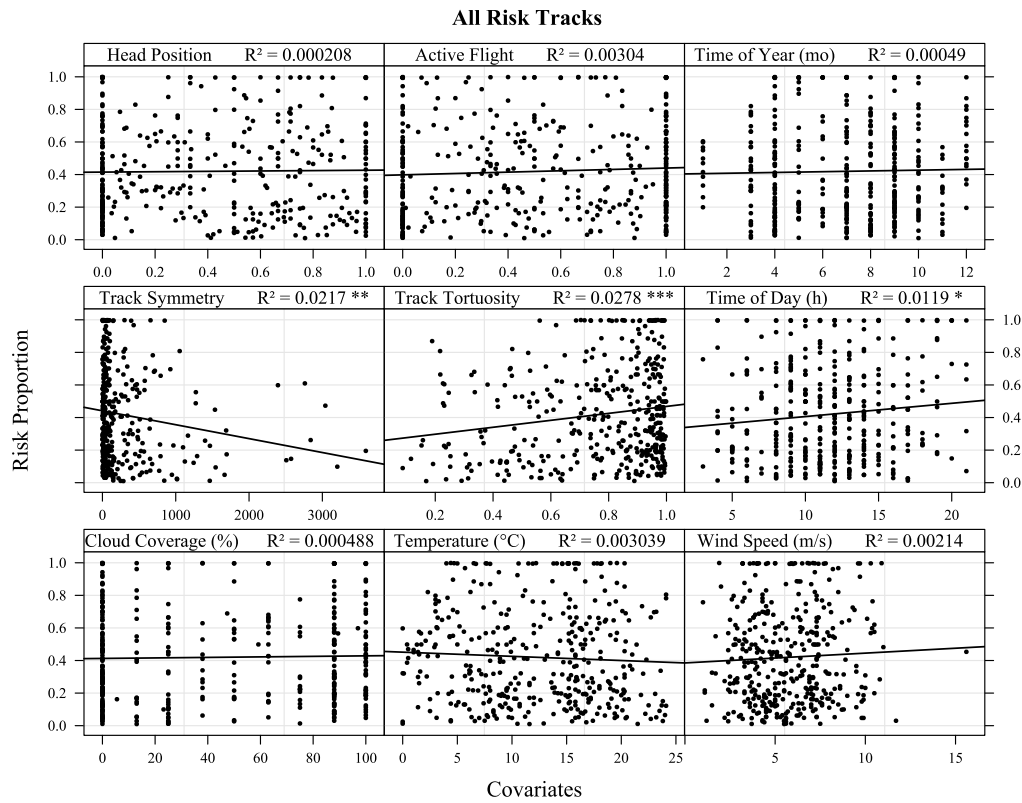
Figure 5. Proportion time spent in risk zone as a function of each possible explanatory variable. A regression trend line is depicted for each plot along with the coefficient of determination (R^2) and significance level.
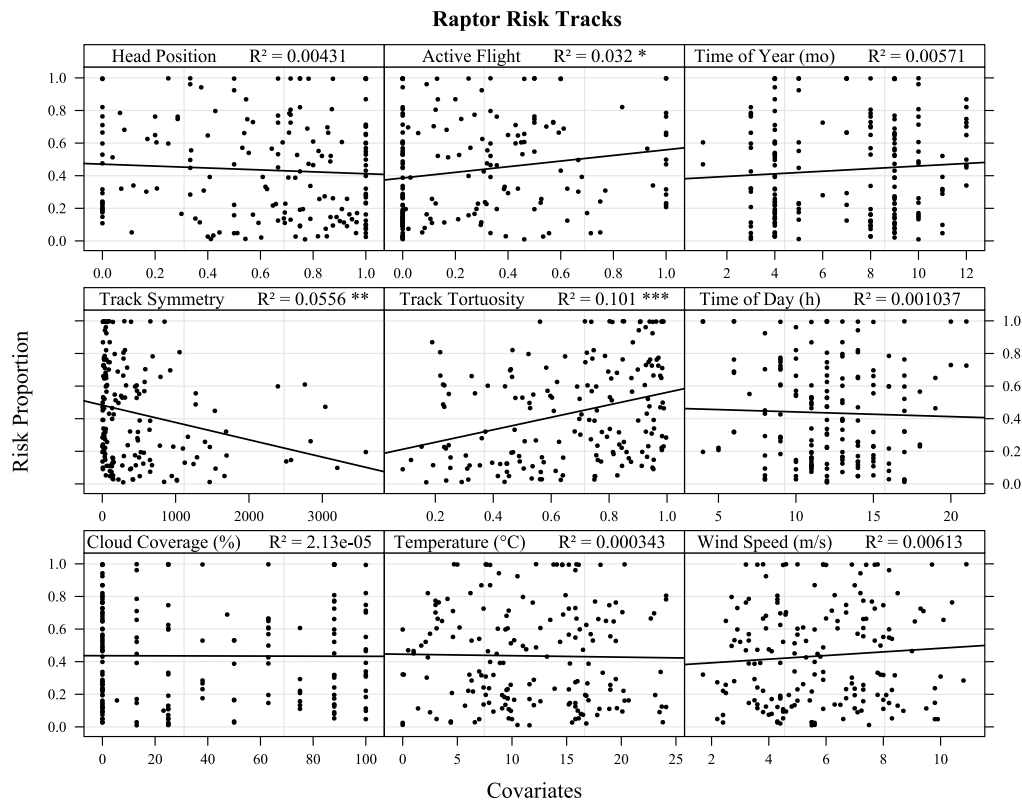
Figure 6. Proportion time spent in risk zone as a function of each possible explanatory variable. A regression trend line is depicted for each plot along with the coefficient of determination (R^2) and significance level.

The relationship between collision risk and track tortuosity became more clear when the assessment only accounted for raptor tracks in the risk zone, showing that track tortuosity was a relatively strong significant predictor of risk ($R^2 = 0.101$, $p < 0.001$) (Figure 6). Moreover, there was a significant relationship between collision risk and active flight for raptor tracks in the risk zone ($R^2 = 0.0320$, $p < 0.05$).

3.2.1. Collision risk models
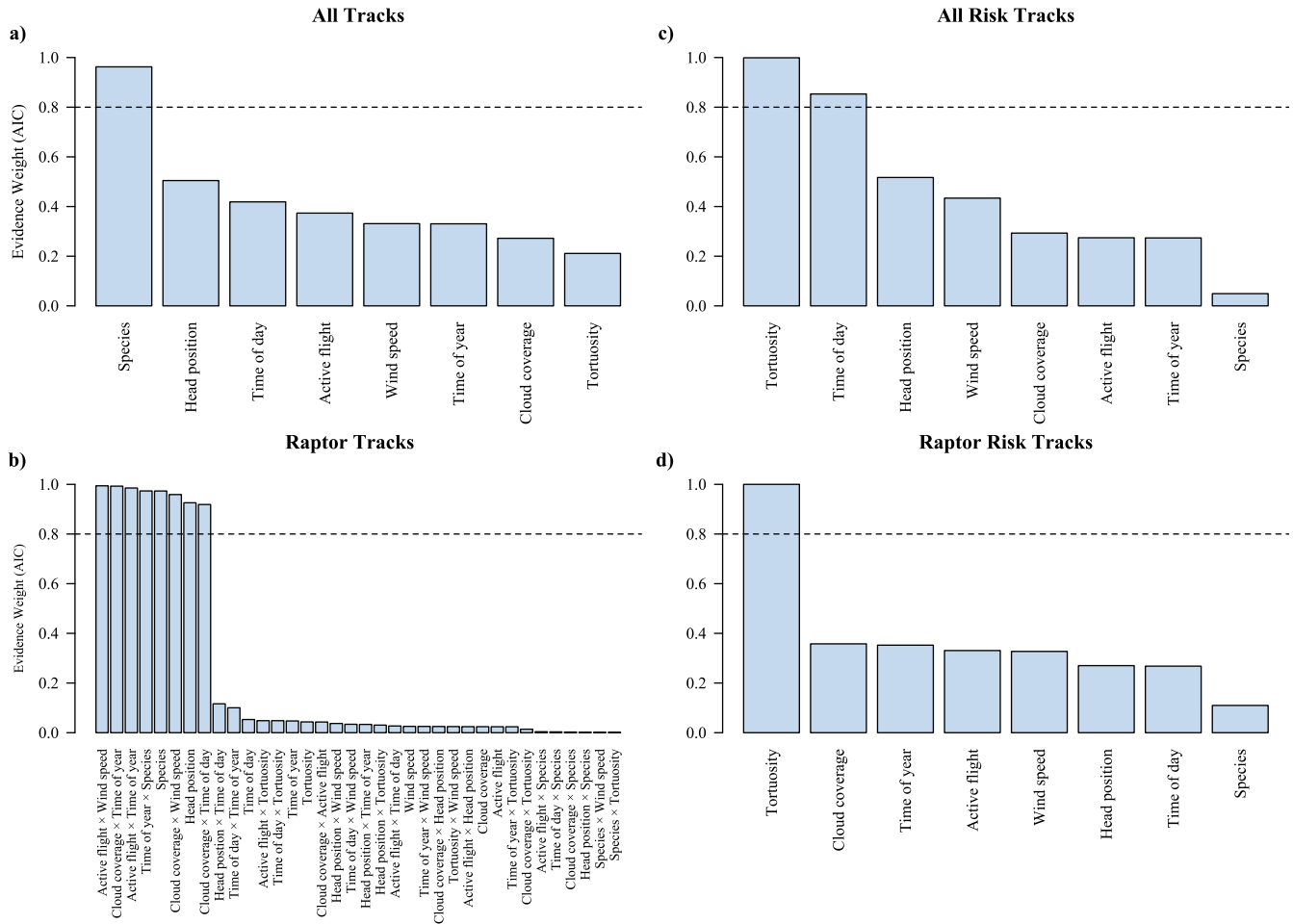
Figure 7. Relative importance of each model term for **a)** all species tracks without interactions, **b)** raptor tracks with interactions, **c)** all tracks in the risk zone without interactions, and **d)** only raptor tracks in the risk zone without interactions. Each term's relative importance was estimated with the automated model selection as the sum of Akaike evidence weights of all models in which the term appears.

The comparison of models with and without interactions, indicated the simpler of the two models to be the better choice for all tracks, all risk tracks and raptor risk tracks. For raptor risk tracks the addition of interaction terms significantly improved the model's goodness of fit (Appendix I). The automated model selection without interactions for all tracks indicated that species (evidence weight = 0.962) was the most important model term, and the only covariate that significantly contributed to explaining the variation of the response, as it was the only covariate with an evidence weight over the threshold of 0.8 (Figure 7a). Whereas, active flight × wind speed (evidence weight = 0.994), cloud coverage × time of year ((evidence weight = 0.993), active flight × time of year (evidence weight = 0.985), time of year × species (evidence weight = 0.973), species (evidence weight = 0.973), cloud coverage × wind speed (evidence weight = 0.959), head position (evidence weight = 0.926), and cloud coverage × time of day (evidence weight = 0.919) were the most important model terms for the model selection for raptor tracks with interactions (Figure 7b). When excluding tracks outside the risk zone the automated model selection without interactions for all species tracks indicated that tortuosity (evidence weight = 1.00), and time of day (evidence weight = 0.853) were the two covariates that significantly

contributed to explaining the variation of the response (Figure 7c). When considering only raptor tracks in the risk zone tortuosity (evidence weight = 1.00) was the single most important model term, and the only covariate with an evidence weight over the threshold in the model selection without interactions (Figure 7d). It should be emphasized that the absolute results from the collision risk models should only be interpreted as indications and should not be taken literally.

3.3. Species-specificity of flight behavioral traits
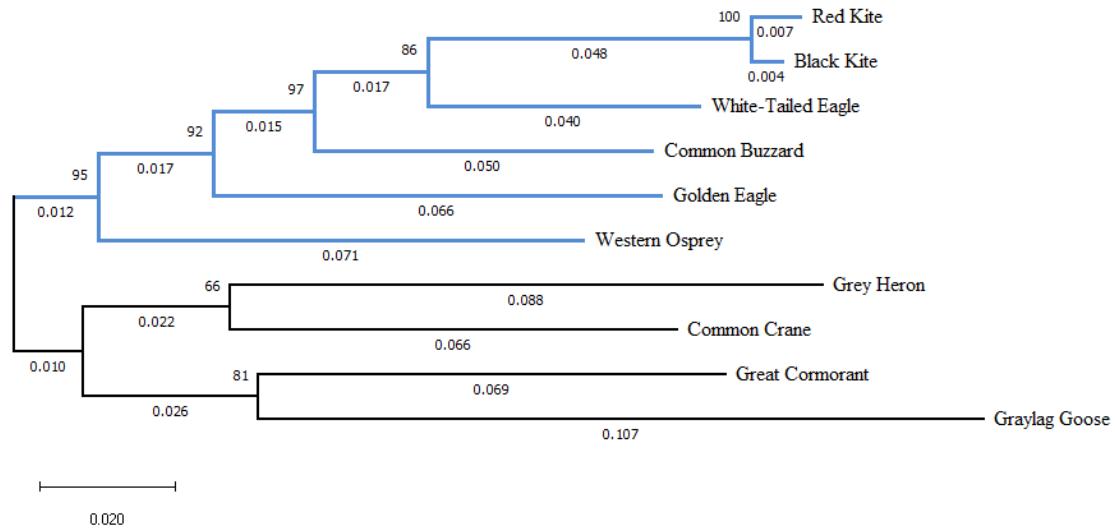
Figure 8. Evolutionary history between the selected bird species. Branch length values are noted under each branch and bootstrap values (%) above the branches. Blue branches represent raptor species.
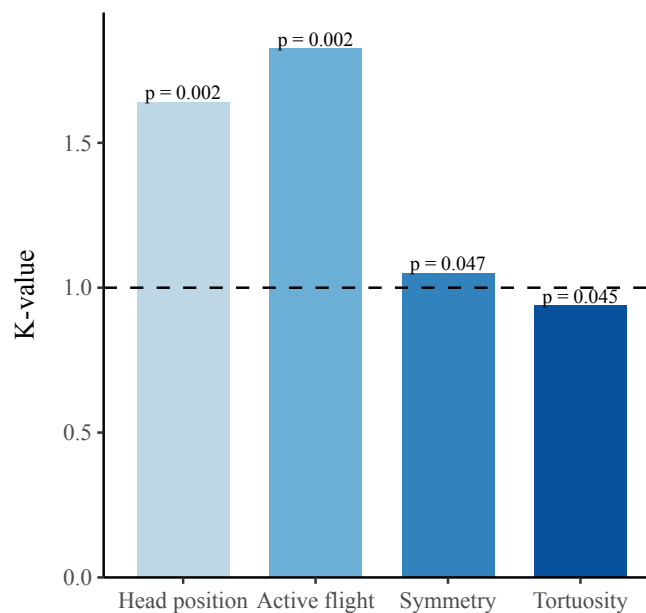
Figure 9. Phylogenetic signal in flight behavior traits using K. The horizontal dotted line represents a K-value of 1, which indicates strong phylogenetic signal that follows Brownian motion perfectly. K-values above this line indicate phylogenetically conserved traits.

The three behavioral traits, head position ($K = 1.64, p = 0.002$), active flight ($K = 1.83, p = 0.002$), and track symmetry ($K = 1.05, p = 0.047$), exhibited statistically significant levels of phylogenetic signal, with K-values greater than 1. For the trait, track tortuosity ($K = 0.939, p = 0.045$), the phylogenetic signal was not stronger than expected under Brownian motion, with a K-value under the threshold of 1.

4. Discussion

4.1. Flight behavior as a predictor of collision risk

Track tortuosity was found to be an important predictor of collision risk, with an evidence weight = 1.00 for risk tracks and raptor risk tracks (Figure 7). The univariate analysis also indicated a significant but weak relationship between track tortuosity and collision risk for all tracks in the risk zone ($R^2 = 0.0278$, $p < 0.001$) (Figure 5). This relationship was more apparent for raptor tracks in the risk zone ($R^2 = 0.101$, $p < 0.001$), with the relationship being strongest for golden eagle tracks in the risk zone ($R^2 = 0.138$, $p < 0.01$) (Figure 6 and Appendix H.14). This association between collision risk and tortuosity indicated that higher collision risk was associated with less tortuous tracks for raptor species in the case study. Thus, disproving the hypothesis that more tortuous tracks yield a higher collision risk and contradicting the same assumption made by Linder *et al.* [28]. Tortuous tracks can be a result of birds utilizing thermal soaring, as shown by the results of Linder *et al.* [28], hence, collision risk was reduced when the birds utilized thermal soaring. This is in agreement with Peron [47] and Janss [15] who found that collision risk was lowest for birds utilizing thermal soaring. Active flight was also weighed as a relatively important risk predictor for raptor tracks, in the automated model selection, with an evidence weight > 0.85 (Figure 7b). The univariate analysis for raptor tracks showed increased active flight to be a significant but weak predictor of increased collision risk ($R^2 = 0.0116$, $p < 0.05$) (Appendix H.2). Thus, contradicting the initial expectation that an increased utilization of active flight would result in a low collision risk, but further confirming the previous result that less tortuous tracks increase collision risk, as Linder *et al.* [28] found that a high utilization of active flight was associated with a low track tortuosity. Moreover, the results indicate a general tendency in which species with low track tortuosity had a high utilization of active flight, e.g. gray heron and great cormorant (Figure 3b and c). However, for the individual non-raptor species, there were no significant relationships between these two respective predictor variables and collision risk (Appendix H).

The relationship between active flight and track tortuosity and their respective relationships with collision risk for raptors may explain why white-tailed eagles generally had a higher collision risk than the other raptor species, as white-tailed eagles also spent more time on active flight and had less tortuous tracks compared to the other raptor species, with the exception of western osprey (Figure 3b, d and e). These differences in active flight and thereby collision risk may be linked to morphological differences between the raptor species. Peron [47] suggested that species with lower aspect ratios (ratio of wing span to chord) are more willing to use active flight i.e. more willing to leave thermals before reaching optimal height. Thus, possibly explaining why white-tailed eagles are more willing to utilize active flight compared to golden eagles, as white-tailed eagles also have a lower aspect ratio, i.e. white-tailed eagles have a larger wing area relative to their wing span. Contrary to the expectation that birds that spent a large proportion of tracks looking down would result in an increased collision risk, this was not proven by the results in this case study. The univariate analysis indicated a negative relationship between risk proportion and time spent looking down for raptor tracks, i.e. time spent looking down did not increase collision risk. In the multivariate analysis for raptor tracks, head position was also weighed as an important predictor of collision risk (Figure 7b).

For white-tailed eagle tracks there was a significant but weak negative relationship between temperature and collision risk ($R^2 = 0.0428$, $p < 0.01$) (Appendix H). For all raptor tracks there was a significant relationship between collision risk and temperature ($R^2 = 0.0163$, $p < 0.01$). A significant but weak relationship was found for between collision risk and and time of day ($R^2 = 0.0119$, $p < 0.05$) (Figure 5).

Moreover, no clear strong relationships were found in the univariate analysis between collision risk and the weather and temporal variables, respectively. However, for all raptor tracks and white-tailed eagle tracks there was a weak negative relationship between collision risk and temperature and for all risk tracks there was a positive, but weak relationship between collision risk and time of day. Moreover, time of year, time of day, wind speed, and cloud coverage were important predictors of collision risk in the multivariate analysis for raptor tracks, where these four variables were included in six of the eight model terms with an evidence weight > 0.8 (Figure 7b). Furthermore, the multivariate analysis for all species tracks collectively indicated species to be the single most important predictor of collision risk. Thus, indicating that collision risk is species-specific, confirming the hypothesis that collision risk could be predicted by species.

4.2. Species-specificity of behavioral traits

The behavioral traits head position and active flight appear to be species-specific (Figure 3c and d). Raptors generally spent more time looking down compared to the other study species, particularly, grey heron, great cormorant, common crane, and goose spp. (Figure 3c). These species generally did not spend any time looking down (*median* = 0.00). The differing foraging ecology between these species and the raptor species is a highly plausible reason for this finding, as all raptor species in this study, with the exception of western osprey, also foraged within the study site. These differences in

foraging ecology are also conveyed by species differences in track tortuosity and symmetry, where raptors generally had more tortuous and asymmetric tracks (Figure 3a and b). Foraging ecology as a potential determining factor in regard to time spent looking down and track tortuosity and asymmetry is further supported by Linder *et al.* [28] who found a positive correlation between time spent looking down and track asymmetry and tortuosity, respectively, i.e. birds spending more time looking down also have more tortuous and asymmetric tracks. Thus, making it likely that these behavioral traits all being associated with the same determining factor, e.g. foraging ecology. Furthermore, head position, and track tortuosity and symmetry have also been linked to different flight strategies, as the utilization of soaring flight is associated with birds spending more time looking down and having asymmetric and tortuous tracks [28]. In this study, raptors generally spent little time on active flight, whereas, most other study species, e.g. grey heron, great cormorant, common crane, crow spp., and gull spp., spent more than 50% of frames engaging in active flight (Figure 3d). These differences in active flight can be linked to morphological differences between these species.

A phylogenetic signal was found for the flight behavioral traits, head position, active flight, and track symmetry, thus, confirming that these behavioral traits were correlated with phylogenetic relatedness. For track tortuosity the phylogenetic signal was weaker than expected under Brownian motion ($K < 1$). Blomberg *et al.* [23] found that behavioral traits tend to show less phylogenetic signal than morphological traits. This is presumed to be due to the faster evolution rate of behavioral traits compared to morphological traits [23,48]. However, this was not the case in this study as three of the behavioral traits had K-values> 1, indicating that these behavioral traits are phylogenetically conserved i.e. close relatives had more similar flight behavior in regard to these to traits than expected under Brownian motion [25]. More specifically, the K-value for active flight was the highest, which may be associated with the close relation between this behavioral trait and morphological traits e.g. wing loading and aspect ratio. Furthermore, a high phylogenetic signal was also found for head position. This behavioral trait is presumably linked to the variation in foraging behaviors between the species and Weeks *et al.* [49] found foraging behavior to be significantly correlated with morphological traits, hence, a possible correlation between head position and morphological traits may explain the high phylogenetic signal. The phylogenetic signal was not as apparent for track symmetry and tortuosity, with both K-values≈ 1. Similar to head position and active flight these two behavioral tracks are also associated with both foraging ecology and morphological traits. However, track symmetry and tortuosity are presumably more dependent on other factors, e.g. obstacle avoidance.

5. Conclusion

To our knowledge this is the first study quantifying species-specific flight behavior in association with turbine collision risk. The findings of species-specific flight behavior was confirmed by a strong phylogenetic signal for the behavioral traits, head position and active flight. Track tortuosity and track symmetry were also species-specific, but the phylogenetic signal was not stronger than expected under Brownian motion. All four behavioral traits were also shown to be important predictors of collision risk. The results of this study can be used to identify risk prone species based on flight behavior and phylogenetic relatedness. However, collision risk is also site-specific and the results of the case study are, therefore, not directly applicable to site-specific conservation practices, but they can be used to give a general indication of risk prone species. Thus, suggesting which species are relevant to further investigate in site-specific contexts. It should be noted that these results are based on the proportion time spent within 100 meters proximity to the nearest turbine as a proxy for collision risk, more accurate results can only be achieved if it is possible to observe the behavior of individuals prior to actual collisions with wind turbines. It would take a large amount of time to collect such data collection due to the infrequency of collisions.

Appendix A. Study site
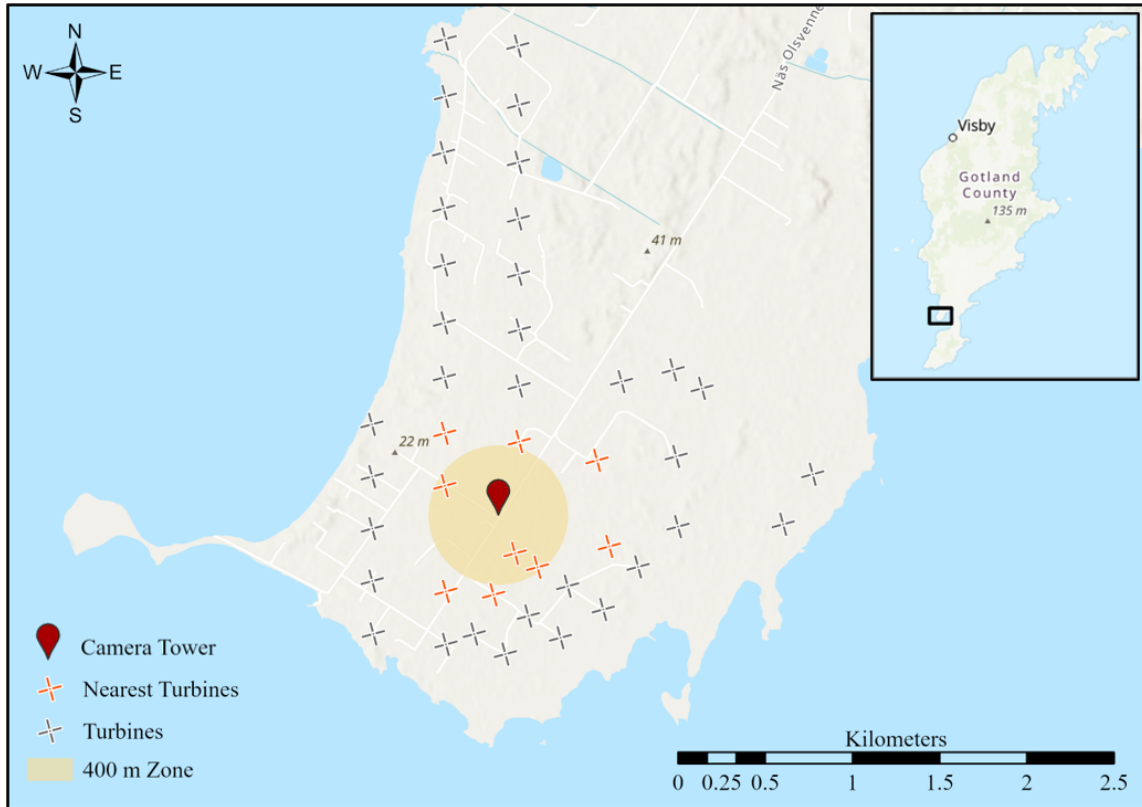
Figure A.1. The IdentiFlight tower (red drop) and the observational area (orange circle), i.e. a 400 meter zone around the tower. The nine wind turbines covered by the camera system (orange crosses) and other turbines (grey crosses) within the wind farm [28].

Appendix B. IdentiFlight system

Appendix B.1. IdentiFlight Camera System

Figure B.1. Camera tower at study site.

Appendix B.2. Curtailment prescription

For each turbine an outer and inner cylinder are predefined. If a bird that has been classified by the system as a protected species enters the inner cylinder a curtailment order is issued, resulting in the curtailment of the specific turbine. If the bird is present in the area between the outer and inner cylinder a curtailment order is only issue when certain criteria are met e.g. the bird is flying towards the particular turbine with a high flight speed (Table B.1) [28].

Table B.1. Turbine details in relation to curtailment for covered and partially covered wind turbines [28].

Model	Number of turbines	Rotor diameter (m)	Hub height (m)	Radius of outer cylinder (m)	Radius of inner cylinder (m)	Height of outer cylinder (m)	Height of inner cylinder (m)
Covered							
Vestas V27	1	27	31	700	250	300	200
Vestas V29	1	29	31	700	250	300	200
Vestas V90	1	90	80	700	400	400	250
Partially covered							
Kenersys 2500 100	1	100	85	600	300	400	250
Vestas V47	2	47	45	600	300	300	200
Vestas V90	2	90	80	700	300	400	250
Vestas V100	1	95	100	700	400	400	250
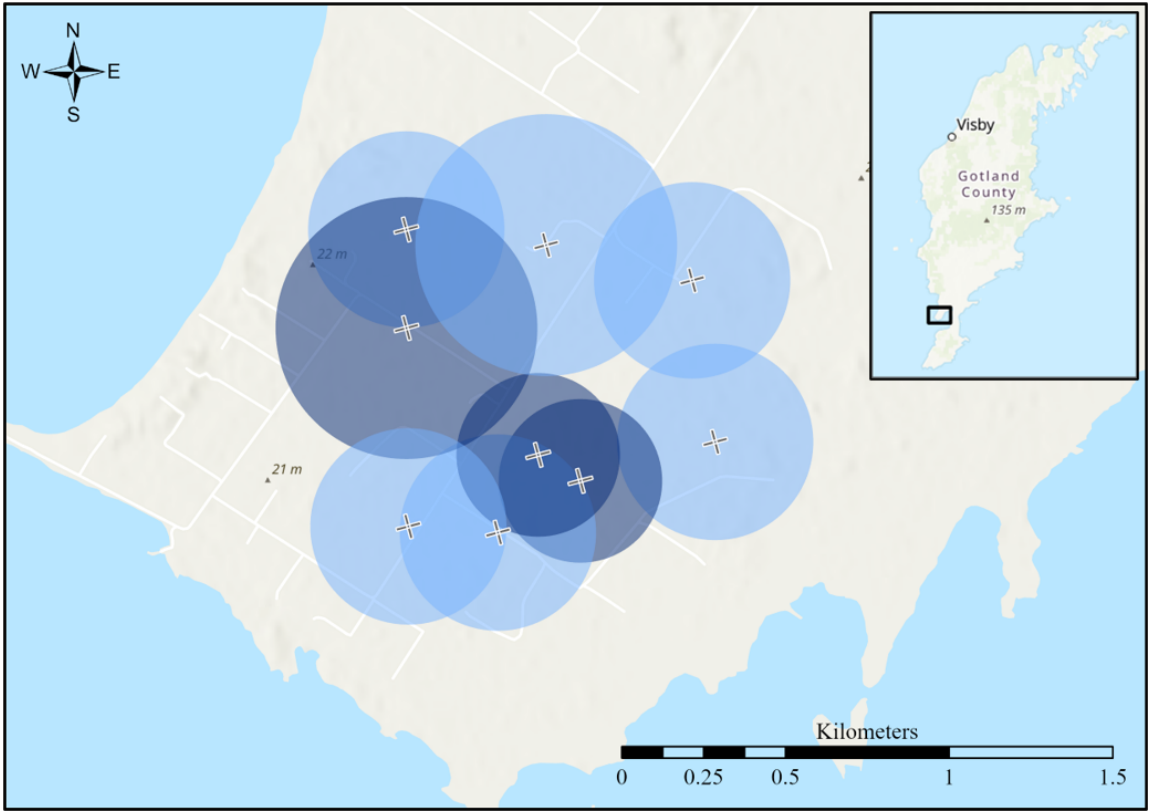
Figure B.2. The radius of the inner cylinder for each turbine also indicating if the turbine is fully covered (dark blue) or partially covered (light blue) by the IdentiFlight camera tower.

Appendix C. Operational days

Table C.1. Number of days where the camera system was operational, number of days with observations of the selected bird species.

Year	Month	Operational days	Days with birds
2020	February	20	15
2020	March	31	31
2020	April	30	28
2020	May	31	28
2020	June	14	14
2020	July	15	15
2020	August	22	22
2020	September	30	27
2020	October	31	15
2020	November	30	13
2020	December	31	17
2021	January	31	20
2021	February	28	23
2021	March	31	28
Total	**155**	**145**	

Appendix D. Tracks

Table D.1. Species and number of tracks for each species that are included in the analyses.

Species	Number of tracks
Golden eagle	85
White-tailed eagle	178
Red kite	42
Black kite	16
Common buzzard	85
Western osprey	6
Grey heron	135
Great cormorant	83
Common crane	18
Goose spp.	28
Crow spp.	97
Gull spp.	114
Total	**887**

Appendix E. Calculations of track tortuosity and symmetry

Appendix E.1. Track tortuosity
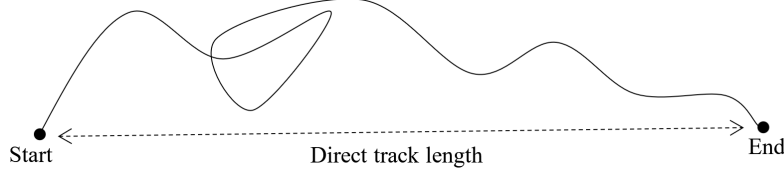
Figure E.1. Portrayal of a track, showing direct track length (the dotted arrow) in comparison to actual track length [28].

Track tortuosity was calculated for each track using Equation A1 (Figure E.1) [28]. This resulted in a measure of deviations from the shortest flight path, where a value of 1 indicates a completely straight flight path, i.e. a low tortuosity. The lower the ratio the more tortuous the flight path [28].

$$Track\ tortuosity = \frac{Direct\ track\ length}{Actual\ track\ length} \tag{A1}$$

Appendix E.2. Track symmetry

An individuals track consists of multiple points connected in a chronological order [28]. Each turn an individual makes can therefore be described by the angle between the connected points. The track angles ranged from $-180°$ to $180°$, thus, distinguishing between left and right turns (Figure E.2) [28].
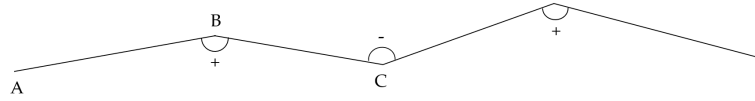
Figure E.2. Track model in which right turns ranged from 0 to $180°$ and left turns from -180 to $0°$ [28].

The angles of each track were calculated using the inverse trigonometric function of cosine (arccos) (Equation A2) [28]. A, B and C represent track points , where AB is the distance from point A to point B, and BC is the distance between point B and C, etc. (Figure E.2).

$$\angle B = arccos\left(\frac{AB^2 + BC^2 - AC^2}{2 \cdot AB \cdot BC}\right) \tag{A2}$$

Equation A3 was used to calculate the track symmetry for each track, where a value of 0 represents a perfectly symmetrical track. Hence, the larger the value the more asymmetrical the track [28].

$$Track\,symmetry = \left|\sum_{i=1}^{n} \angle_i\right| \tag{A3}$$

Appendix F. Risk zones

Table F.1. Model type, number of turbines, rotor diameter and the radius of risk zone around each turbine.

Model	Number of turbines	Radius of rotor (m)	Radius of risk zone (m)
Covered			
Vestas V27	1	13.5	113.5
Vestas V29	1	14.5	114.5
Vestas V90	1	45	145
Partially covered			
Kenersys 2500 100	1	50	150
Vestas V47	2	23.5	123.5
Vestas V90	2	22.5	122.5
Vestas V100	1	47.5	147.5

Appendix G. Data exploration

Appendix G.1. Variance inflation factor analysis

A variance inflation factor (VIF) analysis was used to assess the collinearity of the explanatory variables. A backward selection was used, removing the variable with the highest VIF value and recalculating the VIF values for the remaining variables after each iteration, until all VIF values were smaller than 2 [50].

Table G.1. Variance inflation factor (VIF) values for the explanatory variables.

Covariate	All tracks	Raptor tracks	All risk tracks	Raptor risk tracks
Initial VIF values (iteration 1)				
Head position	1.42	1.23	1.52	1.39
Active flight	1.34	1.17	1.44	1.26
Track symmetry	1.50	1.51	1.64	1.57
Track tortuosity	1.64	1.56	1.82	1.83
Cloud coverage	1.18	1.21	1.22	1.41
Temperature	1.52	1.64	1.45	9.75
Wind speed	1.10	1.13	1.09	1.44
Time of year	1.49	1.54	1.50	9.08
Time of day	1.04	1.06	1.07	1.23

Appendix G.2. Spearman's correlation coefficient and pairwise scatter-plots

　　To assess collinearity Spearman's correlation coefficient was calculated among the covariates and pairwise scatter-plots were created to detect obvious correlations among the covariates.
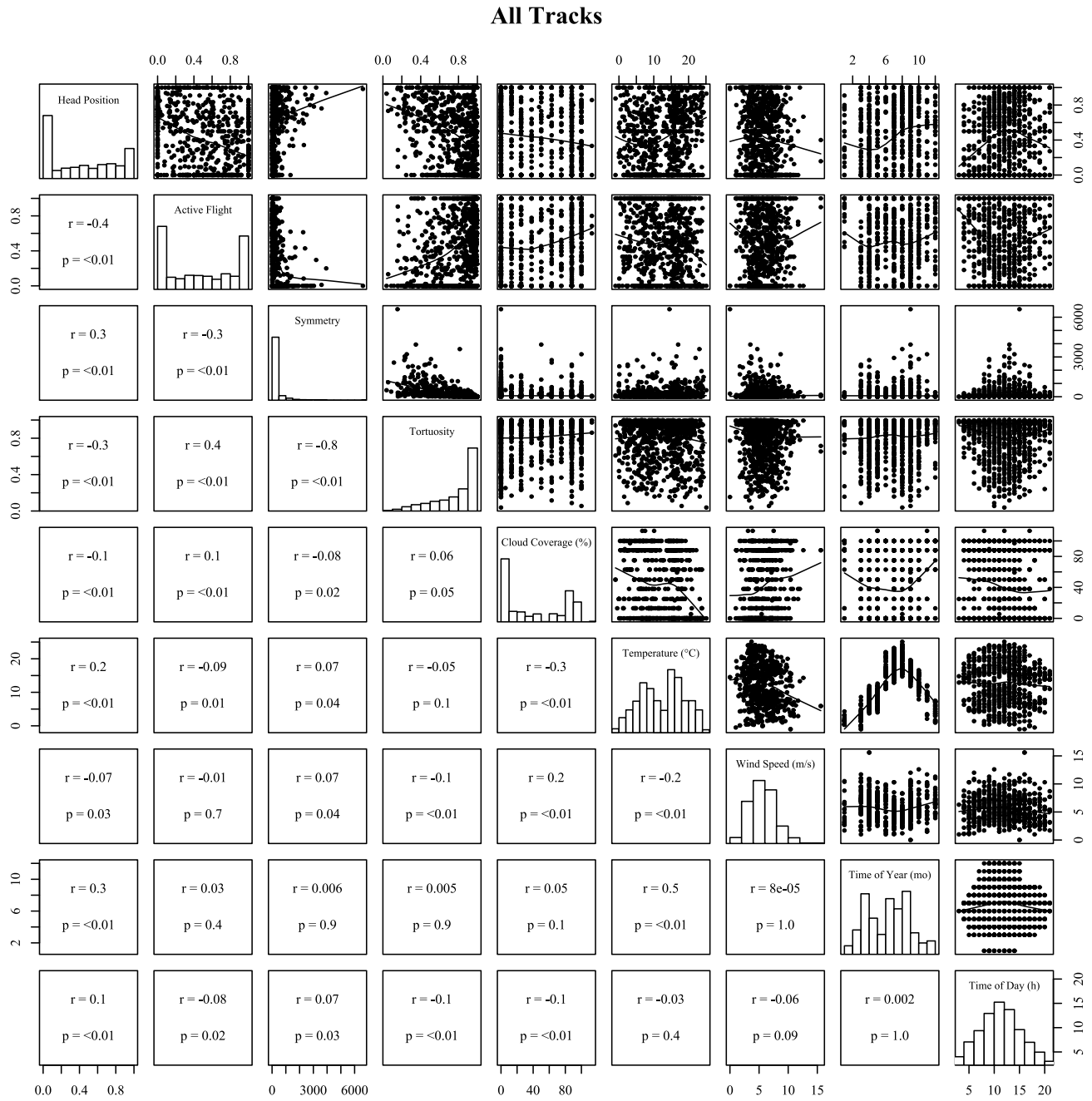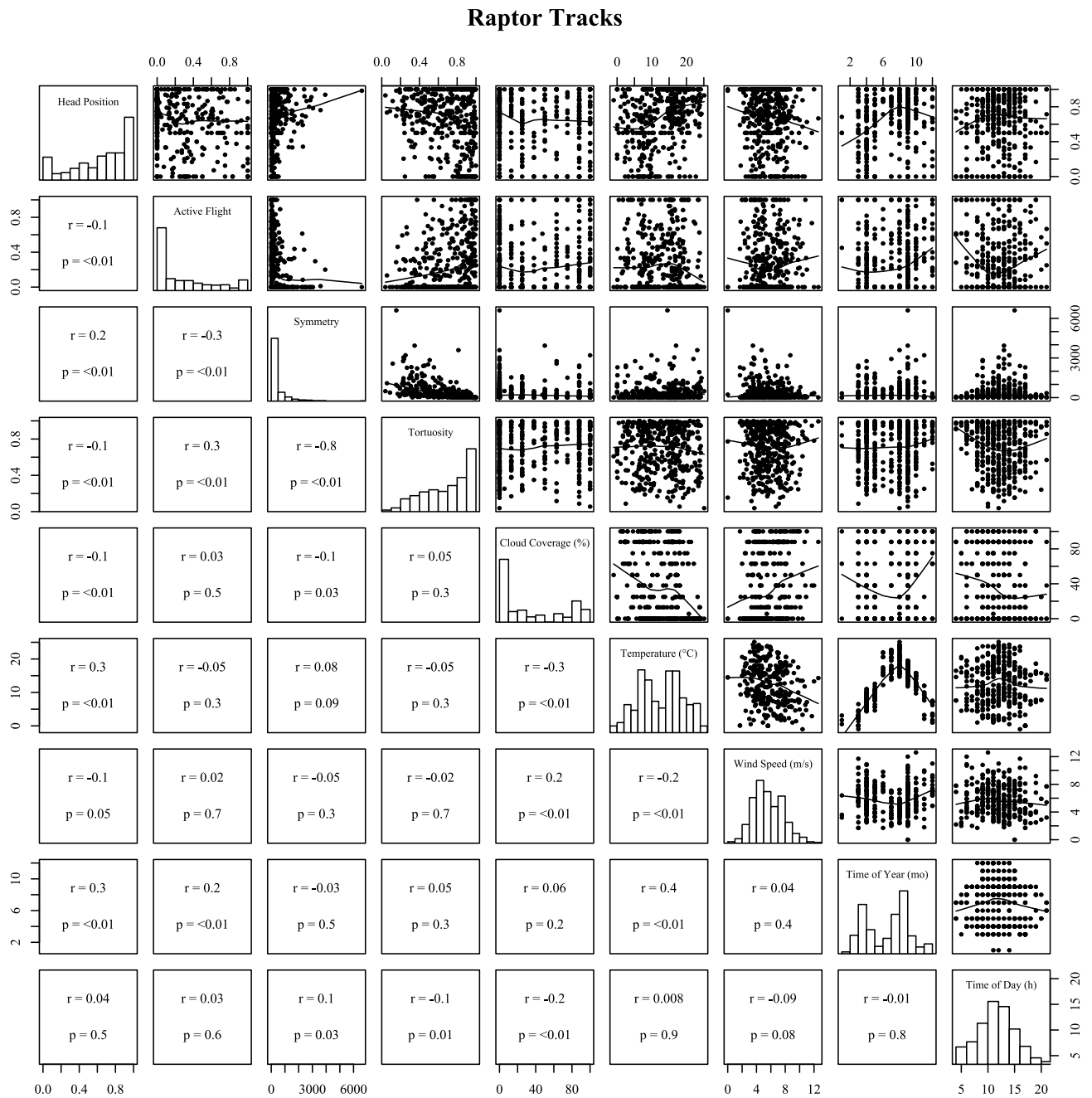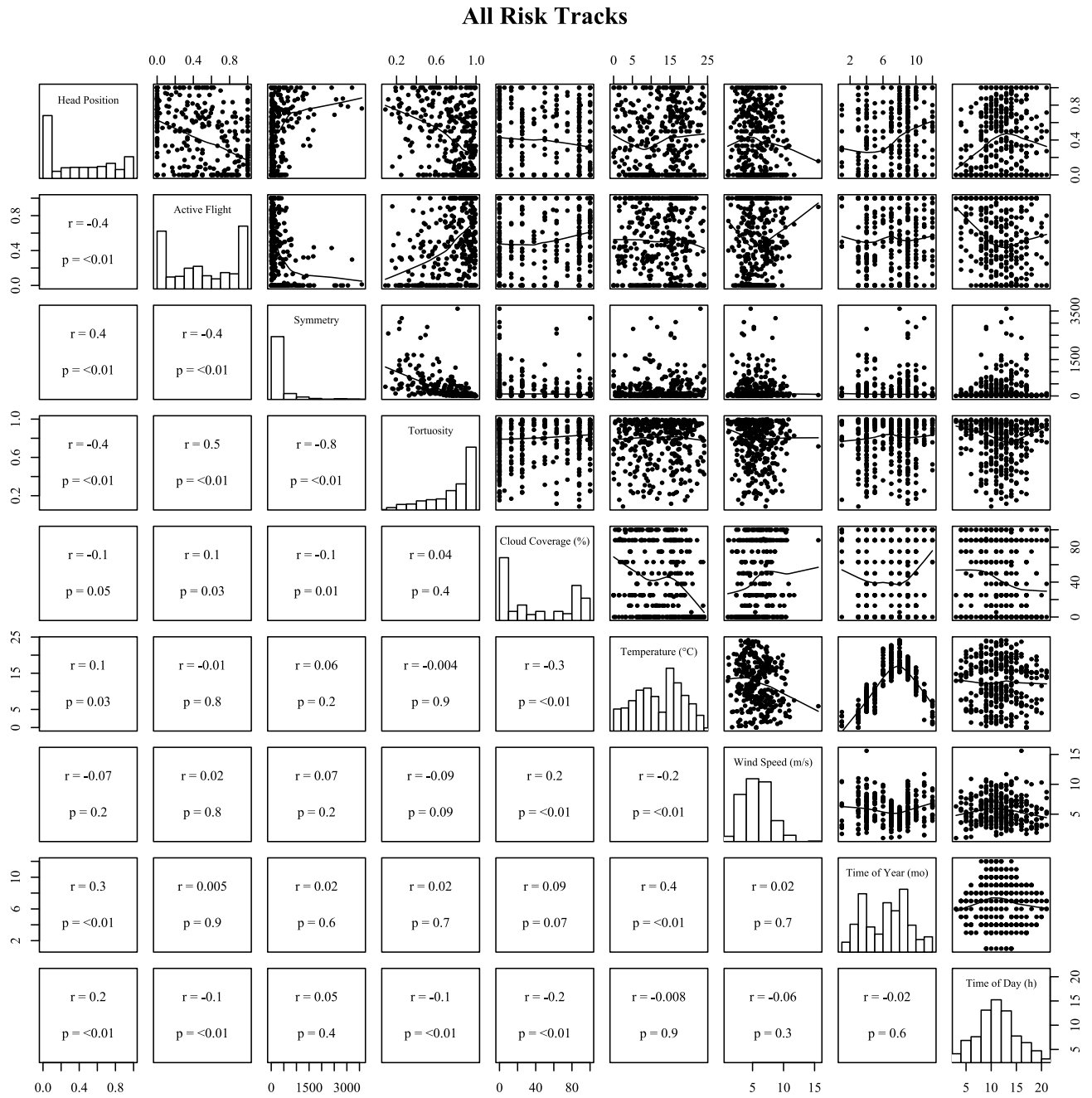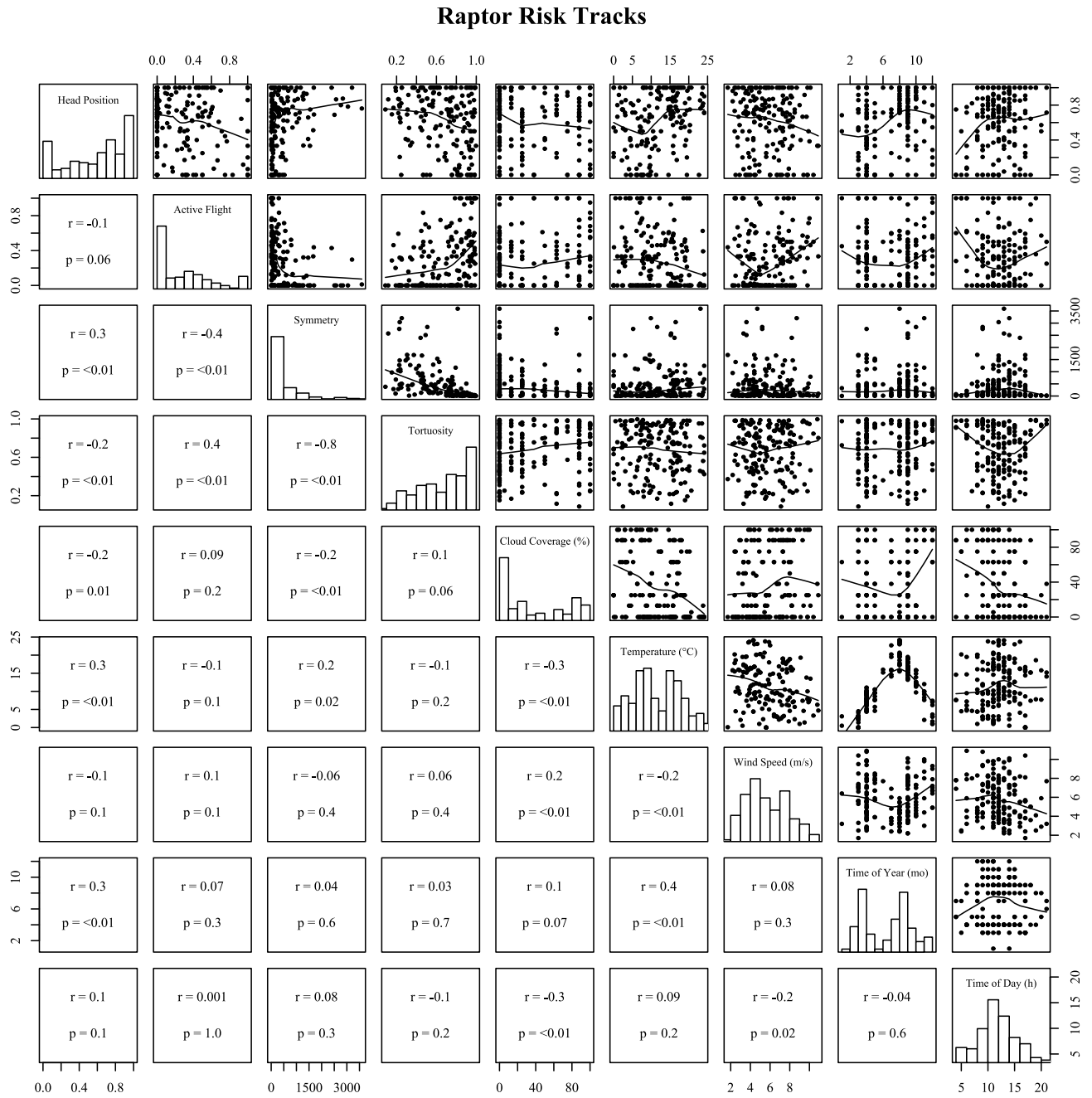
All Tracks

**Figure G.1.** Correlation between the different continuous predictor variables for all tracks.

Figure G.2. Correlation between the different continuous predictor variables for raptor tracks.

Figure G.3. Correlation between the different continuous predictor variables for all risk tracks.

Figure G.4. Correlation between the different continuous predictor variables for raptor risk tracks.
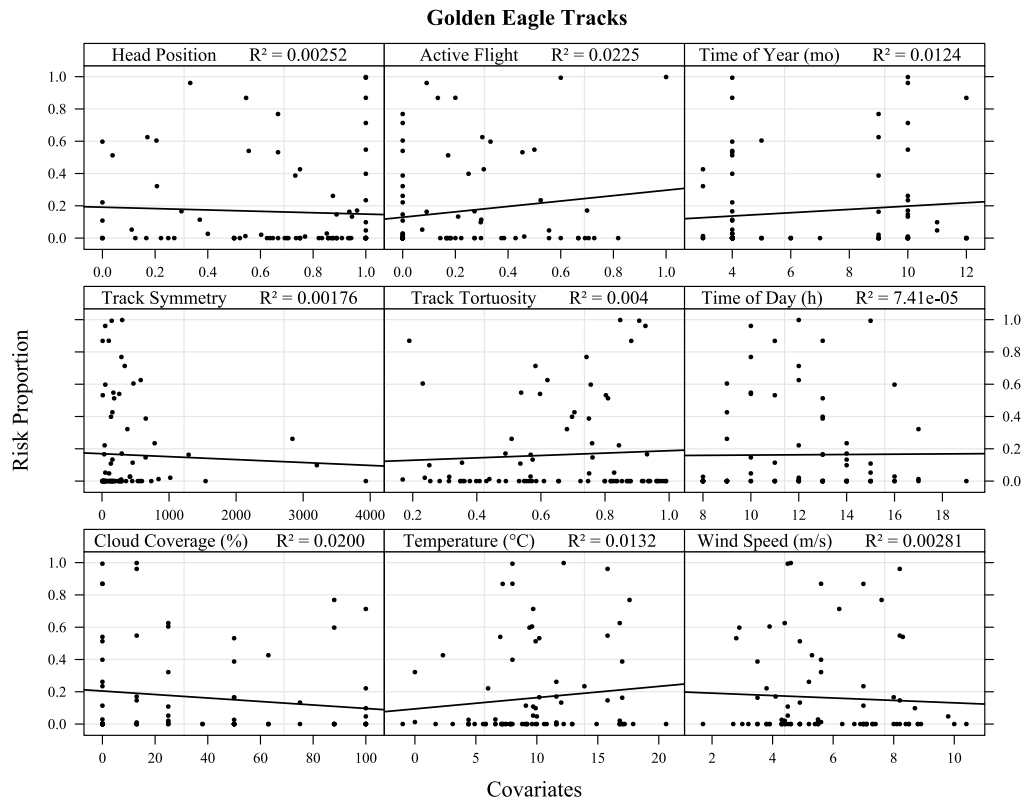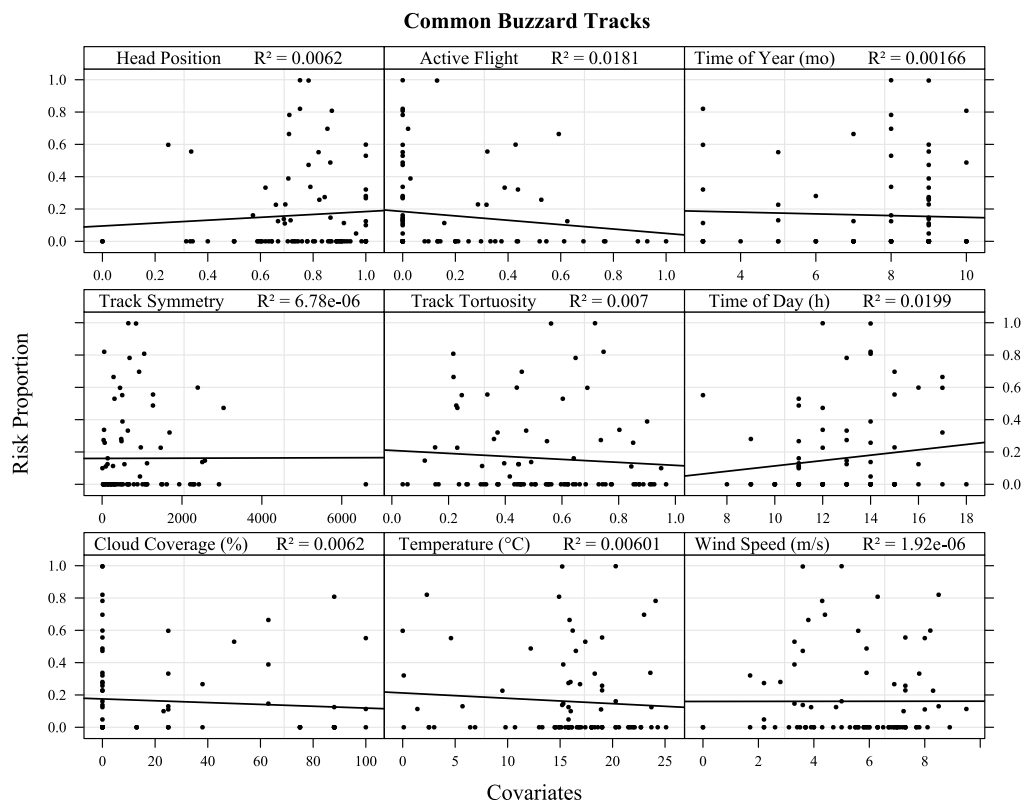
Appendix H. Univariate results
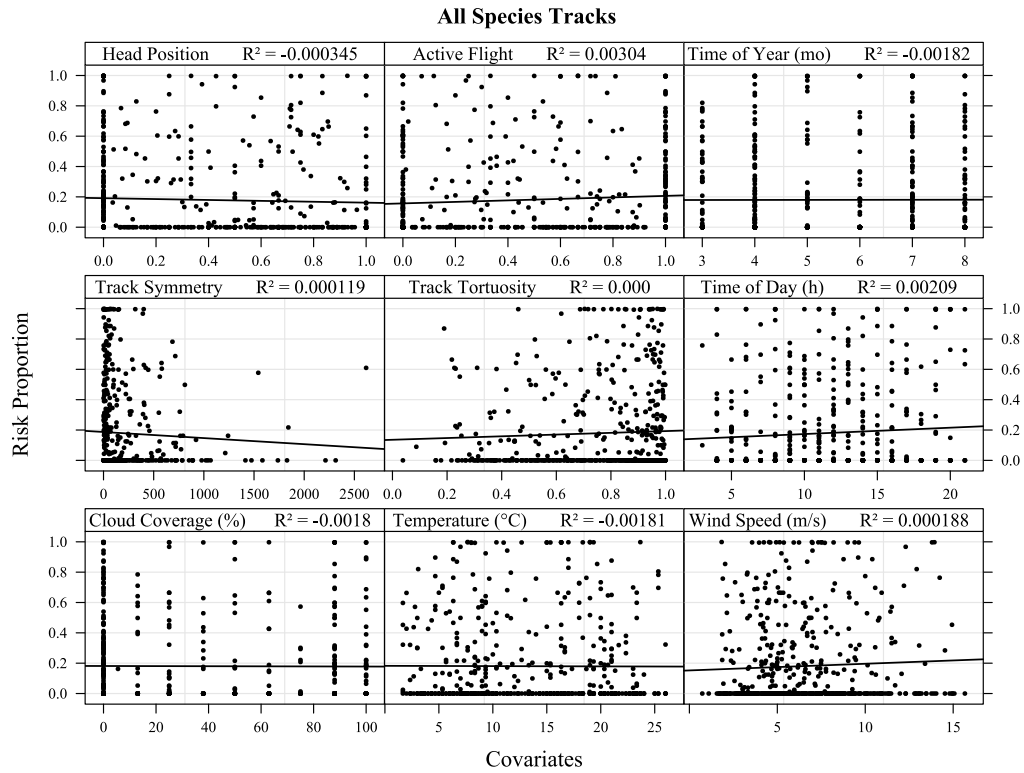
Figure H.1. Proportion time spent in risk zone as a function of each possible explanatory variable. A regression trend line is depicted for each plot along with the coefficient of determination (R^2) and significance level.
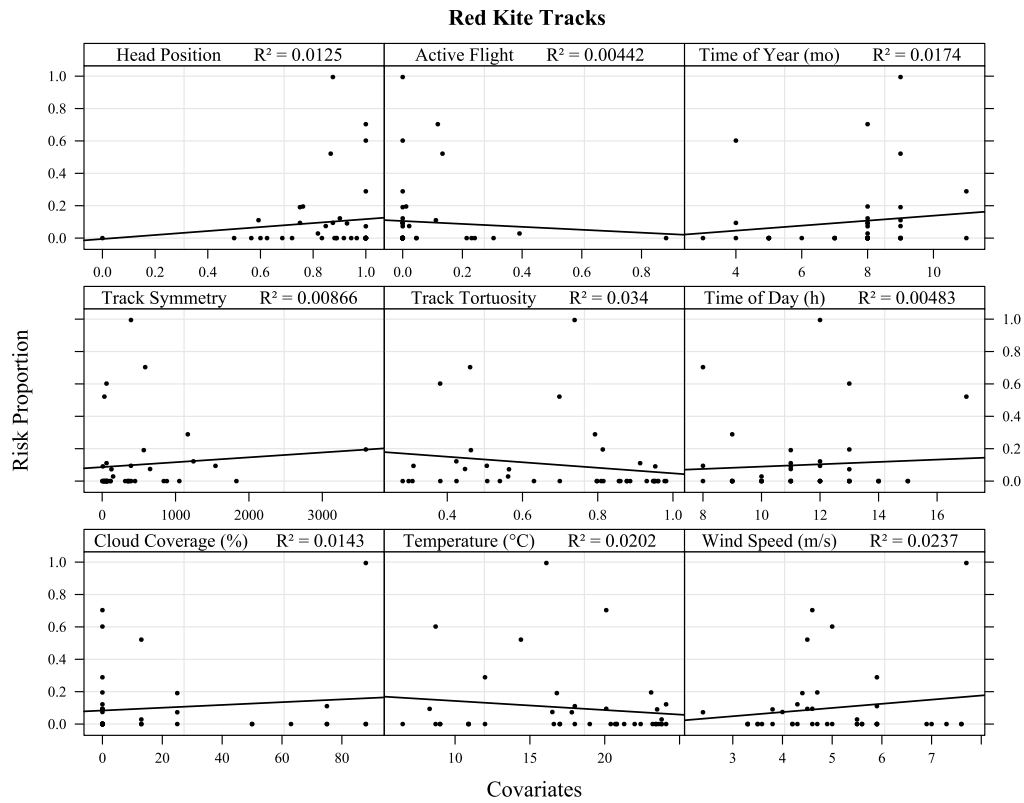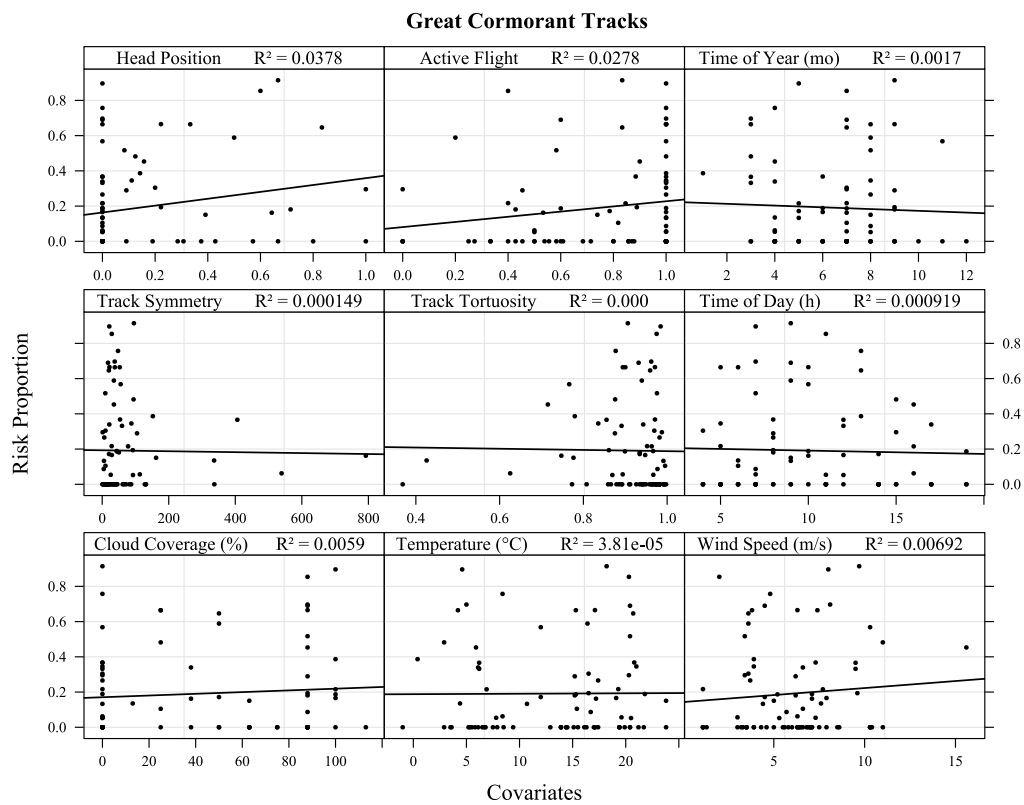
Raptor Tracks
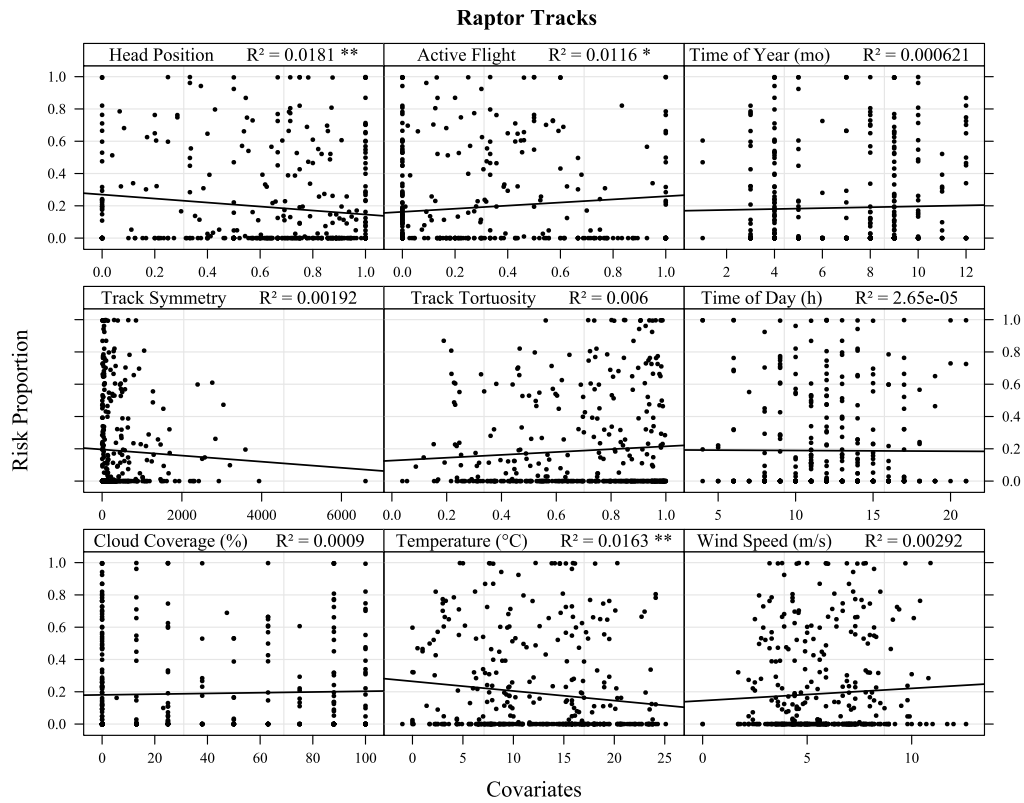
Figure H.2. Proportion time spent in risk zone as a function of each possible explanatory variable. A regression trend line is depicted for each plot along with the coefficient of determination (R^2) and significance level.

White-Tailed Eagle Tracks
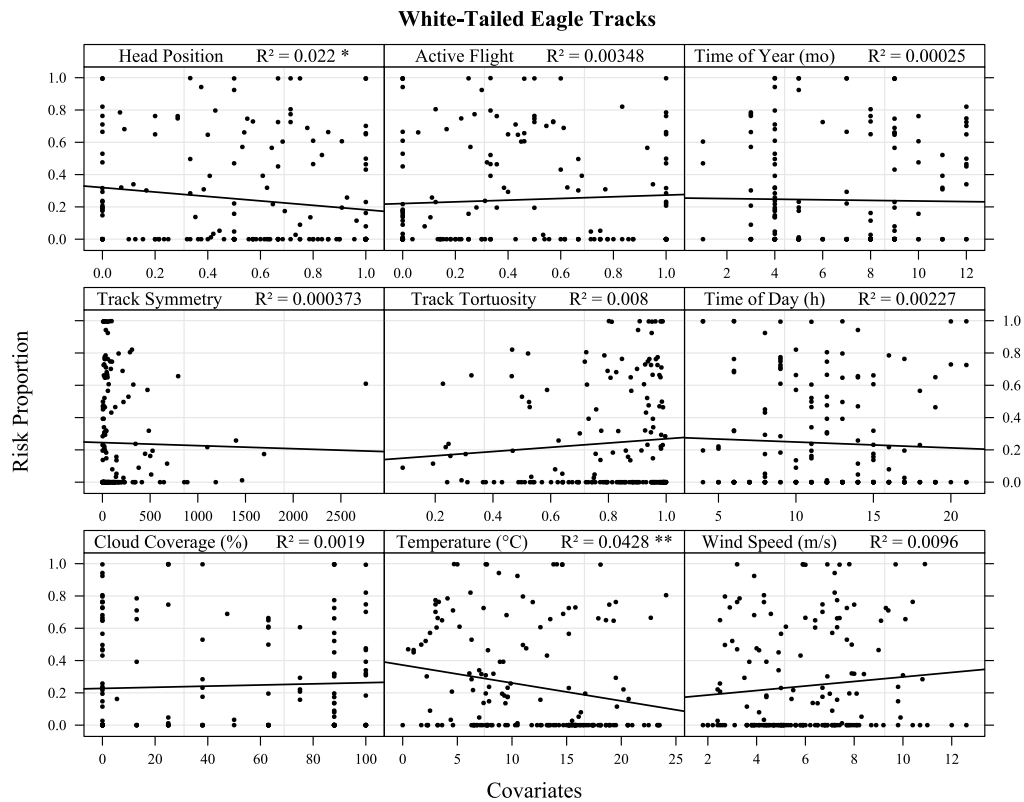
Figure H.3. Proportion time spent in risk zone as a function of each possible explanatory variable. A regression trend line is depicted for each plot along with the coefficient of determination (R^2) and significance level.
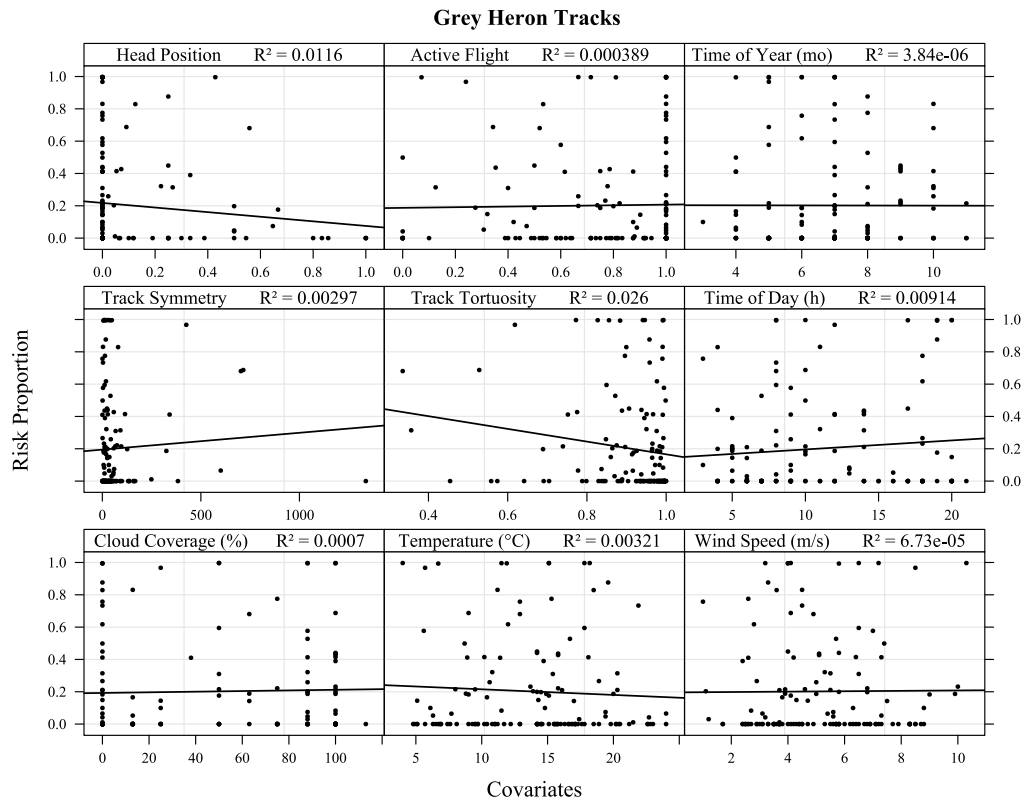
Golden Eagle Tracks

Figure H.4. Proportion time spent in risk zone as a function of each possible explanatory variable. A regression trend line is depicted for each plot along with the coefficient of determination (R^2) and significance level.
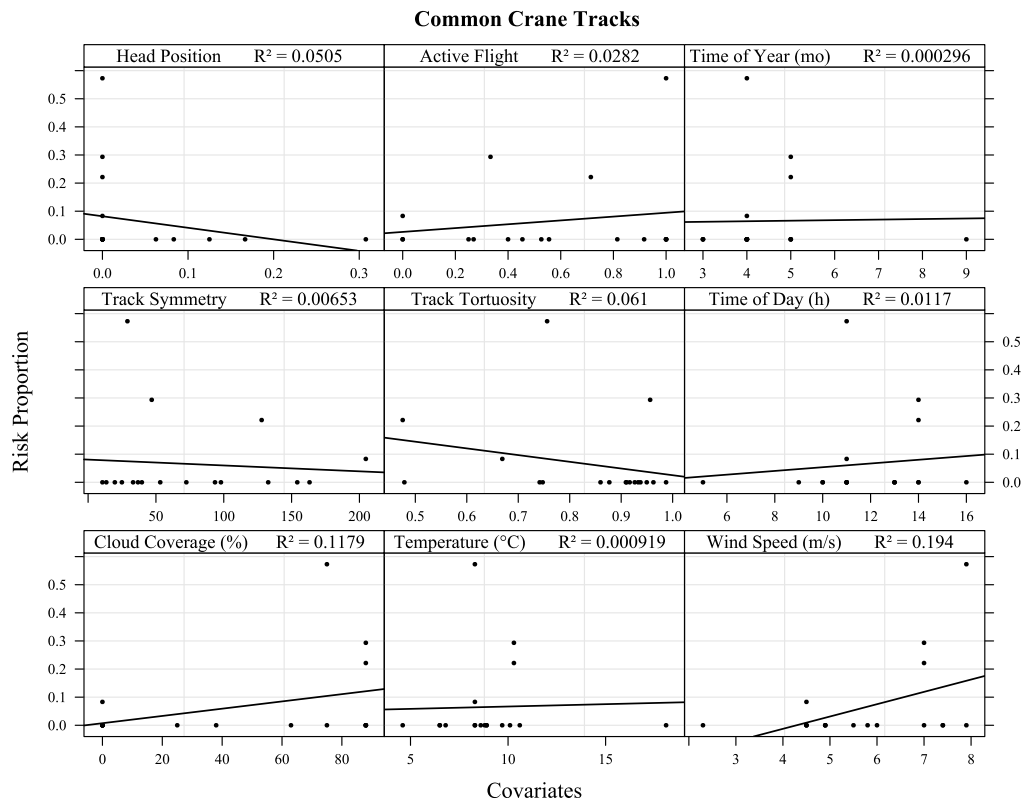
Common Buzzard Tracks

Figure H.5. Proportion time spent in risk zone as a function of each possible explanatory variable. A regression trend line is depicted for each plot along with the coefficient of determination (R^2) and significance level.

Red Kite Tracks

Figure H.6. Proportion time spent in risk zone as a function of each possible explanatory variable. A regression trend line is depicted for each plot along with the coefficient of determination (R^2) and significance level.
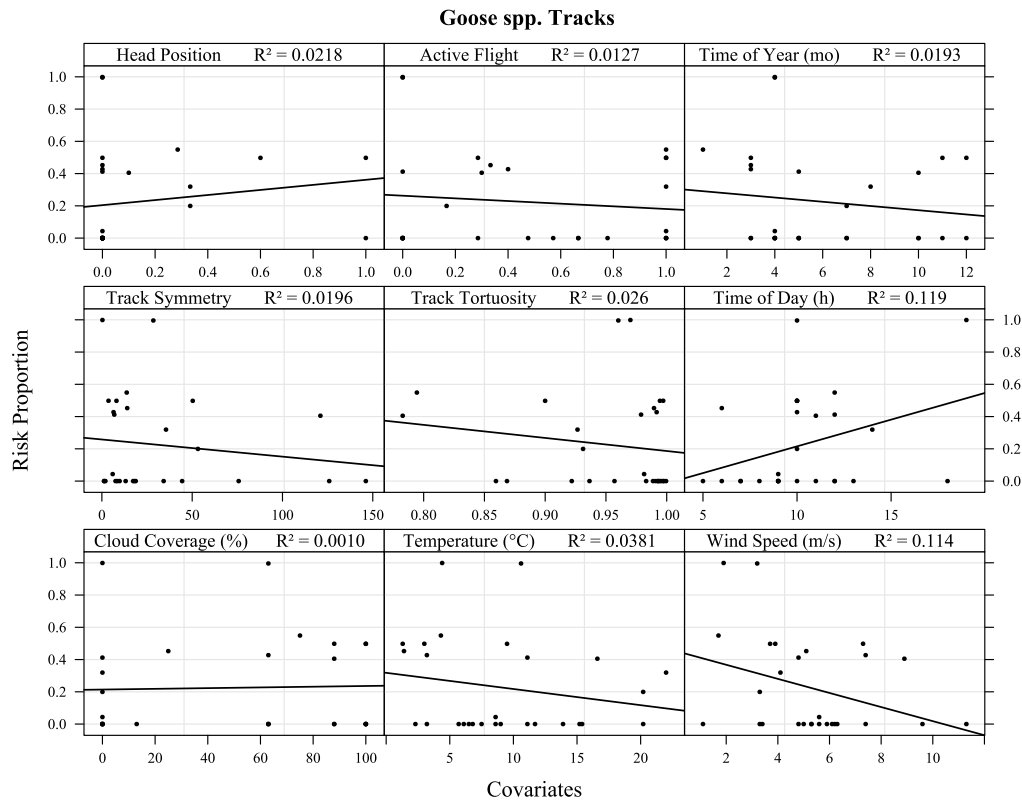
Great Cormorant Tracks

Figure H.7. Proportion time spent in risk zone as a function of each possible explanatory variable. A regression trend line is depicted for each plot along with the coefficient of determination (R^2) and significance level.
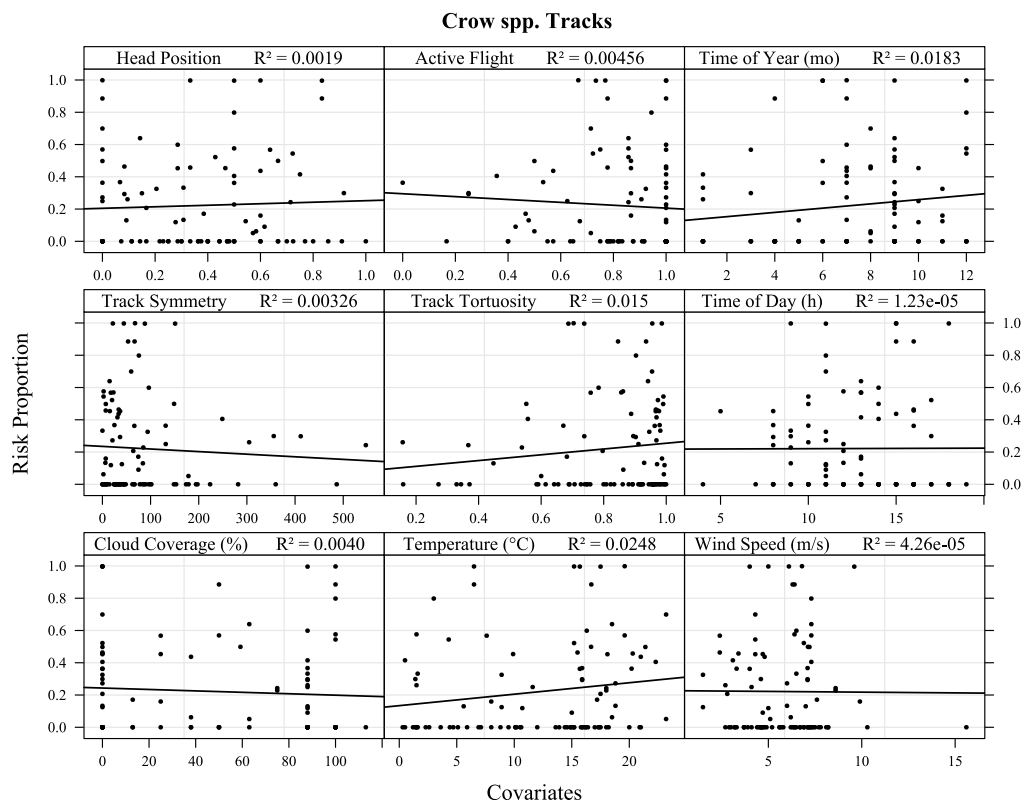
Grey Heron Tracks

Figure H.8. Proportion time spent in risk zone as a function of each possible explanatory variable. A regression trend line is depicted for each plot along with the coefficient of determination (R^2) and significance level.

Common Crane Tracks

Figure H.9. Proportion time spent in risk zone as a function of each possible explanatory variable. A regression trend line is depicted for each plot along with the coefficient of determination (R^2) and significance level.
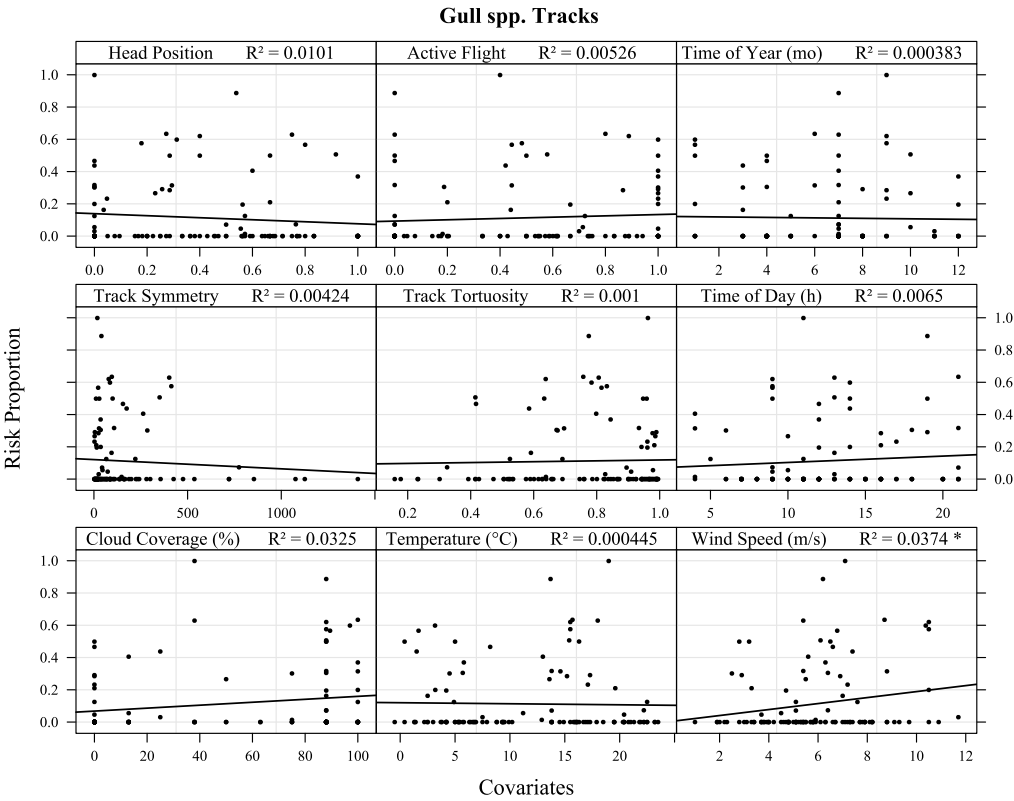
Goose spp. Tracks

Figure H.10. Proportion time spent in risk zone as a function of each possible explanatory variable. A regression trend line is depicted for each plot along with the coefficient of determination (R^2) and significance level.
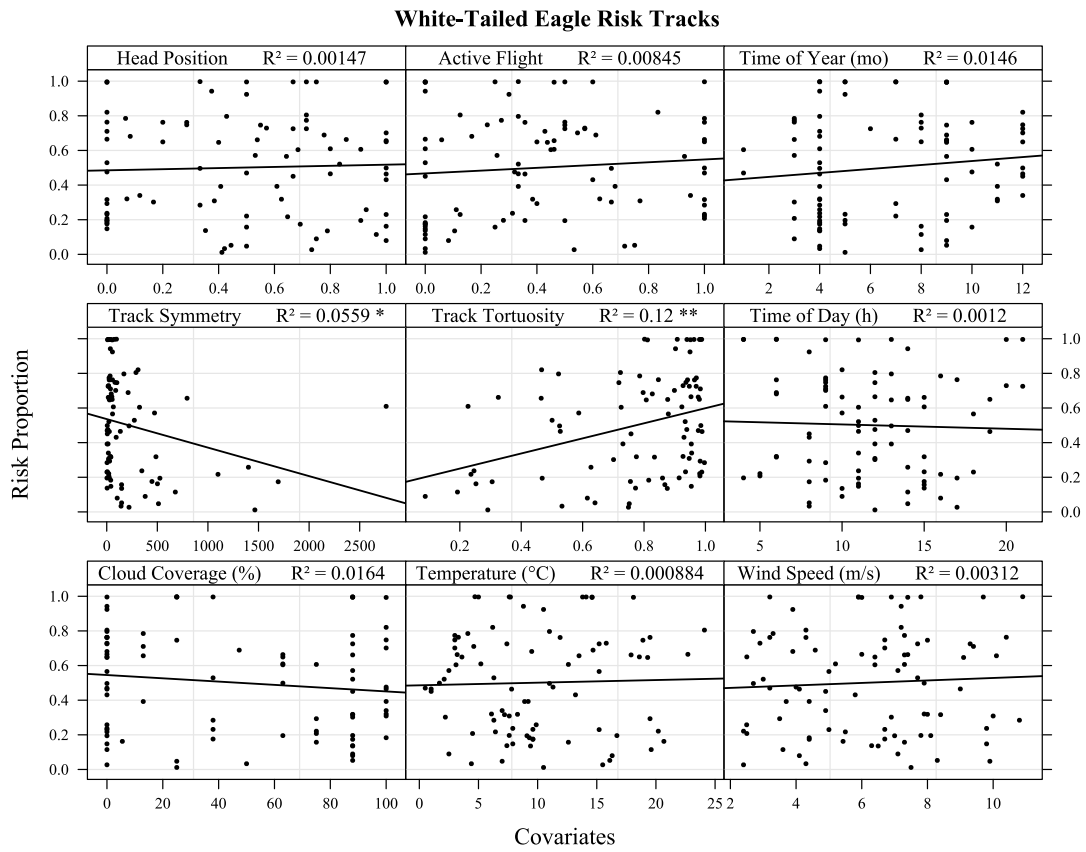
Crow spp. Tracks

Figure H.11. Proportion time spent in risk zone as a function of each possible explanatory variable. A regression trend line is depicted for each plot along with the coefficient of determination (R^2) and significance level.

Figure H.12. Proportion time spent in risk zone as a function of each possible explanatory variable. A regression trend line is depicted for each plot along with the coefficient of determination (R^2) and significance level.

Figure H.13. Proportion time spent in risk zone as a function of each possible explanatory variable. A regression trend line is depicted for each plot along with the coefficient of determination (R^2) and significance level.
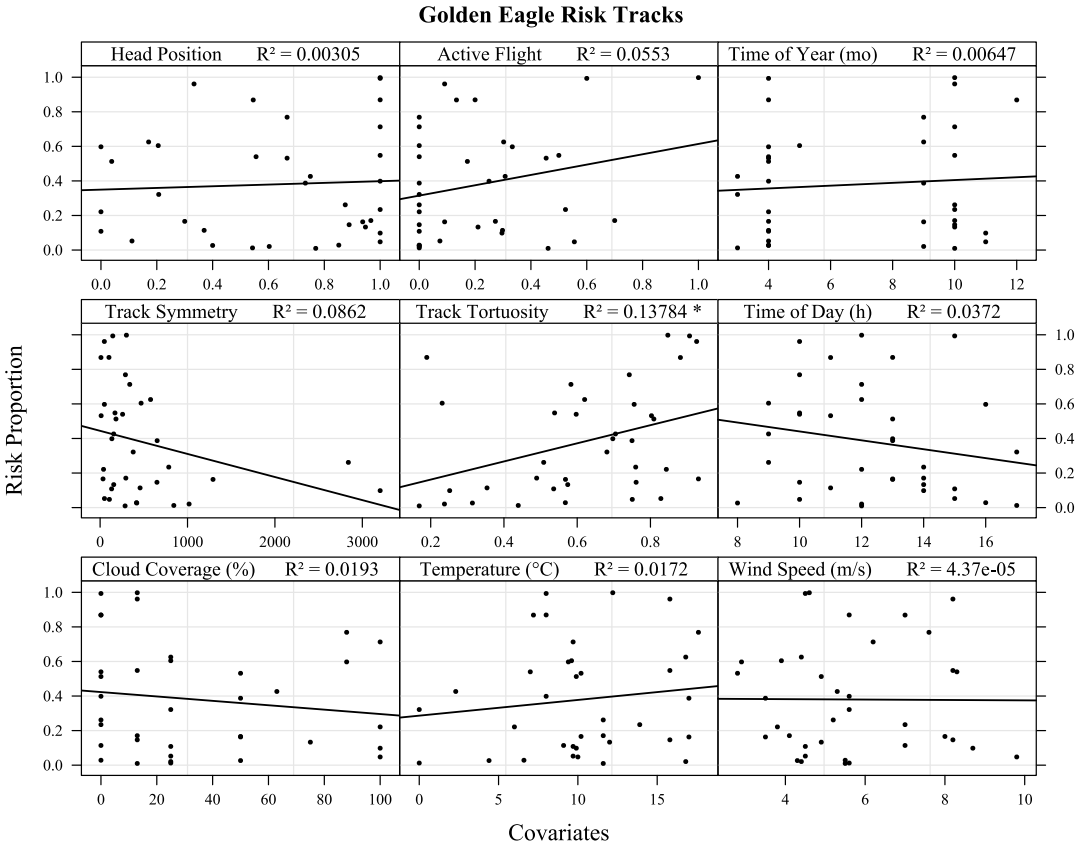
Golden Eagle Risk Tracks

Figure H.14. Proportion time spent in risk zone as a function of each possible explanatory variable. A regression trend line is depicted for each plot along with the coefficient of determination (R^2) and significance level.
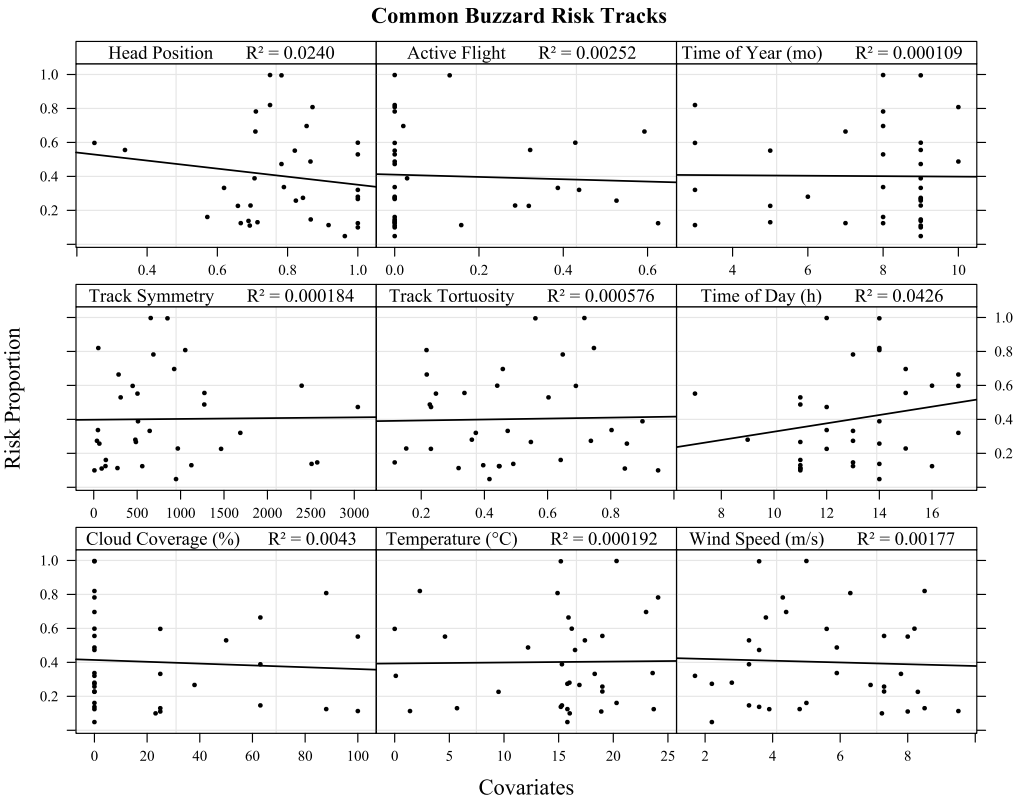
Figure H.15. Proportion time spent in risk zone as a function of each possible explanatory variable. A regression trend line is depicted for each plot along with the coefficient of determination (R^2) and significance level.

Figure H.16. Proportion time spent in risk zone as a function of each possible explanatory variable. A regression trend line is depicted for each plot along with the coefficient of determination (R^2) and significance level.
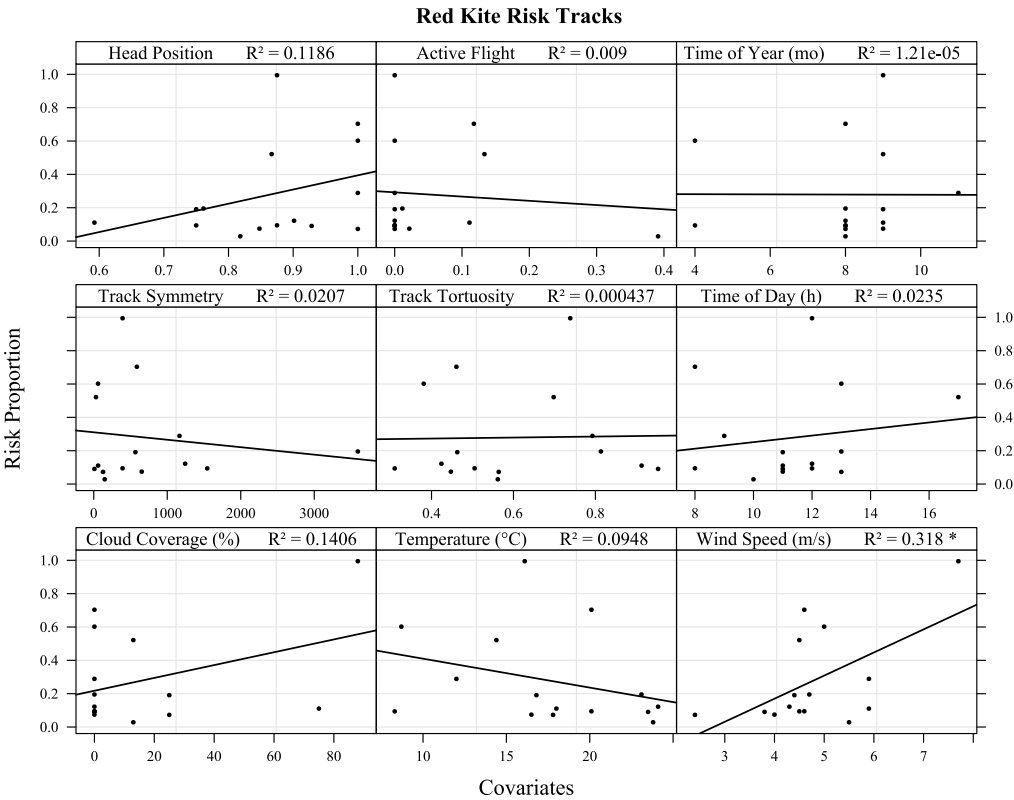
Figure H.17. Proportion time spent in risk zone as a function of each possible explanatory variable. A regression trend line is depicted for each plot along with the coefficient of determination (R^2) and significance level.
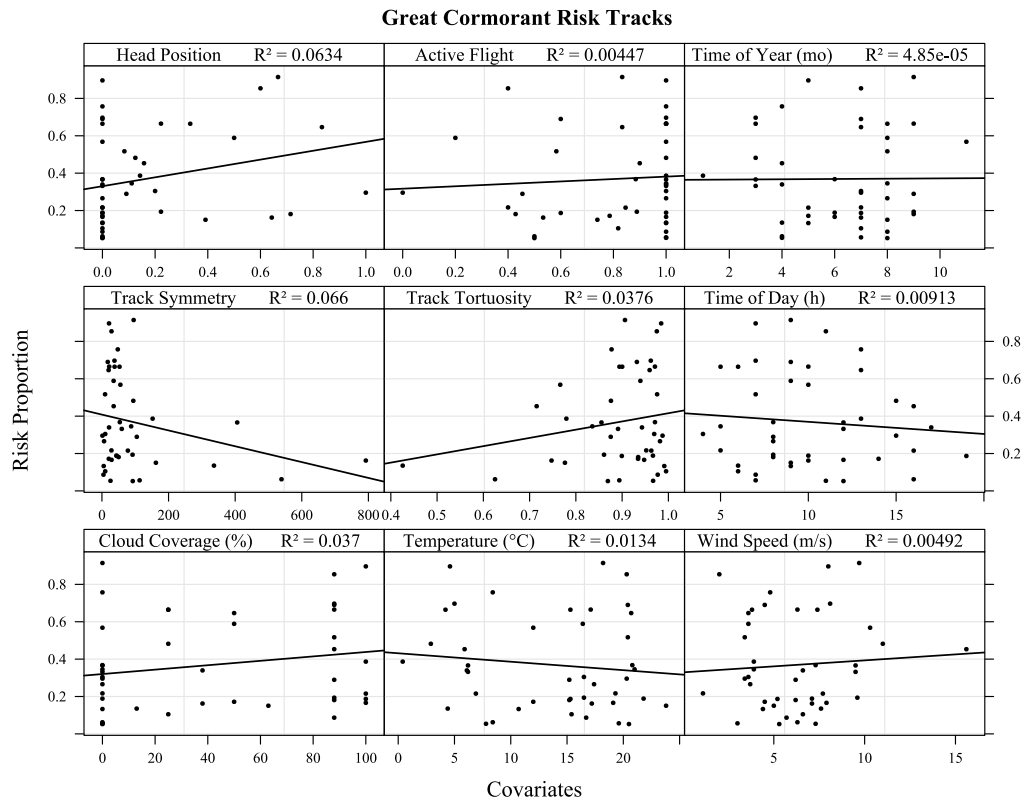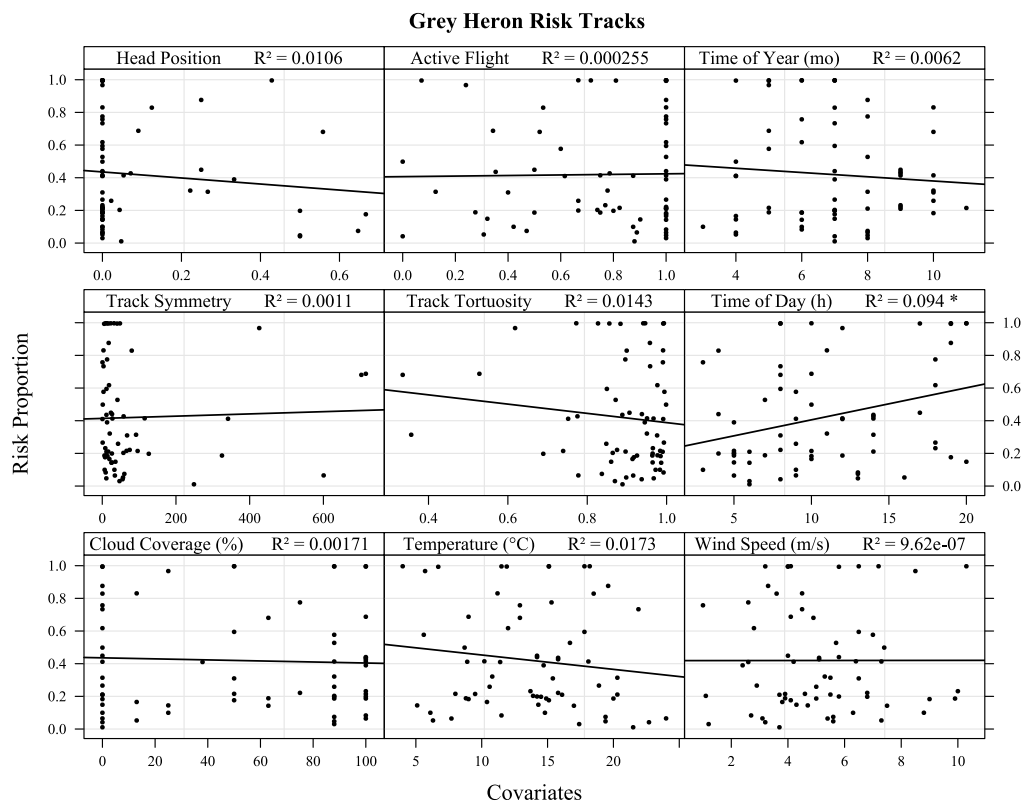

Figure H.18. Proportion time spent in risk zone as a function of each possible explanatory variable. A regression trend line is depicted for each plot along with the coefficient of determination (R^2) and significance level.

Appendix I. Model selection

The automated model selection was carried out for models both with and without interactions for all tracks, raptor tracks, all risk tracks, and raptor risk tracks. For each subset the models with and without interactions were compared based on their respective AIC values. Moreover, an Anova test using the χ^2 test statistic was also used to assess the goodness of fit of the nested regression models, i.e. the models with and without interactions [39]. The model with interactions was selected as the best model if the addition of interaction terms significantly increased the model's goodness of fit, if not the simpler of the two models, i.e. the model without interactions, was selected. The models that were not selected as the best models are presented below.

Table I.1. Details of the automated model selection completed with *glmulti*. The * annotation indicates that the addition of interaction terms significantly improved the model's goodness of fit.

Name	No. of tracks	No. of generations	Best AIC
All tracks			
Without interactions	886	250	274
With interactions	886	640	274
Raptor tracks*			
Without interactions	411	250	155
With interactions	411	550	153
All risk track			
Without interactions	387	250	130
With interactions	387	690	128
Raptor risk tracks			
Without interactions	178	250	65.7
With interactions	178	460	61.7
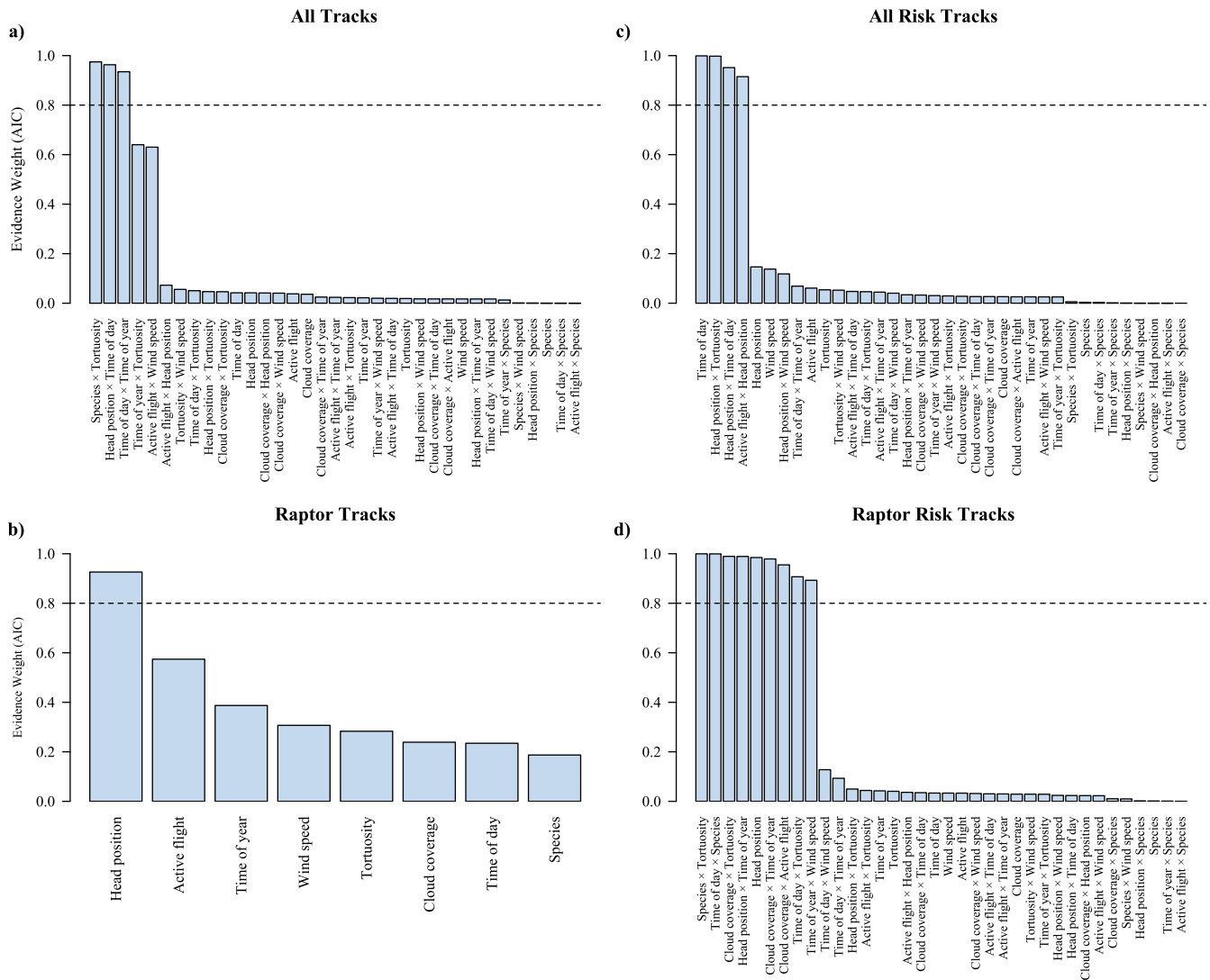
Figure I.1. Each term's estimated importance computed as the sum of the relative weights of all models in which the term appears.

References

1. Drewitt, A.L.; Langston, R.H.W. Assessing the Impacts of Wind Farms on Birds. *Ibis* **2006**, *148*, 29–42. doi:10.1111/j.1474-919X.2006.00516.x.

2. Madders, M.; Whitfield, D.P. Upland Raptors and the Assessment of Wind Farm Impacts. *Ibis* **2006**, *148*, 43–56. doi:10.1111/j.1474-919X.2006.00506.x.

3. de Lucas, M.; Janss, G.F.E.; Whitfield, D.P.; Ferrer, M. Collision Fatality of Raptors in Wind Farms does not Depend on Raptor Abundance. *Journal of Applied Ecology* **2008**, *45*, 1695–1703. doi:10.1111/j.1365-2664.2008.01549.x.

4. Smallwood, K.S.; Thelander, C. Bird Mortality in the Altamont Pass Wind Resource Area, California. *The Journal of Wildlife Management* **2008**, *72*, 215–223. doi:10.2193/2007-032.

5. Bevanger, K.; Berntsen, F.; Clausen, S.; Dahl, E.L.; Flagstad, Ø.; Follestad, A.; Halley, D.; Hanssen, F.; Johnsen, L.; Kvaløy, P.; Lund-Hoel, P.; May, R.; Nygård, T.; Pedersen, H.C.; Reitan, O.; Røskaft, E.; Steinheim, Y.; Stokke, B.; Vang, R. *Pre- and Post-construction Studies of Conflicts Between Birds and Wind Turbines in Coastal Norway (Bird-Wind). Report on Findings 2007-2010*, 2010.

6. Katzner, T.E.; Brandes, D.; Miller, T.; Lanzone, M.; Maisonneuve, C.; Tremblay, J.A.; Mulvihill, R.; Jr, G.T.M. Topography Drives Migratory Flight Altitude of Golden Eagles: Implications for On-Shore Wind Energy Development. *Journal of Applied Ecology* **2012**, *49*, 1178–1186. doi:10.1111/j.1365-2664.2012.02185.x.

7. Loss, S.R.; Will, T.; Marra, P.P. Estimates of Bird Collision Mortality at Wind Facilities in the Contiguous United States. *Biological Conservation* **2013**, *168*, 201–209. doi:10.1016/j.biocon.2013.10.007.

8. Marques, A.T.; Batalha, H.; Rodrigues, S.; Costa, H.; Pereira, M.J.R.; Fonseca, C.; Mascarenhas, M.; Bernardino, J. Understanding Bird Collisions at Wind Farms: An Updated Review on the Causes and Possible Mitigation Strategies. *Biological Conservation* **2014**, *179*, 40–52. doi:10.1016/j.biocon.2014.08.017.

9. Watson, R.T.; Kolar, P.S.; Ferrer, M.; Nygård, T.; Johnston, N.; Hunt, W.G.; Smit-Robinson, H.A.; Farmer, C.J.; Huso, M.; Katzner, T.E. Raptor Interactions with Wind Energy: Case Studies from Around the World. *The Journal of Raptor Research* **2018**, *52*, 1–18.

10. Perold, V.; Ralston-Paton, S.; Ryan, P. On a Collision Course? The Large Diversity of Birds Killed by Wind Turbines in South Africa. *Journal of African Ornithology* **2020**, *91*, 228–239. doi:10.2989/00306525.2020.1770889.

11. Powlesland, R.G. Impacts of Wind Farms on Birds: A Review. *Science for Conservation* **2009**, *289*.

12. Barrios, L.; Rodríguez, A. Behavioural and Environmental Correlates of Soaring-bird Mortality at On-shore Wind Turbines. *Journal of Applied Ecology* **2004**, *41*, 72–81. doi:10.1111/j.1365-2664.2004.00876.x.

13. Martin, G.R.; Portugal, S.J.; Murn, C.P. Visual Fields, Foraging and Collision Vulnerability in *Gyps vultures*. *Ibis* **2012**, *154*, 626–631. doi:10.1111/j.1474-919X.2012.01227.x.

14. Potier, S.; Duriez, O.; Cunningham, G.B.; Bonhomme, V.; O'Rourke, C.; Fernàndez-Juricic, E.; Bonadonna, F. Visual Field Shape and Foraging Ecology in Diurnal Raptors. *Journal of Experimental Biology* **2018**, *221*, jeb177295. doi:10.1242/jeb.177295.

15. Janss, G. Avian mortality from power lines: a morphologic approach of a species-specific mortality. *Molecular Biology and Evolution* **2000**, *10*, 512–526.

16. Therkildsen, O.R.; Elmeros, M.; Kahlert, J.; Desholm, M. Baseline Investigations of Bats and Birds at Wind Turbine Test Centre Østerild. *Scientific Report from DCE - Danish Centre for Environment and Energy* **2012**, *28*.

17. Navarrete, L.; Griffis-Kyle, K.L. Sandhill Crane Collisions with Wind Turbines in Texas. *Proceedings of the North American Crane Workshop* **2016**, *13*, 380.

18. Powlesland, R.G. Bird Species of Concern at Wind Farms in New Zealand. *DOC Research & Development Series* **2009**, *317*.

19. Johnston, N.N.; Bradley, J.E.; Otter, K.A. Increased Flight Altitudes Among Migrating Golden Eagles Suggest Turbine Avoidance at a Rocky Mountain Wind Installation. *PloS one* **2014**, *9*, e93030. doi:10.1371/journal.pone.0093030.

20. Murgatroyd, M.; Photopoulou, T.; Underhill, L.G.; Bouten, W.; Amar, A. Where Eagles Soar: Fine-Resolution Tracking Reveals the Spatiotemporal Use of Differential Soaring Modes in a Large Raptor. *Ecology and Evolution* **2018**, *8*, 6788–6799. doi:10.1002/ece3.4189.

21. Marques, A.T.; Santos, C.D.; Hanssen, F.; Muñoz, A.; Onrubia, A.; Wikelski, M.; Moreira, F.; Palmeirim, J.M.; Silva, J.P. Wind Turbines Cause Functional Habitat Loss for Migratory Soaring Birds. *Journal of Animal Ecology* **2019**, *89*, 93–103. doi:10.1111/1365-2656.12961.

22. May, R.; Hoel, P.L.; Langston, R.; Dahl, E.L.; Bevanger, K.; Reitan, O.; Nygård, T.; Pedersen, H.C.; Røskaft, E.; Stokke, B.G. *Collision Risk in White-tailed Eagles. Modelling Collision Risk using Vantage Point Observations in Smøla Wind-power Plant*, 2010.

23. Blomberg, S.P.; Garland Jr, T.; Ives, A.R. Testing for Phylogenetic Signal in Comparative Data: Behavioral Traits are More Labile. *Evolution* **2003**, *57*, 717–745.

24. Losos, J.B. Phylogenetic Niche Conservatism, Phylogenetic Signal and the Relationship Between Phylogenetic Relatedness and Ecological Similarity Among Species. *Ecology Letters* **2008**, *11*, 995–1003. doi:10.1111/j.1461-0248.2008.01229.x.

25. Kamilar, J.M.; Cooper, N. Phylogenetic Signal in Primate Behaviour, Ecology and Life History. *Philosophical Transactions of the Royal Society B* **2013**, *368*, 20120341. doi:10.1098/rstb.2012.0341.

26. Blomberg, S.P.; Garland Jr, T. Tempo and Mode in Evolution: Phylogenetic Inertia, Adaptation and Comparative Methods. *Journal of Evolutionary Biology* **2002**, *15*, 889–910. doi:10.1046/j.1420-9101.2002.00472.x.

27. Herrera-Alsina, L.; Villegas-Patraca, R.; Eguiarte, L.E.; Artia, H.T. Bird communities and wind farms: a phylogenetic and morphological approach. *Biodiversity and Conservation* **2013**, *22*, 2821–2836. doi:10.1007/s10531-013-0557-6.

28. Linder, A.; Lyhne, H.; Laubek, B.; Bruhn, D.; Pertoldi, C. Quantifying Raptors' Flight Behavior to Assess Collision Risk and Avoidance Behavior to Wind Turbines. *Preprints* **2021**, *2021020391*. doi:10.20944/preprints202102.0391.v1.

29. McClure, C.J.W.; Martinson, L.; Allison, T.D. Automated Monitoring for Birds in Flight: Proof of Concept with Eagles at a Wind Power Facility. *Biological Conservation* **2018**, *224*, 26–33. doi:10.1016/j.biocon.2018.04.041.

30. McClure, C.J.W.; Rolek, B.W.; Dunn, L.; McCabe, J.D.; Martinson, L.; Katzner, T. Eagle Fatalities are Reduced by Automated Curtailment of Wind Turbines. *Journal of Applied Ecology* **2021**, *58*, 446–452. doi:10.1111/1365-2664.13831.

31. Esri.; HERE.; Garmin.; FAO.; NOAA.; USGS. *World Topographic Map*, 2020. http://www.esri.com/.

32. Wirdheim, A.; Corell, M. *Fågelrapport*, 2015.

33. Aldén, L.; Ottvall, R.; Soares, J.P.D.S.; Klein, J.; Liljenfeldt, J. *Rapport: Samexistens Örnar och Vindkraft på Gotland*, 2017.

34. Esri. *ArcGIS Pro 2.5.0*, 2020. http://www.esri.com/.

35. SMHI, S.M.; Institute, H. *SMHI, Swedish Meteorological and Hydrological Institute*. Norrköping, 2020. www.smhi.se.

36. R Core Team. *R version 4.0.3*. R Foundation for Statistical Computing, Vienna, Austria, 2020.

37. Zuur, A.F.; Ieno, E.N.; Elphick, C.S. A Protocol for Data Exploration to Avoid Common Statistical Problems. *Methods in Ecology and Evolution* **2010**, *1*, 3–14. doi:10.1111/j.2041-210X.2009.00001.x.

38. Calcagno, V.; de Mazancourt, C. glmulti: An R Package for Easy Automated Model Selection with (Generalized) Linear Models. *Journal of Statistical Software* **2010**, *34*. doi:10.18637/jss.v034.i12.

39. Zuur, A.F.; Ieno, E.N.; Walker, N.J.; Saveliev, A.A.; Smith, G.M. *Mixed Effects Models and Extensions in Ecology with R*; Statistics for Biology and Health, Springer New York: New York, NY, 1009.

40. Kumar, S.; Stecher, G.; Li, M.; Knyaz, C.; Tamura, K. MEGA X: Molecular Evolutionary Genetics Analysis across Computing Platforms. *Molecular Biology and Evolution* **2018**, *35*, 1547–1549.

41. Tamura, K.; Nei, M. Estimation of the Number of Nucleotide Substitutions in the Control Region of Mitochondrial DNA in Humans and Chimpanzees. *Molecular Biology and Evolution* **1993**, *10*, 512–526.

42. Hillis, D.M.; Bull, J.J. An Empirical Test of Bootstrapping as a Method for Assessing Confidence in Phylogenetic Analysis. *Systematic Biology* **1993**, *42*, 182–192. doi:10.2307/2992540.

43. Pacheco, M.A.; Battistuzzi, F.U.; Lentino, M.; Aguilar, R.F.; Kumar, S.; Escalante, A.A. Evolution of Modern Birds Revealed by Mitogenomics: Timing the Radiation and Origin of Major Orders. *Molecular Biology and Evolution* **2011**, *28*, 1927–1942. doi:10.1093/molbev/msr014.

44. Benson, D.A.; Cavanaugh, M.; Clark, K.; Karsch-Mizrachi, I.; Lipman, D.J.; Ostell, J.; Sayers, E.W. GenBank. *Nucleic Acids Research* **2017**, *45*, D37–D42. doi:10.1093/nar/gkw1070.

45. Edgar, R.C. MUSCLE: a Multiple Sequence Alignment Method with Reduced Time and Space Complexity. *BMC Bioinformatics* **2003**, *5*, 113. doi:10.1186/1471-2105-5-113.

46. Swenson, N.G. *Functional and Phylogenetic Ecology in R*; Use R!, Springer New York: New York, NY, 2014.

47. Peron, b. The energy landscape predicts flight height and wind turbine collision hazard in three species of large soaring raptor. *Molecular Biology and Evolution* **2017**, *10*, 512–526.

48. Adams, D.C. Comparing Evolutionary Rates for Different Phenotypic Traits on a Phylogeny Using Likelihood. *Systematic Biology* **2013**, *62*, 181–192. doi:10.1093/sysbio/sys083.

49. Weeks, B.C.; Naeem, S.; Winger, B.M.; Cracraft, J. The Relationship Between Morphology and Behavior in Mixed-Species Flocks of Island Birds. *Ecology and Evolution* **2020**, *10*, 10593–10606. doi:10.1002/ece3.6714.

50. Zuur, A.F.; Ieno, E.N.; Smith, G.M. *Analysing Ecological Data*; Statistics for Biology and Health, Springer New York: New York, NY, 2007.

Is Virtual Fencing an Effective Way of Enclosing Cattle? Personality, Herd Behavior and Welfare

Anne Cathrine Linder [1]*

1   Department of Chemistry and Bioscience — Section of Biology and Environmental Science, Aalborg University, Fredrik Bajers Vej 7, 9220 Aalborg, Denmark
*   Correspondence: c.linder04@gmail.com

Simple Summary: Virtual fences provide boundaries without physical barriers. Virtual fencing systems utilize a collar and GPS technology for tracking animals and delivering audio warnings and electric impulses to the animals when approaching the designated virtual boundary. These GPS-based fencing systems have the potential to improve grazing management. This article examines the use of the Nofence© virtual fencing system to keep a group of twelve Angus cows within a virtual enclosure without compromising animal welfare. Within 139 days the cows had learned to respond to the auditory warnings, thus, respecting the virtual boundaries. The virtual fence was generally successful in keeping the cows within the virtual enclosure. The virtual enclosure was expanded and subsequently made smaller several times, and the animals did not show significant issues adapting to the new border placement. The cattle did not express any significant changes in their behavior upon receiving an electrical impulse from the collar. However, they did display inter-individual differences, indicating that the personality of the cows should be taken into account when selecting animals for placement in virtual enclosures. The cows also reacted to herd mates receiving electric impulses showing that they are influenced by their herd mates.

Abstract: In modern nature conservation and rewilding there is a need for controlling the movements of large grazers in extensively managed areas. The inflexibility of physical fencing can be a limitation in nature management, and the physical boundaries created by physical fencing can have detrimental effects on wildlife. Virtual fencing systems provide boundaries without physical structures. These systems utilize collars with GPS technology to track animals and deliver auditory or electric cues to encourage the animals to stay within the predefined boundaries. This study aims to assess the use of virtual fencing (Nofence©) to keep twelve Angus cows (*Bos taurus*) within a virtual enclosure without compromising their welfare. As such, the study examines inter-individual differences between the cows as well as their herd behavior, when reacting and learning to respond appropriately to virtual fencing. Moreover, the activity of the cows was used as an indicator of welfare. The virtual fencing was successful in keeping the herd within the designated area. Moreover, the cattle learned to avoid the virtual border and respond to auditory cues, where the cows received significantly more auditory warning and electric impulses per week throughout the first 14 days than the remaining 125 days ($p < 0.001$). The cows were found to express both inter-individual differences ($p < 0.001$) and herd behavior. The cattle did not express any significant changes in their activity upon receiving an electrical impulse from the collar. Thus, indicating that there were little to no acute welfare implications associated with the use of virtual fencing in this study. This study clearly supports the potential for virtual fencing as a viable alternative to physical electric fencing. However, it also shows that both individual differences in personality and herd structure should be considered when selecting individuals for virtual fencing.

Keywords: virtual fencing; Nofence©; Angus cattle; animal welfare; animal behavior; animal personality; nature conservation

1. Introduction

In recent years, nature conservationists have become aware of the beneficial effects of rewilding, with large organizations such as the European Union expressing interest in the subject [1]. Rewilding utilizes large grazers in large areas to achieve the desired effects on the composition of vegetation in the landscape, increasing the need for large peripheral fencing. Physical barriers, such as those created by physical electric fencing, can have detrimental effects on wildlife [2,3]. Moreover, physical fencing cannot be readily adapted to changing circumstances. The inflexibility of physical fencing is often described as a limitation in nature management, e.g., when dealing with seasonal changes in vegetation, or periods when animals need to be excluded from environmentally-sensitive areas [4,5]. Virtual fencing has, therefore, been developed as an alternative to physical fencing. This type of fencing using GPS technology has been shown to be an effective way of keeping animals within an area [6–10]. This could prove to be a flexible fencing option for extensive grazing of large areas.

Virtual fencing works by attaching a collar to each animal that can administer auditory warnings (82 dB, 1 m) and low energy electric impulses (0.2 J, 3 kV, 1.0 s). However, this is illegal in a number of European countries including

Denmark, under current regulations. Moreover, animal welfare has been shown to be a concern for the public when it comes to implementing virtual fencing technology [11]. Thus, to determine whether virtual fencing is suitable for use in nature conservation, it has to be ensured, that welfare is not compromised. When referring to animal welfare in this paper the term is mainly associated with the basic health and functioning of the animals in relation to the animals' behavior. It is, therefore, crucial that the animals are capable of learning to respond to audio cues to avoid unnecessary stress responses.

Previous studies have shown that animal welfare in virtual enclosures is comparable to physical electric fencing, and that cattle and sheep can learn to respond to audio cues and thereby avoid electric impulses [5,12–18]. Thus, suggesting that virtual fencing does not have a negative impact on animal welfare compared to current practices, i.e., physical electric fencing. However, several of these studies investigated the cattle collectively as a group but noted a high inter-individual variance, thus, calling for further research accounting for inter-individual differences [8,12,14,19,20]. Many factors can influence this intra-specific variation in behavior, but one important factor to consider when choosing individuals for virtual fencing could be the expression of personality [21,22]. Animal personality can be defined as individual differences in behavioral traits that are consistent over time and across contexts [23,24]. Another apparent problem with pooling individuals in welfare assessments is the fact that cattle are social animals living together in herds. Therefore, they cannot be considered as completely independent units as they will experience socially facilitated learning, as well as possibly reacting to a herd mate being exposed to a stressful situation, such as receiving an electric impulse [20,25–27]. Thus, there is a need for an assessment of individual cow welfare in virtual enclosures and their individual learning ability to respond appropriately to the auditory cues [20,28].

Virtual fencing could provide useful in the establishment of the new nature national parks that are underway. Enclosing these large areas with physical fencing has been subject to some public opposition. Using virtual fencing eliminates the presence of a physical barrier, thus, eliminating many of the concerns associated with physical fencing. However, the current regulations in Denmark prohibit the use of virtual fencing, due to the unfamiliarity of such systems and their effect on animal welfare. Therefore, this study aims to assess the use of the Nofence© system to keep a group of cattle within a virtual enclosure with minimal welfare implications, i.e., without impairing the cattle's basic health and functioning. This was achieved by studying the individual behavior of twelve Angus cows (*Bos taurus*) in a virtual enclosure wearing Nofence© collars, along with the behavior of the entire herd collectively. It was hypothesized that the Nofence© virtual fencing system would be successful in keeping the cows within the virtual enclosure. Furthermore, the cows were hypothesized to learn to respond appropriately to the virtual fence, i.e., reacting to the audio cues alone and receiving fewer electric impulses. In order to thoroughly assess the use of the virtual fencing system in practice, this study also explored individual and herd factors affecting learning capacity. It was hypothesized that the cows in this experiment would express inter-individual differences. The cows were also hypothesized to express herd behavior by reacting to electric impulses received by herd mates. Lastly, the activity of the cattle was utilized as an indicator of welfare. Here, it was hypothesized that the general level of activity of the cows would not differ immediately before and after receiving an electric impulse, indicating no effect on their basic health and functioning.

2. Methods

2.1. Animals and Location

The study took place on the east coast of the island of Fanø in the southwest of Denmark (Figure 1). The area consisted of 65 ha of coastal meadows to the east and a dune landscape with both dry (heath) and wet parts, with scattered vegetation of trees and bushes to the west. As a sort of border between the two habitat types, a gravel road runs through the study area from north to south, and further two summer residences are nestled on two small dune tops (Figure 1). The animals had access to lush grass close to the waterline and dry areas for resting further inland. The experiment was carried out utilizing twelve Angus cows aged between four and nine years at the start of the experiment. All cows were pregnant and calved during the experiment. The cows were used to traditional physical electric fencing, but not familiar with virtual fencing prior to the study.

2.2. Virtual Fencing System

All data in this experiment was collected using collars developed by the company Nofence© (https://www.nofence.no/en/, accessed on 25 March 2022) fitted around the neck of the animals (Table 1) (Appendix A) [29]. The collars weighed 1446 g and were composed of a silicone strap, placed on top of the animals' neck, connected to two chains that held up a box suspended below the animals' neck, containing the battery, two small solar panels and a GPS receiver. The collars measured the position, heading and speed of the animals. An animal's position is triangulated using the GNSS positioning system (GPS and GLONASS). Heading and speed are continuously calculated from the last two positions of the animal. Each collar had a unique serial number that was included in every message sent by the collar, which

remained constant during the experiment. All cows except one, wore the same collar during the entire experiment. Data points from the animal that had a change in collar were given the same serial number during analysis. This means that each cow had a unique serial number used to reference the animal.
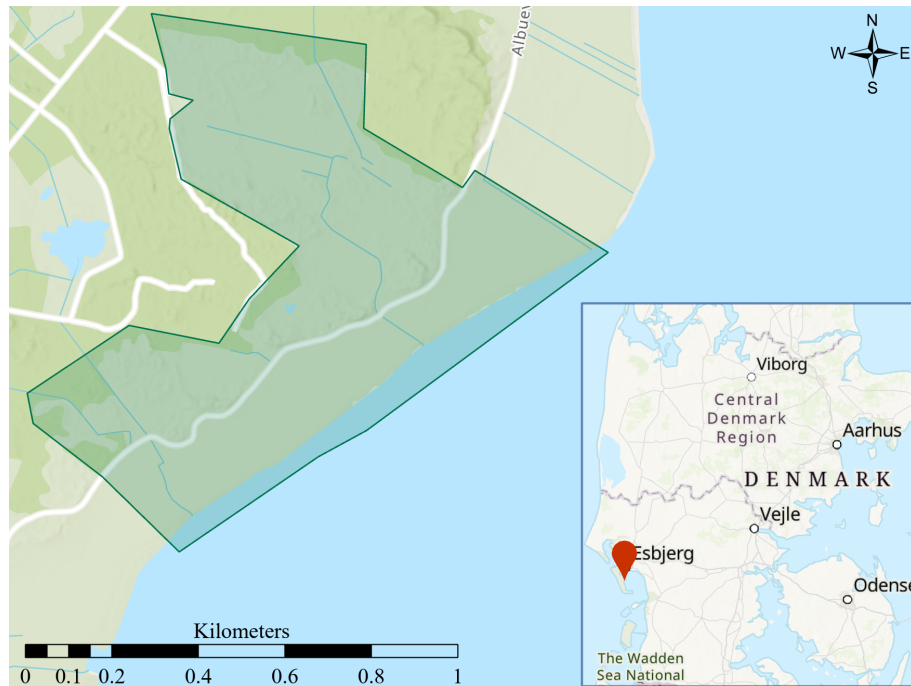
Figure 1. The 65 ha study area on Fanø in the southwest of Denmark. The dark green area marks the area encompassing the largest iteration of the virtual enclosure. The coordinates of the upper left corner of the map frame are 8°26′33″ E 55°24′28″ N.

A virtual boundary was specified, and the collar then used an animal's GPS position to determine if the animal was approaching the virtual boundary (Figure 1). If the animal was found to be approaching the boundary the collar would emit a series of warning sounds, consisting of multiple 82 dB tones increasing in pitch for a duration of 5–20 s, based on whether the animal continued to ignore the warning or turned around. If the animal continued and was in risk of crossing the virtual border, as determined by position, heading, and speed, it would receive an electric impulse of 0.2 J at 3 kV for one second. If the animal slowed down, changed heading, or stopped, the animal did not receive an electric impulse. The animal would continue to receive electric impulses if it did not return to the virtual enclosure up to a maximum of three impulses. If the animal had received three impulses and had not returned to the enclosure the collar would send a notification to the owner, that the animal had escaped. The collar would continue to monitor the animal's position, but the animal would not receive further warnings or electric impulses. If, however, the animal returned to the virtual enclosure the collar returned to normal function and would again administer both warnings and electric impulses when the animal approached the virtual fence. These settings were predetermined by Nofence©.

Table 1: Overview and description of data collected for the data analysis with each message type sent from the Nofence© collars.

Type	Frequency	Description	No. of Obs.
Poll	Every 15 min	Positional data	157,120
Seq	Every 30 min	Activity data	79,633
Warning	After receiving warning	Positional data	1949
Zap	Upon receiving electric impulse	Positional data	197

The experiment began on 29 May 2021 and data collection for this study concluded on 14 October 2021. During the experiment the collars continuously monitored the cows' GPS positions, but only logged GPS data every 15 min and every time a warning or electric impulse was given. Furthermore, the collar recorded the cows' movement and logged their activity every 30 min. The activity of the animals was measured using an accelerometer as a unitless value, as it was

originally developed for sheep. Information about warnings and electric impulses were recorded and transmitted at the time of the event (Table 1).

2.3. Experimental Protocol

On 28 May 2021, twelve cows were placed in an enclosure of about 6.5 hectares, with all four sides being physically electrically fenced. After two days the southern fence line was removed and replaced by a virtual border and the experiment began (Appendix B, Version L.1). This border was then moved about 20 m further south after an additional six days (Appendix B, Version L.2). Then, the border was moved further 20 m twice after three days each (Appendix B Versions L.3 and L.4). On day 14 of the experiment the remaining three sides of the electric fence were removed and the cows were allowed to move freely within a completely virtual enclosure of 35 hectares (Appendix B, Version 1.1). In the following month and a half the enclosure was progressively expanded to 49 hectares until day 62 of the experiment when the cows were then limited to an area of 28 hectares for twelve days and then 15 hectares the following 14 days (Appendix B, Versions 1.1–2.1). After having been limited to a smaller area, the enclosure was then re-expanded to encompass 65 hectares (Appendix B, Versions 2.2–2.6). During the entire experiment, all animals were provided with pasture water pumps but no supplementary food was given. The experiment concluded after 139 days.

2.4. Data and Statistical Analysis

Data was collected as different message types (Table 1). *Poll* messages were sent periodically every 15 min and contain the collar status. The collar status includes the time, the cow's position (latitude and longitude), and the battery voltage in centivolts. *Seq* messages describe the solar charge gathered in the last 30 min and the number of "steps" the cow has moved in the last 30 min. The number of steps was given as a unitless value, as the accelerometer was originally developed for sheep. *Warning* messages were sent when the collar has finished playing a warning sound, either because the cow has turned around, i.e., understanding the warning sound, or because the cow has received an electric pulse. *Warning* messages also contain the duration of the warning sound in milliseconds. *Zap* messages were sent when the collar gives of an electric pulse. One of the cows had its collar changed during the experiment, and for that reason, one day of data was removed for that single individual. No other problems with the collars were discovered.

In total 238,899 messages were recorded by the GPS collars over the course of the 139-day experiment. Of these messages 157,120 were *poll* messages, 79,633 were *seq* messages, 1949 were *warning* messages, and 197 were *zap* messages. For statistical analysis, data was subdivided by message type and the individual from which the data was collected. The data was further divided into three separate periods. *The learning period* being from the beginning of the experiment until day 14, where the remaining physical electric fence was removed, enlarging the enclosure, which now only consisted of virtual borders. *The first period* within the complete virtual enclosure, thus, began on day 15 and lasted until, but not including day 75 where the enclosure size was considerably reduced. *The second period* consequently lasted from day 75 until the end of the experiment on day 139. All data was plotted and sorted in QGIS [30] and all statistical analyses were carried out in R version 4.1.2 [31]. Non-parametric tests were used in the statistical analysis, as the data was not normally distributed.

2.4.1. Distribution within the Virtual Enclosure

In order to evaluate if the Nofence© system was successful in keeping the cows within the virtual enclosure, a heatmap was created for each version of the virtual enclosure, thus, portraying the cows' distribution in relation to the virtual borders throughout the study (Appendix C).

2.4.2. Learning Ability

To determine whether the cows were able to learn to respond appropriately to virtual fencing, thus, receiving fewer warnings and electric impulses with time, the cumulative number of warnings was calculated for each individual and assessed in relation to changes in the virtual border. Differences between the three periods were investigated by comparing the average number of warnings received by the individuals per week for the respective periods using the Mann-Whitney U test. The average number of electric impulses received by the individuals per week was also compared across the three periods with the Mann-Whitney U test.

2.4.3. Inter-Individual Differences

In order to assess any inter-individual differences between the cows, the individuals were compared in regard to the number of auditory warnings and electric impulses they received. The Kruskal Wallis test was used to determine if there was a significant difference between individuals in regard to the number of warnings and electric impulses

received, respectively. These individual differences were further investigated by conducting pairwise comparisons between all individuals using the Mann-Whitney U Test with Bonferroni's correction. Furthermore, the relationship between the number of warnings and number of electric impulses received by the individuals throughout the experiment was tested with Spearman's rank correlation (r_s). This relationship was assessed for the entire experiment and each of the three periods, respectively. Moreover, the number of warnings that each individual received within a given period was compared to that of the other two periods with Spearman's rank correlation (r_s). Likewise, the number of electric impulses that each individual received within a given period was also compared to that of the other two periods with Spearman's rank correlation (r_s).

2.4.4. Herd behavior

To assess the herd behavior of the cows, i.e., cows reacting to a herd mate being exposed to a stressful situation, the reaction of each individual cow was investigated in response to a herd mate receiving an electric impulse. Every time a collar gave an electric impulse to any cow (except following a social panic reaction), the distance from each individual to the virtual border was measured 15, 30, 45 and 60 min prior to the electric impulse and 15, 30, 45 and 60 min after the electric impulse. The difference in median distance to the virtual border, before and after an electric impulse, was tested for each individual using the Mann-Whitney test as well as for the median distance of the herd. This was done separately for each of the three periods.
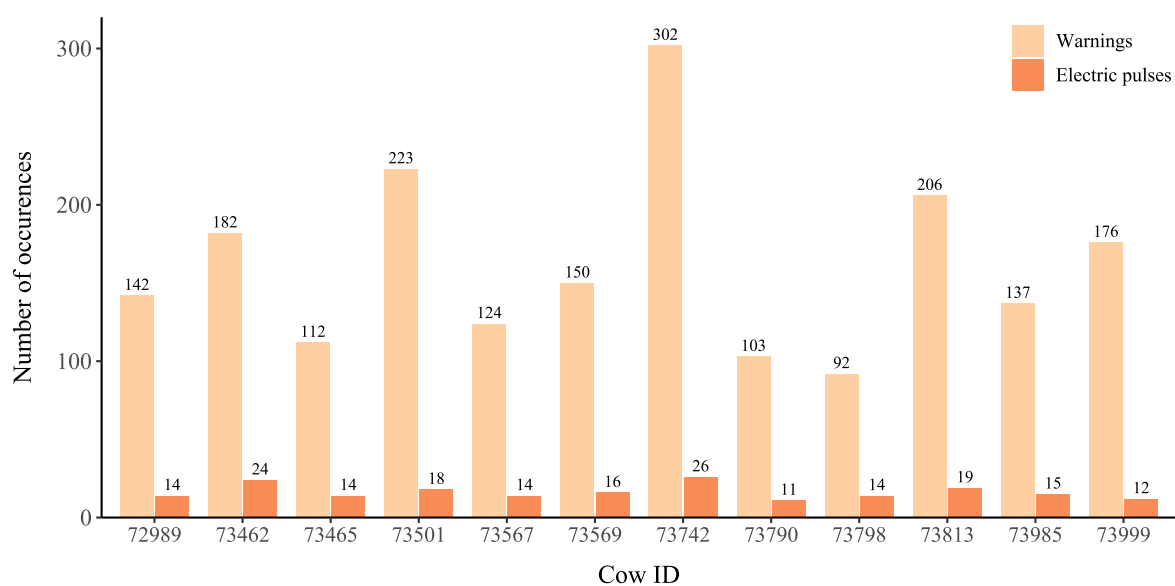
2.4.5. Reactions to Electric Impulse

To investigate whether the activity level of the cows differed after receiving an electric impulse, the total activity of an individual was recorded two hours prior to and two hours following an electric impulse, respectively. Differences in activity before and after receiving an electric impulse were assessed using the Mann-Whitney test. If several electric impulses were administered to an individual in close succession, the activity was only measured two hours before and after the first electric impulse. Additionally, a single occurrence of an individual receiving an electric impulse was removed from the data set as it was not possible to get a representative measure of activity due to the collar failing to record the activity data for a three hour period.

3. Results

3.1. Interactions with the Virtual Border

The twelve cows received 197 electric impulses with each cow receiving between 11 and 26 electric impulses. The cows received 1949 warnings with each cow receiving between 92 and 302 auditory warnings (Figure 2). The virtual fence successfully kept the cows within the virtual boundaries for the majority of the experiment (Appendix C). On four separate occasions, a single cow escaped the enclosure alone, with one other breakout involving three cows.
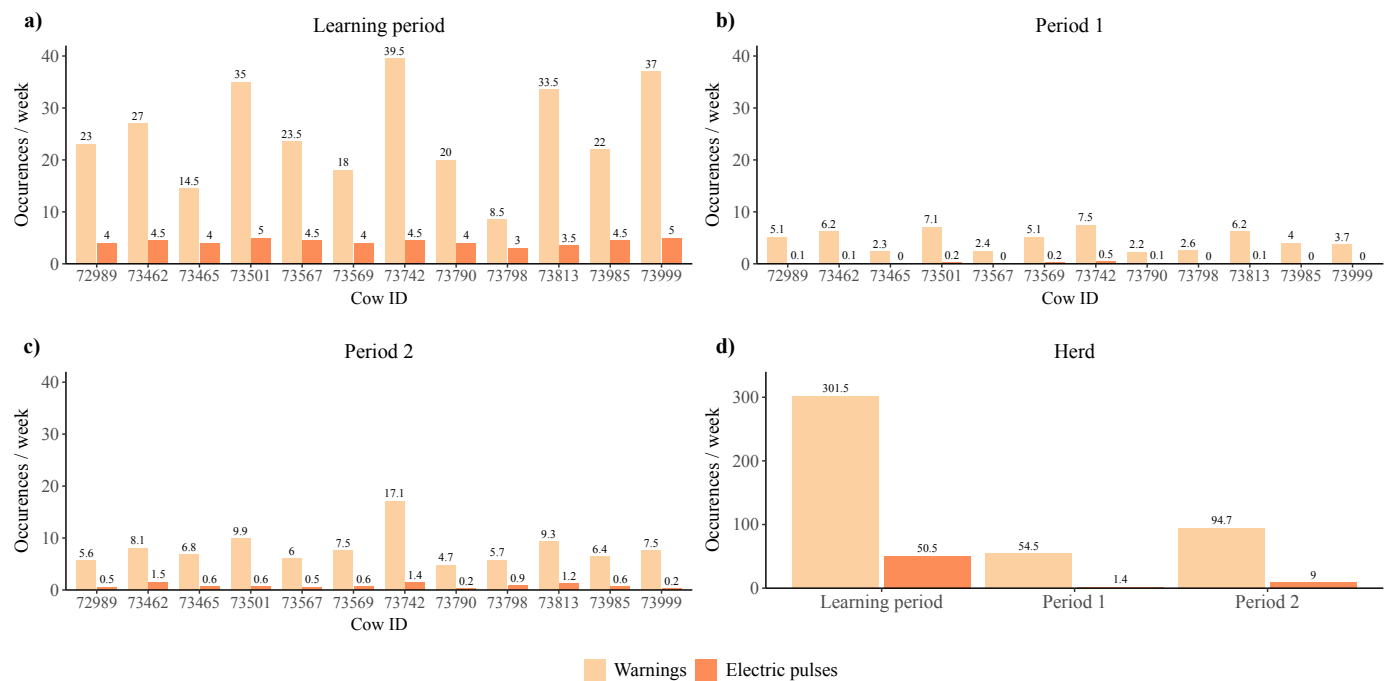

Figure 2. The number of auditory warnings and electric impulses that each individual received throughout the 139-day experiment.

Furthermore, twice all twelve cows escaped and once eight cows escaped due to a social panic reaction. The first time was during the first day of the experiment when the cows experienced the electric impulse for the first time. The second time the virtual border had been placed immediately on the other side of a ditch from the cows, which meant that when the cows tried to cross the ditch they received an electric impulse in the middle of crossing, meaning their only option was to continue forward and out of the enclosure. The border was subsequently moved to avoid further incidents. The final stampede occurred when a journalist flew a drone in low altitude towards and directly above the herd. All escaped cows were brought back to the enclosure within short time. Note that these three social panic reactions account for 104 of the electric impulses received throughout the study and 220 of the warnings received. However, these social panic reactions generally did not affect the results (Appendix F).

3.2. Learning Ability

The cows received significantly more auditory warnings and electric impulses per week during the 14 day *learning period* than during the other two periods ($p < 0.001$) (Figure 3). The cows also received significantly more warnings and electric impulses in *period 2* compared to *period 1* ($p < 0.01$) (Figure 3). Moreover, the ratio between the number of electric impulses and the number of auditory warnings was highest in *the learning period* for most of the individuals and all individuals had the lowest impulse to warning ratio in *period 1*.


Figure 3. Average number of auditory warnings and electric impulses received per week by (**a**) each individual in *the learning period*, (**b**) each individual in *period 1*, (**c**) each individual in *period 2*, and (**d**) by the entire herd during each of the three periods.

When assessing the cumulative warnings each cow received during the three periods, the warning frequency was largest during the beginning of each period and the frequency began to plateau with time (Figure 4). However, in *period 2* there was an increase in warning frequency after the virtual border was changed on day 113. This change in the virtual border allowed the cows to move freely on either side of a gravel road but not on the road itself. This meant the cows had to follow the border some distance into the enclosure to reach a point of free passage across the road, resulting in a disproportionate number of warnings being given in the last period of the experiment.

3.3. Inter-Individual Differences

There was a positive correlation between the number of warnings and electric impulses an individual received over the entire period of the experiment ($r_s = 0.762$ **) (Appendix D). There was also a positive correlation between the number of warnings an individual cow received in *the learning period* and the number of warnings received in *period 1* ($r_s = 0.660$ *) and *period 2* ($r_s = 0.687$ *), respectively (Appendix D). Moreover, the number of warnings an individual received in *period 1* and the number of warnings received in *period 2* were also positively correlated ($r_s = 0.803$ **).

Furthermore, the individuals significantly differed from one another in the number of warnings and electric impulses they received ($p < 0.001$) (Appendix E).
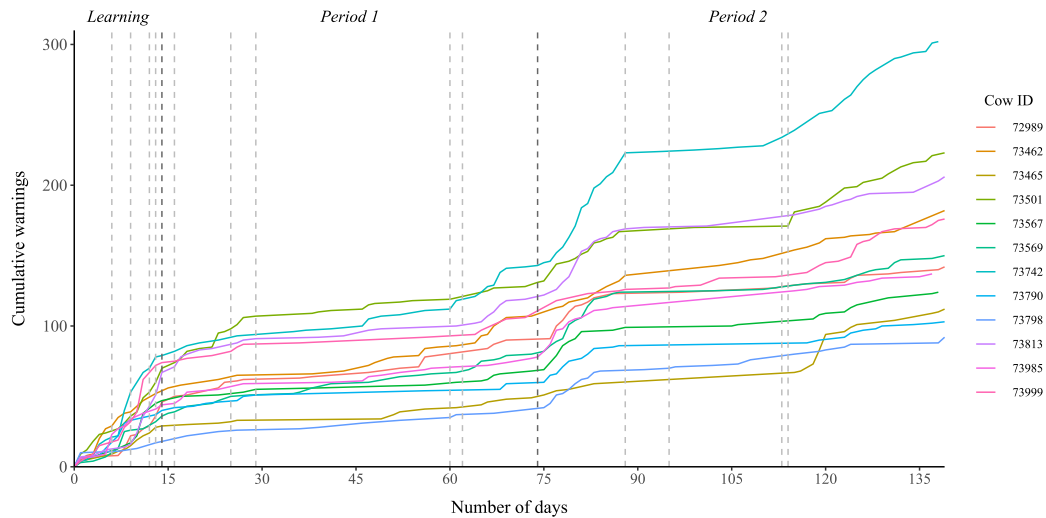
Figure 4. Cumulative number of warnings received by each cow during the three periods. The vertical lines in the plot mark any significant change in the virtual enclosure, where the darker lines indicate the division of the three periods.

3.4. Herd behavior

During *the learning period*, the cows' distance to the virtual border was significantly greater after any one individual received an electric impulse for three of the cows, and for the herd as a whole ($p < 0.05$) (Figure 5a). In the *period 1* of the experiment no significant differences were found in regard to the cows' distance to the virtual border before and after any one individual received an electric impulse (Figure 5b). During *period 2*, the median distance to the virtual border was significantly smaller after any one individual received an electric impulse for six of the twelve cows and for the herd as a whole ($p < 0.05$) (Figure 5c).
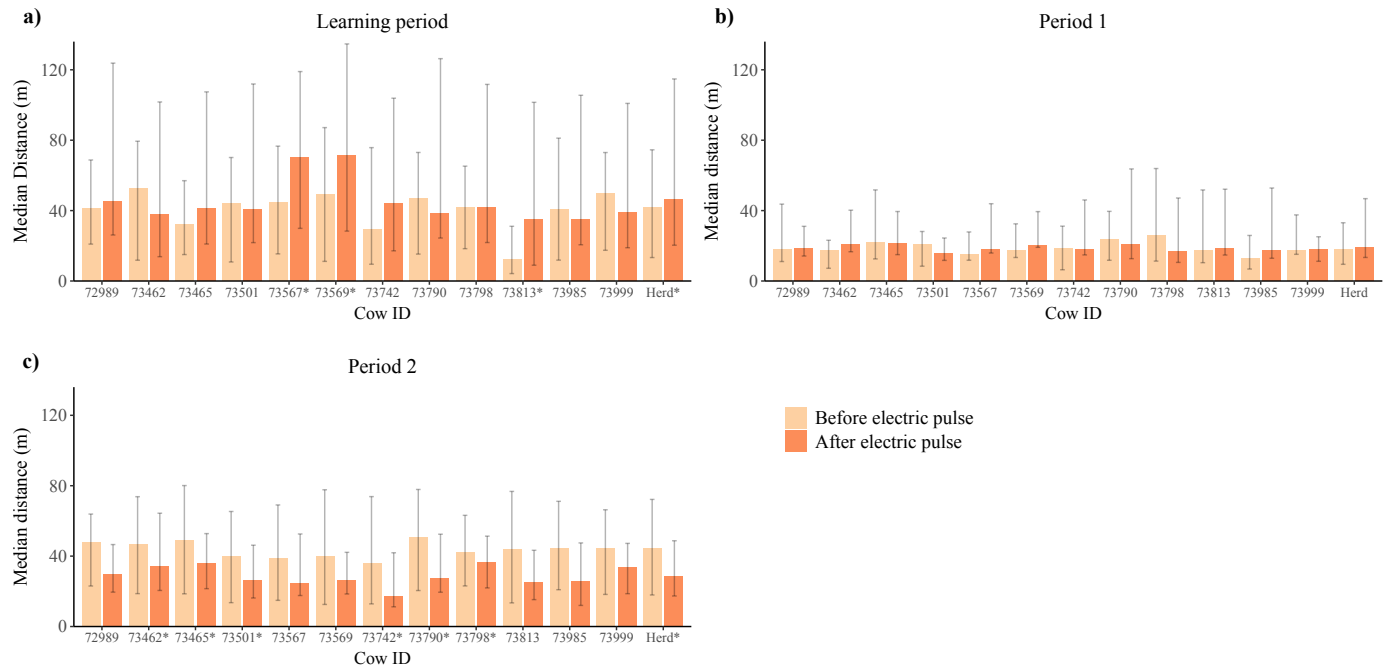
Figure 5. Median distance to the virtual border of each individual cow and the herd collectively, before and after any one individual received an electric impulse during (**a**) *the learning period* ($n = 3077$), (**b**) *period 1* ($n = 402$), and (**c**) *period 2* ($n = 4831$). Error bars represent the interquartile range. An asterisk next to the serial number denotes statistical significance ($p < 0.05$).

3.5. Reactions to Electric Impulse

There were no significant changes in the cows' activity before and after receiving an electric impulse (Figure 6).
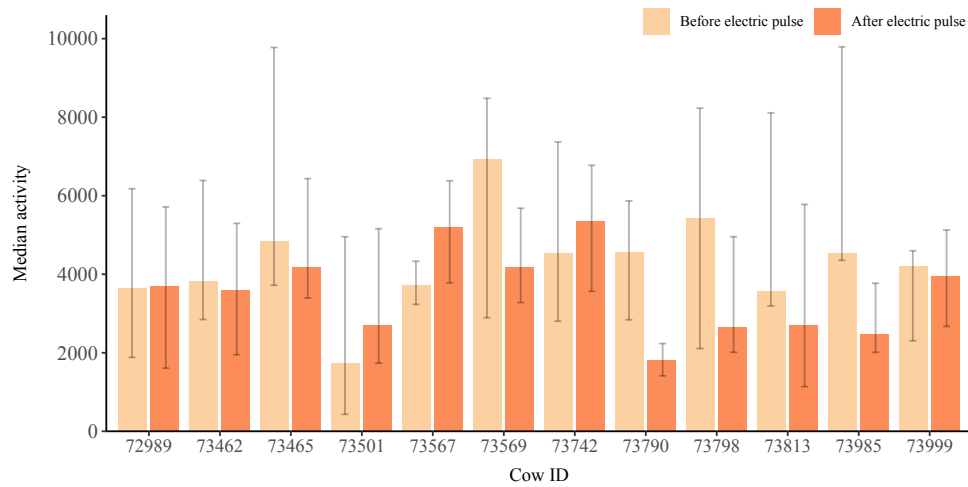
Figure 6. Median activity of each individual two hours before and after receiving an electric impulse ($n = 202$). Error bars represent the interquartile range.

4. Discussion

4.1. Interactions with the Virtual Border

In this study, virtual fencing was successful in keeping the herd of cattle within the specified area for the vast majority of the time, with only four separate breakouts across the entire 139-day period not explained by unfortunate circumstances such as poor fence placement or low flying drones. These results are in accordance with previous studies and underline the potential for virtual fencing in cattle management [7–10,32]. Interestingly, the cows spent most of their time on either lush areas for grazing or higher areas for resting, and did not appear to have much interest in testing the border or breaking out of the enclosure (Appendix C). It was observed, however, that the herd spent more time grazing the fresh, not previously grazed, areas whenever the virtual border was moved out, especially when kept within a smaller area. This could suggest that one should be wary of keeping the cattle in areas with limited feed availability. However, previous studies have found that it is possible to exclude cattle from reaching an area of greater feed availability to some extent [14,19]. However, this study mainly investigated the cattle individually and not as a herd, warranting further studies of whether herding behavior can override the individuals' hesitation to cross the virtual border in the case of low feed availability. This has previously proven to be an issue when testing similar virtual fencing systems on sheep [16,33].

In *the learning period*, the distance to the virtual border was significantly larger after any one individual received an electric impulse than prior to the impulse. This was the case for the herd as a whole and for three of the individual cows (Figure 5a). Interestingly, in *period 2* the distance to the border was significantly smaller after an individual received an electric impulse than before, both for the herd as a whole, and for six out of the twelve individuals (Figure 5c). This may be due to the cows learning the association between the auditory warning and the virtual border, thus, increasing their reliance on these cues to ensure that they remain within the virtual boundary rather than relying upon the response of their conspecifics. Nonetheless, an individual receiving an electric impulse clearly solicited a social response in its herd mates, as suggested by previous studies and supporting the initial hypothesis [25,27].

In this study there were no significant differences in the activity of the cows after receiving an electric impulse, i.e., receiving an electric impulse did not have a long term effect on the cows' activity level. Thus, indicating that the virtual fencing system did not negatively impact the cows' welfare, based on measures associated with the behavior of the cows. Campbell et al. [6] similarly found a minimal impact of the virtual border on cattle behavior. However, McSweeney et al. [17] found cattle to express some signs of stress when kept under virtual fencing. It can, therefore, not be dismissed that under some circumstances virtual fencing may have a negative effect on welfare. Such an effect on welfare could be dependent on the intensity of the electric pulse, where a more intense electric impulse would likely result in a stronger behavioral response. Further studies may provide insight into under which conditions attribute to ensuring optimal animal welfare when using virtual fencing systems. Furthermore, this study only investigated the long term effect of an electric impulse on the cows' behavior. It may, therefore, be relevant to also investigate the acute behavioral effect of receiving an electric impulse.

4.2. Learning Ability

In this study there was a positive correlation between the number of warnings and the number of electric impulses received. As such, this study suggests that an individual receiving a higher number of warnings will also receive a higher number of electric impulses. Likewise, a decrease in the number of warnings received over time will result in the individual receiving fewer electric impulses, i.e., fewer stressful events. However, the results also indicated that the ratio between the number of electric impulses and the number of auditory warnings decreased with time, showing that this relationship between the number of warnings and impulses may be subject to change as the cows improve their response to the auditory warnings alone. Thus, as expected and in accordance with previous studies, the results of this study clearly showed that the cows learned to respond correctly to the virtual fencing system [8,14]. As the number of warnings and thereby electric impulses decreased rapidly over time when the cows learned to respond appropriately to the auditory cues, enabling to avoid the virtual border, the long term welfare implications are expected to be minimal, as has also been suggested by multiple other studies [5,13,18,28,34].

It is obvious, that the cows in this study learned to avoid the virtual border, receiving fewer warnings and electric impulses over time. This corresponds well with findings in previous studies of cattle [14,15,17,19,25,35]. In the context of nature conservation and rewilding, where large grazers are meant to be kept in large areas, these results are promising when considering virtual fencing as a replacement of traditional electric fencing. This is in line with previous studies suggesting virtual fencing could be a good alternative in extensive grazing situations, such as nature conservation [2,32]. The fact that the cows seemingly have to go through a new "exploratory" phase, however, when being restricted to a far smaller area from one day to the next, suggests that such sudden changes in the enclosure should be done with precaution, as it could cause unnecessary stress to the animals. However, another study found no issue when limiting a small heard of cattle to a smaller area, the herd quickly moving into the new allowed area with no significant change in behavior [6]. Nonetheless, future studies should pay more attention to the placement of the virtual border. A few times during the experiment the virtual border was placed sub-optimally, such as right on the other side of a ditch, or on both sides of a road such that only the road was inaccessible. This caused a disproportionately large amount of warnings and electric impulses to be delivered in these areas. Thus, future studies should also investigate optimal placement of the virtual border.

4.3. Inter-Individual Variation

There was a significant inter-individual variation in the number of warnings and electric impulses the cows received in this study. Similar differences between individuals in relation to virtual fencing have also been shown in previous studies [8,12,14,19]. There was clear variation in how many warnings the cows received in the two periods, and how quickly they learned to avoid warnings and electric impulses. Additionally, there was a strong positive correlation between the number of warnings a cow received in each of the three respective periods. This clearly supports the hypothesis that the number of warnings and electric impulses are dependent on the individual cow. It is, therefore, suggested that the personality of each cow is taken into consideration when choosing individuals to be used in virtual fencing. However, this is only realisable in small scale projects. Clearly, it is desirable that cows, both for farming and nature management purposes, using virtual fencing, should have personalities suited to such circumstances [8,20]. This study clearly showed that cows receiving a small number of warnings in a training period will continue to receive few warnings and therefore electric impulses and will most likely be exposed to fewer stressful events.

It is also clear that in future investigations of animal welfare and learning capabilities of cattle, one needs to consider both the personality of each individual as well as socially facilitated behavior. Statistical analyses should as such also take this into consideration, by assessing each individual in addition to pooled herd data. Furthermore, future studies should consider incorporating different breeds of cattle, and the effect of adding bulls to the herd should also be investigated. Another idea for future experimentation is to examine whether virtual fencing is effective in very large enclosures where the cattle would possibly not be subject to warnings or electric impulses for long periods of time. It may be more effective to create smaller virtual enclosures and move them, as the results indicate that cows are quick to adapt to new virtual borders, and previous studies show that virtual fencing is effective at herding cattle into a new area [36].

One aspect this experiment failed to address, is the possible link between personality and social hierarchy as well as possible socially facilitated learning. Previous studies have shown that cattle learned how to respond to virtual fencing, not just by interacting with the fence themselves, but also from observing herd mates [25,27]. Future studies are needed to investigate this potential link between social hierarchy and personality, possibly explaining why some individuals receive more auditory warnings and electric impulses than others, e.g., an individual receiving many warnings may be the dominant cow leading the herd. Future studies could also examine whether this social learning and hierarchical herd

behavior would allow for only a part of the herd to wear collars, without compromising the ability of the virtual fencing to contain the animals, as has been shown to be the case for sheep [26].

5. Conclusion

In conclusion, the Nofence virtual fencing system was effective at confining the herd of cattle to the desired area. No indications that virtual fencing negatively affected animal welfare were found based on the behavioral observations in this study. However, it is difficult to assess whether the welfare implications are larger or smaller compared to traditional electric fence, as no control group was included. Future studies should compare the two fencing methods to reach a conclusion. The animals did, however, show clear signs of learning, receiving fewer warnings and electrical impulses with time. As such, any welfare implications should be significantly reduced over time. Furthermore, the cows reacted to herd members receiving electric pulses, and future studies should not assume independency between the cows, but factor in herd behavior, when doing statistical analyses. Lastly, the cows also expressed inter-individual variations in their responses to the virtual enclosure. This need to be taken into account when choosing animals to be placed in virtually fenced enclosures in order to ensure optimal welfare.

Institutional Review Board Statement: The study was conducted according to the institutional guidelines for animal research (directive 2010/63/EU), and approved by the Animal Experiments Inspectorate of Denmark (2020-15-0201-00588) prior to the start of the study.

Data Availability Statement: The data presented in this study are available on request from the corresponding author.

Conflicts of Interest: The authors declare no conflict of interest.

## Appendix A. Nofence Virtual Fencing System

Figure A1. Nofence collar (Photo: J. Frikke).

Appendix B. Virtual Enclosures

Table 2: Activation date and effective size of each version of the virtual enclosure. Each version of the enclosure was active from the date specified in the table until the next version was created. Only versions of the enclosure that were in effect for more than 12 h are included.

|	Version	Date	Size (ha)
Learning	L.1	29 May 2021	11.92
	L.2	4 June 2021	12.08
	L.3	7 June 2021	12.55
	L.4	10 June 2021	12.26
Period 1	1.1	12 June 2021	34.94
	1.2	14 June 2021	37.41
	1.3	23 June 2021	37.23
	1.4	27 June 2021	45.80
	1.5	28 July 2021	48.93
	1.6	30 July 2021	27.98
Period 2	2.1	11 August 2021	15.08
	2.2	25 August 2021	64.72
	2.3	1 September 2021	64.80
	2.4	19 September 2021	63.03
	2.5	20 September 2021	69.50
	2.6	23 September 2021	70.36
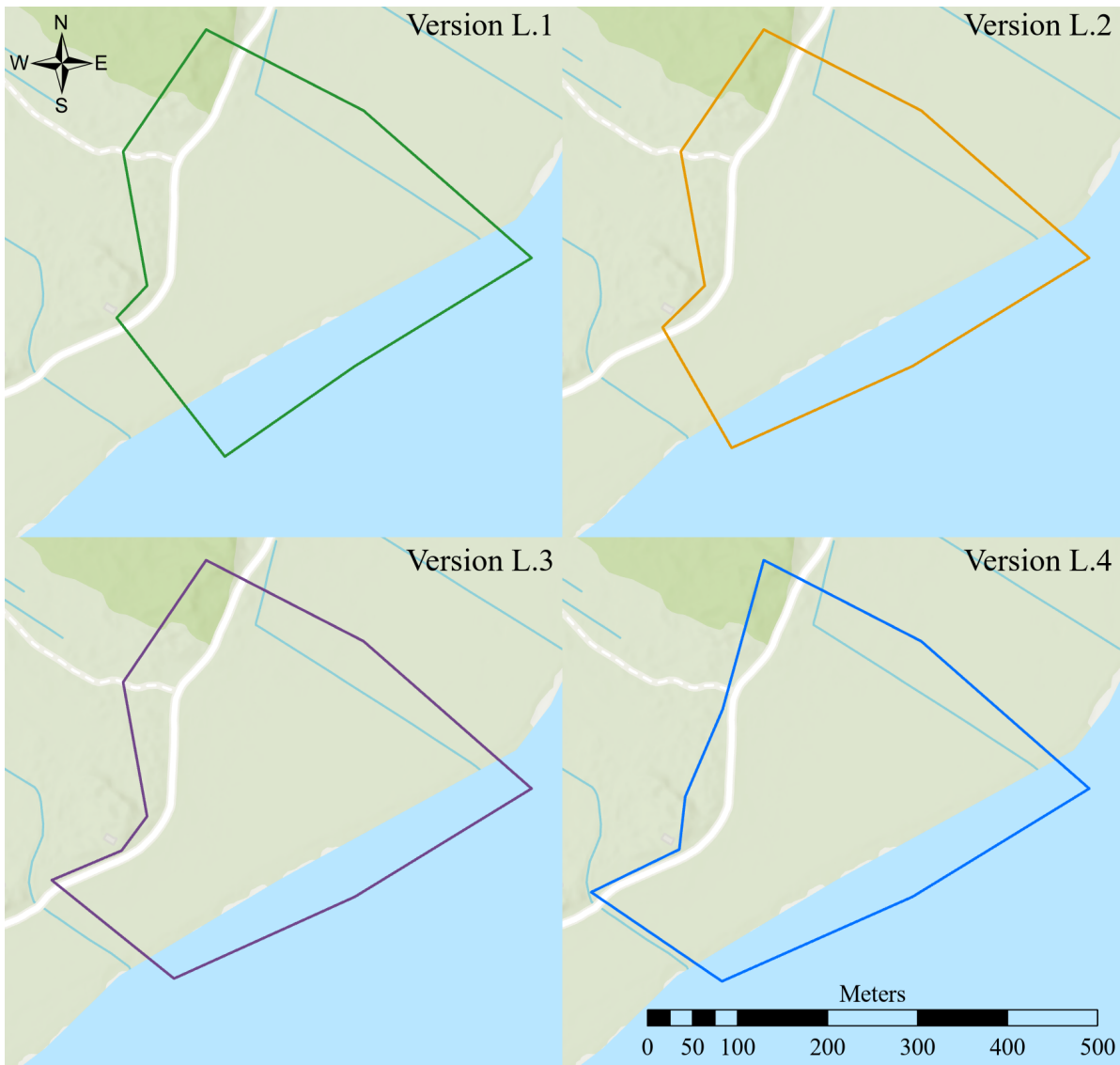
Figure A2. The virtual enclosure during *the learning period*. The coordinates of the lower right corner of each map frame are 8°27′59″ E 55°24′4″ N.
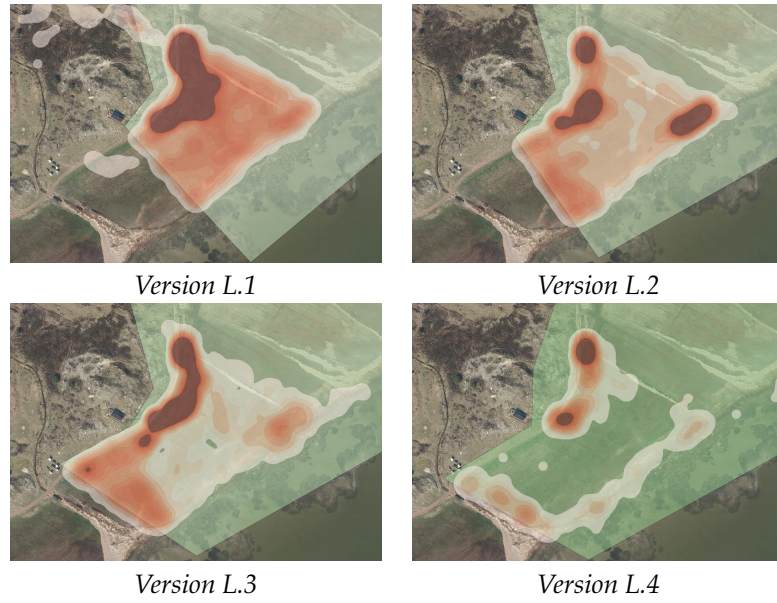
Figure A3. The virtual enclosure during *period 1*. The coordinates of the lower right corner of each map frame are 8°27′59″ E 55°23′46″ N.
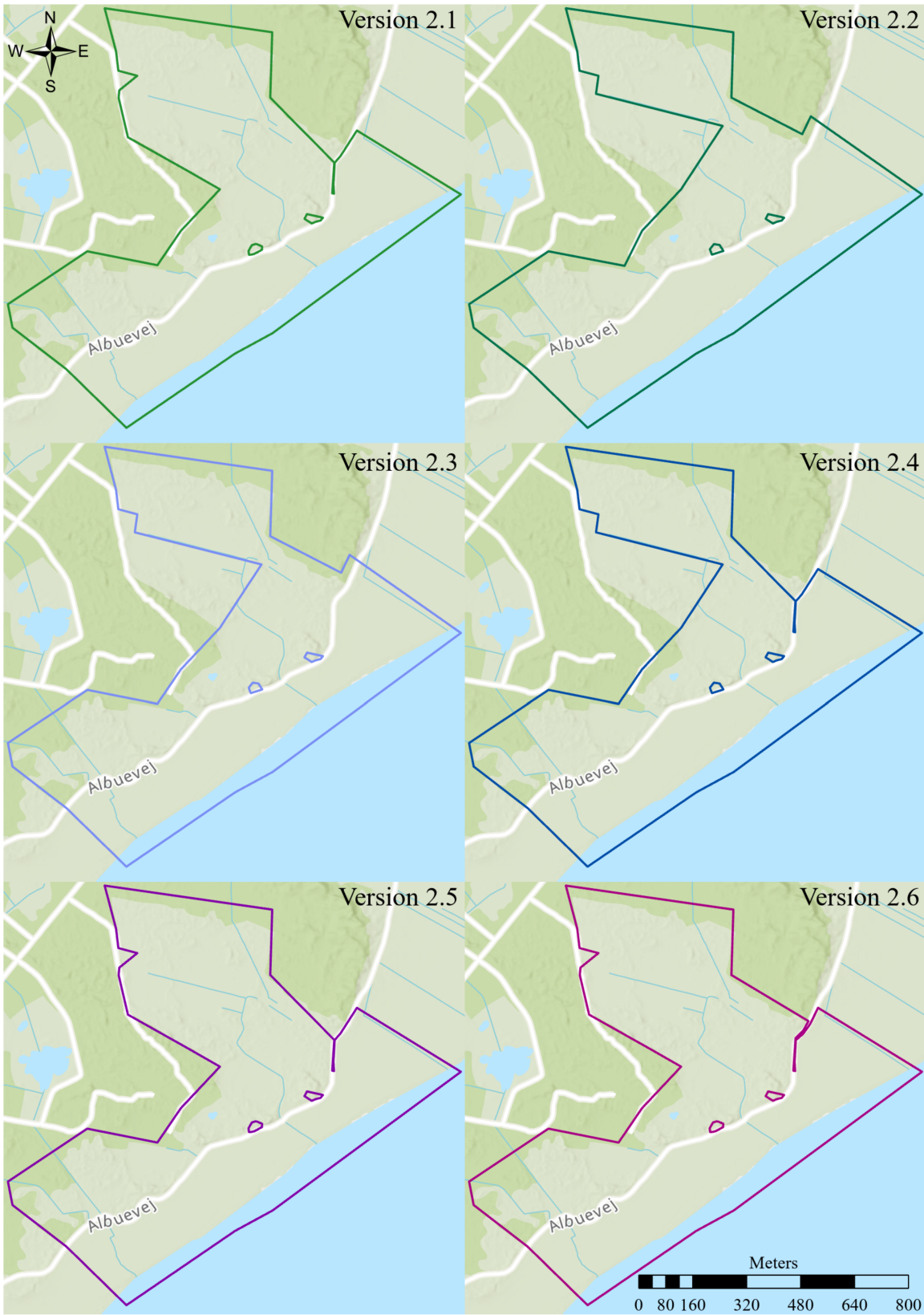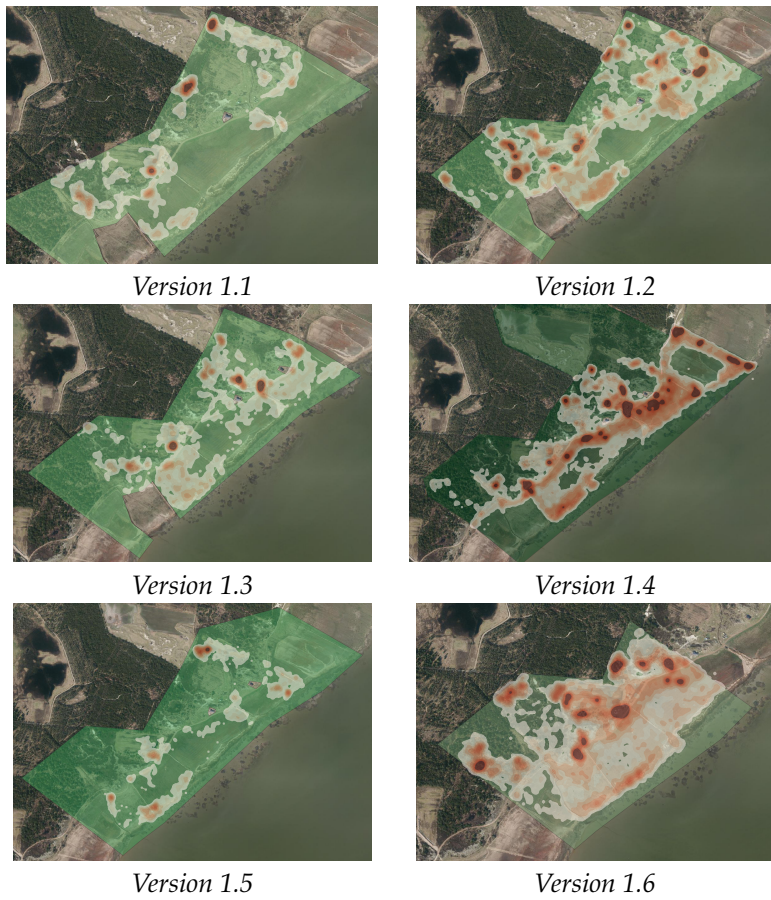
Figure A4. The virtual enclosure during *period 2*. The coordinates of the lower right corner of each map frame are 8°27′59″ E 55°23′50″ N.

Appendix C. Heatmaps

Version L.1

Version L.2
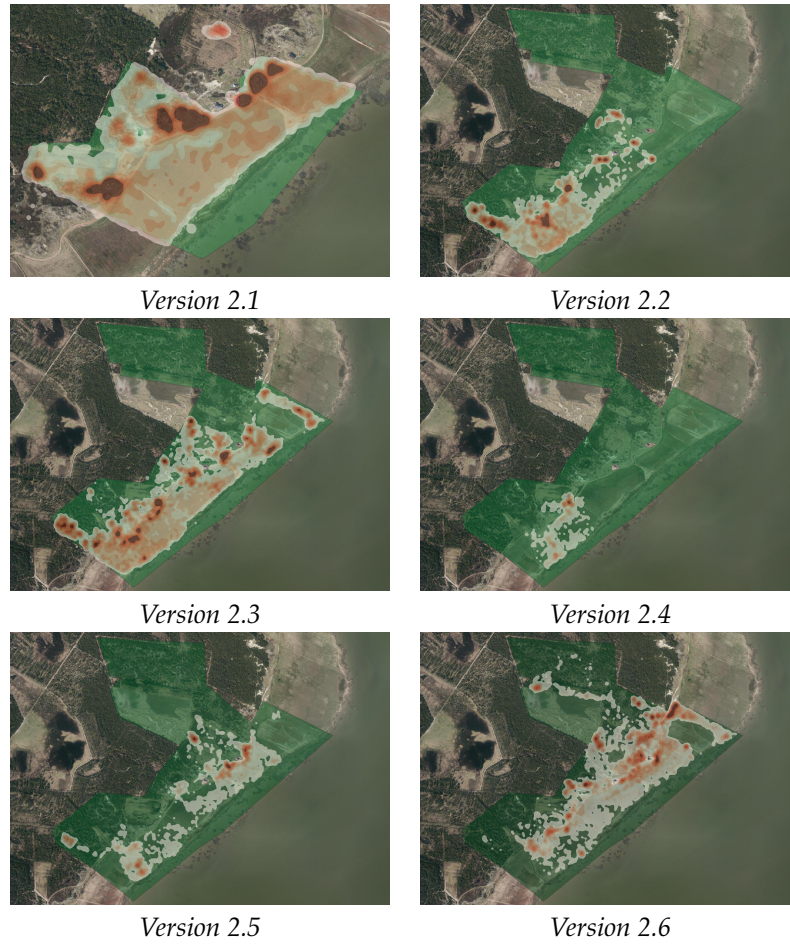
Version L.3

Version L.4

Figure A5. Heatmaps showing the cows' distribution within the different versions of the virtual enclosure during the learning period. The light green area represents the area of the virtual enclosure for each version.


Version 1.1

Version 1.2

Version 1.3

Version 1.4

Version 1.5

Version 1.6

Figure A6. Heatmaps showing the cows' distribution within the different versions of the virtual enclosure during period 1. The light green area represents the area of the virtual enclosure for each version.

Version 2.1

Version 2.2

Version 2.3

Version 2.4

Version 2.5

Version 2.6

Figure A7. Heatmaps showing the cows' distribution within the different versions of the virtual enclosure during period 2. The light green area represents the area of the virtual enclosure for each version.

Appendix D. Correlations
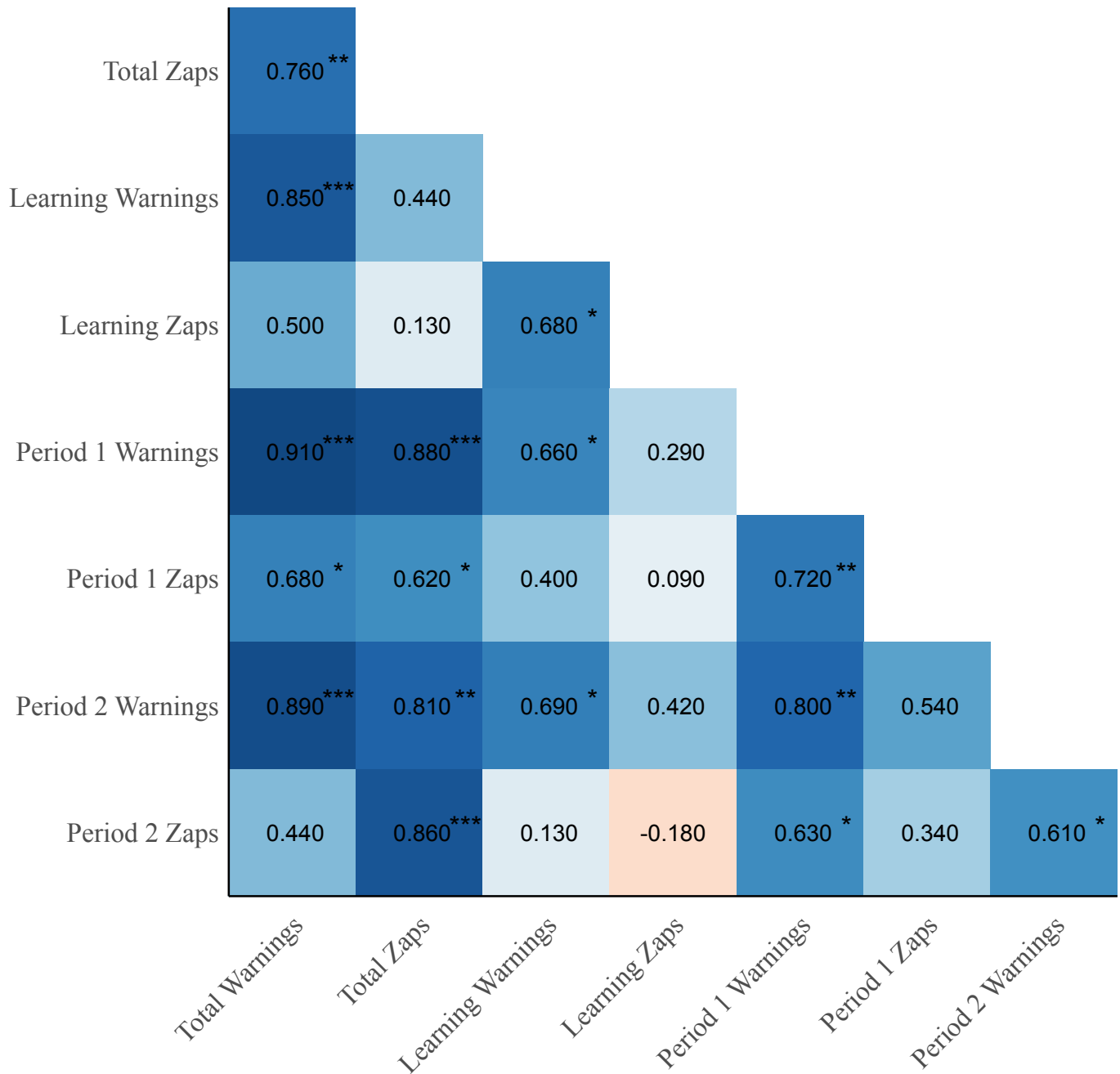
Figure A8. Correlation between auditory warnings and electric pulses received throughout the entire experiment and those received in each of the three periods. The values indicating the Spearman correlation coefficient with the significance level (* $p < 0.05$; ** $p < 0.01$; *** $p < 0.001$).

Appendix E. Pairwise Comparisons between Individuals

Results of pairwise comparisons between the individuals using the Mann-Whitney U Test with corrections for multiple testing using the Bonferroni correction.

Table 3: Individual differences in the number of auditory warnings and electric pulses they received throughout the entire experiment, the learning period, period 1, and period 2, respectively. The percentage of pairwise comparisons that showed significant differences between the individuals along with the significance level of the pairwise comparisons.

Period	Message	Total Significant Differences (%)	No. Siginficant Differences			
			<0.05	<0.01	<0.001	n.s.
All	Warnings	70.0%	4	2	40	20
	Electric impulses	70.0%	4	2	40	20
Learning	Warnings	53.0%	3	4	28	31
	Electric impulses	9.10%	1	4	1	60
Period 1	Warnings	62.1%	2	6	33	25
	Electric impulses	51.5%	19	0	15	32
Period 2	Warnings	53.0%	2	6	27	31
	Electric impulses	22.7%	3	3	9	51

Appendix F. Results when Removing the Social Panic Reaction Data

This appendix includes results where data from three days has been removed (29 May 2021; 10 June 2021; 20 September 2021). Two of these days all twelve cows escaped due to a social panic reaction, and the last day eight of the cows escaped due to a social panic reaction. Each time a cow escapes it has received three electric impulses before the system registers the cow as 'escaped'.

Appendix F.1. Interactions with the Virtual Border
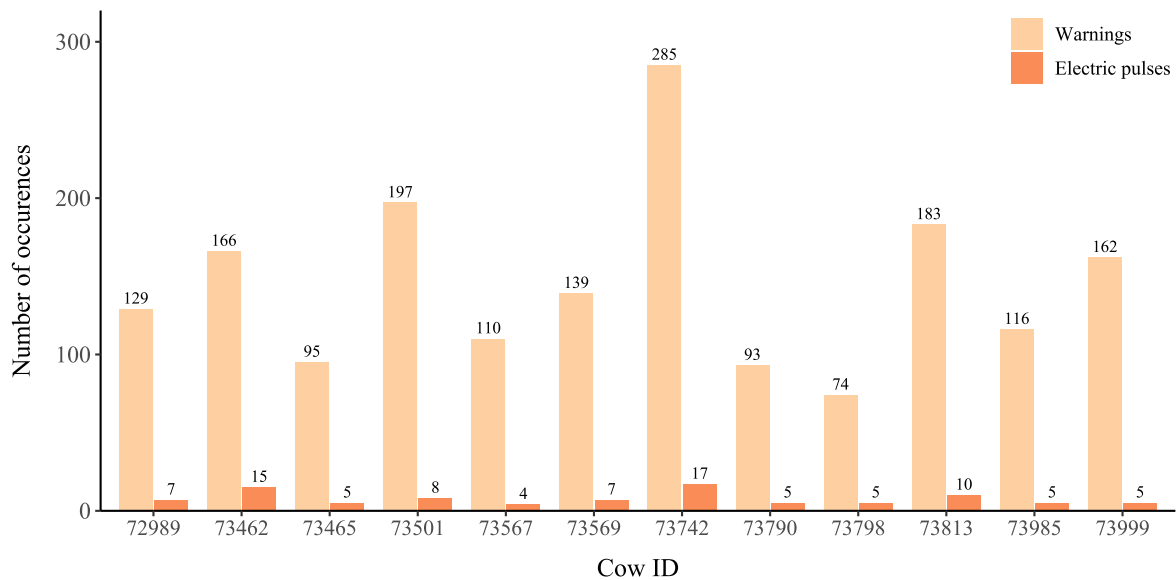
Figure A9. The number of auditory warnings and electric impulses that each individual received throughout the 139-day experiment, excluding those received on days where a social panic reaction occurred.

Appendix F.2. Learning Ability

The cows received significantly more auditory warnings and electric impulses per week during the 14 day *learning period* than during the other two periods ($p < 0.05$) (Figure A10). The cows also received significantly more warnings and electric impulses in *period 2* compared to *period 1* ($p < 0.05$) (Figure A10). Moreover, the ratio between the number of electric impulses and the number of auditory warnings was highest in *the learning period* for most of the individuals and all individuals had the lowest impulse to warning ratio in *period 1*.
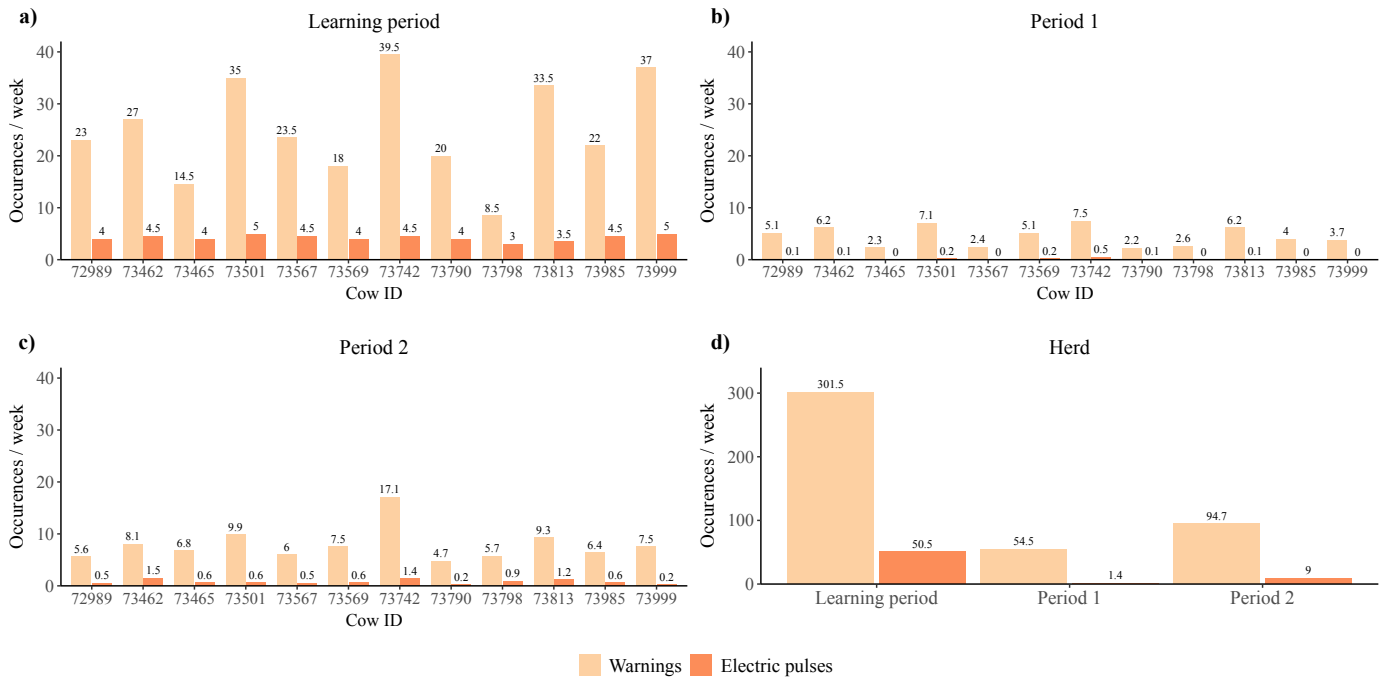
Figure A10. Average number of auditory warnings and electric impulses received per week by (**a**) each individual in *the learning period*, (**b**) each individual in *period 1*, (**c**) each individual in *period 2*, and (**d**) the entire herd during each of the three periods. Excluding days where a social panic reaction occurred.
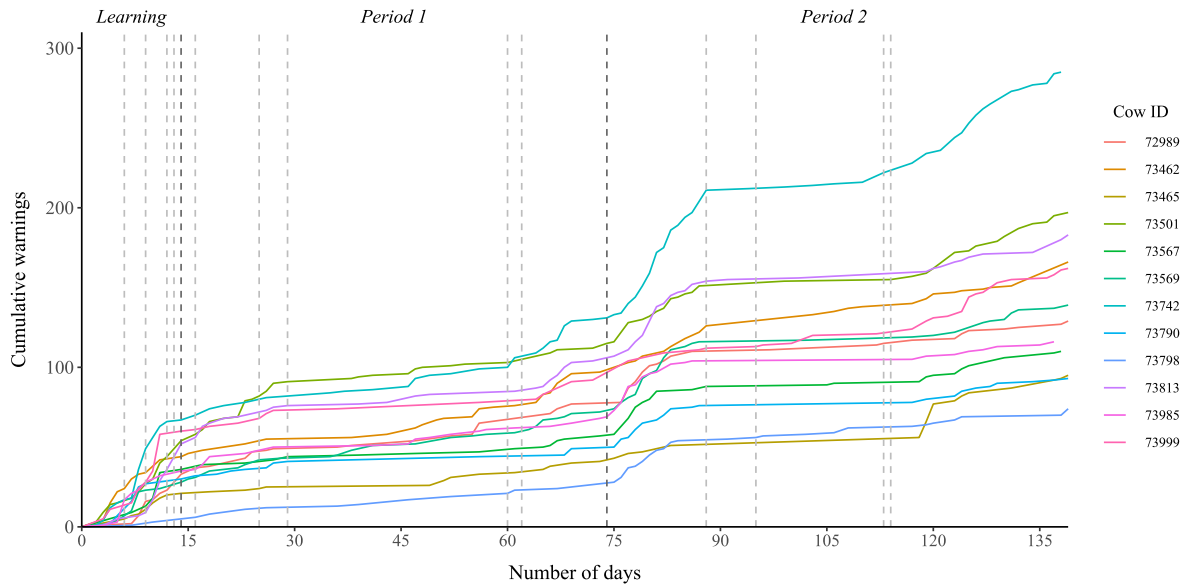
Figure A11. Cumulative number of warnings received by each cow during the three periods. The vertical lines in the plot mark any significant change in the virtual enclosure, where the darker lines indicate the division of the three periods. Excluding days where a social panic reaction occurred.

Appendix F.3. Inter-Individual Differences

There was a positive correlation between the number of warnings and electric impulses an individual received over the entire period of the experiment ($r_s = 0.817$ **). There was also a positive correlation between the number of warnings an individual cow received in *the learning period* and the number of warnings received in *period 1* ($r_s = 0.649$ *) and *period 2* ($r_s = 0.748$ **), respectively. Furthermore, the individuals significantly differed from one another in the number of warnings and electric impulses they received ($p < 0.001$).

Appendix F.4. Reactions to Electric Impulse

There were no significant changes in the cows' activity before and after receiving an electric impulse (Figure A12).
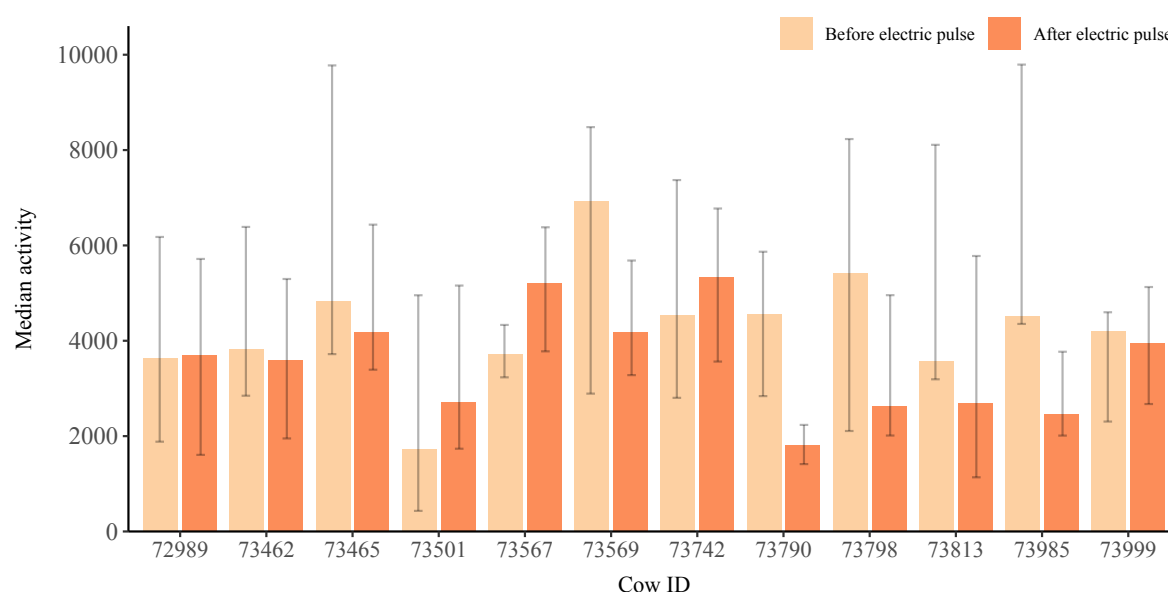
Figure A12. Median activity of each individual two hours before and after receiving an electric impulse ($n = 202$). Error bars represent the interquartile range. An asterisk next to the serial number denotes statistical significance ($p < 0.05$). Excluding data from days where a social panic reaction occurred.

References

1. European Commission. *GRAZELIFE: Grazing for Wildfire Prevention, Ecosystem Services, Biodiversity and Landscape Management (LIFE18PRE/NL00)*; LIFE Programme of the European Union: Brussels, Belgium, 2019.
2. Jachowski, D.S.; Slotow, R.; Millspaugh, J.J. Good Virtual Fences Make Good Neighbors: Opportunities for Conservation. *Anim. Conserv.* **2014**, *17*, 187–196. [CrossRef]
3. Osipova, L.; Okello, M.M.; Njumbi, S.J.; Ngene, S.; Western, D.; Hayward, M.W.; Balkenhol, N. Fencing Solves Human-Wildlife Conflict Locally but Shifts Problems Elsewhere: A Case Study Using Functional Connectivity Modelling of the African Elephant. *J. Appl. Ecol.* **2018**, *55*, 2673–2684. [CrossRef]
4. Umstatter, C. The Evolution of Virtual Fences: A Review. *Comput. Electron. Agric.* **2011**, *75*, 10–22. [CrossRef]
5. Campbell, D.L.M.; Lea, J.M.; Keshavarzi, H.; Lee, C. Virtual Fencing is Comparable to Electric Tape Fencing for Cattle Behavior and Welfare. *Front. Vet. Sci.* **2019**, *6*, 445. [CrossRef] [PubMed]
6. Campbell, D.L.M.; Lea, J.M.; Farrer, W.J.; Haynes, S.J.; Lee, C. Tech-Savvy Beef Cattle? How Heifers Respond to Moving Virtual Fence Lines. *Animals* **2017**, *7*, 72. [CrossRef]
7. Campbell, D.L.M.; Ouzman, J.; Mowat, D.; Lea, J.M.; Lee, C.; Llewellyn, R.S. Virtual Fencing Technology Excludes Beef Cattle from an Environmentally Sensitive Area. *Animals* **2020**, *10*, 1069. [CrossRef] [PubMed]
8. Lomax, S.; Colusso, P.; Clark, C.E. Does Virtual Fencing Work for Grazing Dairy Cattle? *Animals* **2019**, *9*, 429. [CrossRef]
9. Umstatter, C.; Morgan-Davies, J.; Waterhouse, T. Cattle Responses to a Type of Virtual Fence. *Rangel. Ecol. Manag.* **2015**, *68*, 100–107. [CrossRef]
10. Langworthy, A.D.; Verdon, M.; Freeman, M.J.; Corkrey, R.; Hills, J.L.; Rawnsley, R.P. Virtual Fencing Technology to Intensively Graze Lactating Dairy Cattle. I: Technology Efficacy and Pasture Utilization. *J. Dairy Sci.* **2021**, *104*, 7071–7083. [CrossRef]
11. Stampa, E.; Zander, K.; Hamm, U. Insights into German Consumers' Perceptions of Virtual Fencing in Grassland-Based Beef and Dairy Systems: Recommendations for Communication. *Animals* **2020**, *10*, 2267. [CrossRef] [PubMed]
12. Campbell, D.L.M.; Lea, J.M.; Haynes, S.J.; Farrer, W.J.; Leigh-Lancaster, C.J.; Lee, C. Virtual Fencing of Cattle Using an Automated Collar in a Feed Attractant Trial. *Appl. Anim. Behav. Sci.* **2018**, *200*, 71–77. [CrossRef]
13. Lee, C.; Campbell, D.L.M. A Multi-Disciplinary Approach to Assess the Welfare Impacts of a New Virtual Fencing Technology. *Front. Vet. Sci.* **2021**, *8*, 637709. [CrossRef] [PubMed]
14. Lee, C.; Henshall, J.M.; Wark, T.J.; Crossman, C.C.; Reed, M.T.; Brewer, H.G.; O'Grady, J.; Fisher, A.D. Associative Learning by Cattle to Enable Effective and Ethical Virtual Fences. *Appl. Anim. Behav. Sci.* **2009**, *119*, 15–22. [CrossRef]
15. Wredle, E.; Rushen, J.; de Passillé, A.M.; Munksgaard, L. Training Cattle to Approach a Feed Source in Response to Auditory Signals. *Can. J. Anim. Sci.* **2004**, *84*, 567–572. [CrossRef]
16. Brunberg, E.I.; Bøe, K.E.; Sørheim, K.M. Testing a New Virtual Fencing System on Sheep. *Acta Agric. Scand. Sect. A—Anim. Sci.* **2015**, *65*, 168–175. [CrossRef]

17. McSweeney, D.; O'Brien, B.; Coughlan, N.E.; Férard, A.; Ivanov, S.; Halton, P.; Umstatter, C. Virtual Fencing Without Visual Cues: Design, Difficulties of Implementation, and Associated Dairy Cow behavior. *Comput. Electron. Agric.* **2020**, *176*, 105613. [CrossRef]

18. Verdon, M.; Langworthy, A.; Rawnsley, R. Virtual Fencing Technology to Intensively Graze Lactating Dairy Cattle. II: Effects on Cow Welfare and Behavior. *J. Dairy Sci.* **2021**, *104*, 7084–7094. [CrossRef] [PubMed]

19. Verdon, M.; Lee, C.; Marini, D.; Rawnsley, R. Pre-Exposure to an Electrical Stimulus Primes Associative Pairing of Audio and Electrical Stimuli for Dairy Heifers in a Virtual Fencing Feed Attractant Trial. *Animals* **2020**, *10*, 217. [CrossRef] [PubMed]

20. Lee, C.; Colditz, I.G.; Campbell, D.L.M. A Framework to Assess the Impact of New Animal Management Technologies on Welfare: A Case Study of Virtual Fencing. *Front. Vet. Sci.* **2018**, *5*, 187. [CrossRef]

21. Bushby, E.V.; Friel, M.; Goold, C.; Gray, H.; Smith, L.; Collins, L.M. Factors Influencing Individual Variation in Farm Animal Cognition and How to Account for These Statistically. *Front. Vet. Sci.* **2018**, *5*, 15. [CrossRef]

22. Santicchia, F.; Wauters, L.A.; Dantzer, B.; Westrick, S.E.; Ferrari, N.; Romeo, C.; Palme, R.; Preatoni, D.G.; Martinoli, A. Relationships Between Personality Traits and the Physiological Stress Response in a Wild Mammal. *Curr. Zool.* **2019**, *66*, 197–204. [CrossRef] [PubMed]

23. Stamps, J.; Groothuis, T.G.G. The Development of Animal Personality: Relevance, Concepts and Perspectives. *Biol. Rev.* **2010**, *85*, 301–325. [CrossRef] [PubMed]

24. de Azevedo, C.S.; Young, R.J. Animal Personality and Conservation: Basics for Inspiring New Research. *Animals* **2021**, *11*, 1019. [CrossRef] [PubMed]

25. Keshavarzi, H.; Lee, C.; Lea, J.M.; Campbell, D.L.M. Virtual Fence Responses are Socially Facilitated in Beef Cattle. *Front. Vet. Sci.* **2020**, *7*, 711. [CrossRef] [PubMed]

26. Marini, D.; Kearton, T.; Ouzman, J.; Llewellyn, R.; Belson, S.; Lee, C. Social Influence on the Effectiveness of Virtual Fencing in Sheep. *PeerJ* **2020**, *8*, e10066. [CrossRef] [PubMed]

27. Colusso, P.I.; Clark, C.E.F.; Lomax, S. Should Dairy Cattle Be Trained to a Virtual Fence System as Individuals or in Groups? *Animals* **2020**, *10*, 1767. [CrossRef] [PubMed]

28. Kearton, T.; Marini, D.; Cowley, F.; Belson, S.; Keshavarzi, H.; Mayes, B.; Lee, C. The Influence of Predictability and Controllability on Stress Responses to the Aversive Component of a Virtual Fence. *Front. Vet. Sci.* **2020**, *7*, 986. [CrossRef] [PubMed]

29. Berntsen, O.H. Method and System for Fencing Animals Without Using a Physical Fence. European Patent 2 515 633 B1, 31 December 2012.

30. QGIS. QGIS Desktop 3.20. 2021. Available online: http://www.qgis.org/ (accessed on 1 October 2021).

31. R Core Team. *R: A Language and Environment for Statistical Computing*; R Foundation for Statistical Computing, Vienna, Austria, 2021.

32. Bishop-Hurley, G.J.; Swain, D.L.; Anderson, D.M.; Sikka, P.; Crossman, C.; Corke, P. Virtual Fencing Applications: Implementing and Testing an Automated Cattle Control System. *Comput. Electron. Agric.* **2007**, *56*, 14–22. [CrossRef]

33. Brunberg, E.I.; Bergslid, I.K.; Bøe, K.E.; Sørheim, K.M. The Ability of Ewes with Lambs to Learn a Virtual Fencing System. *Animal* **2017**, *11*, 2045–2050. [CrossRef] [PubMed]

34. Kearton, T.; Marini, D.; Cowley, F.; Belson, S.; Lee, C. The Effect of Virtual Fencing Stimuli on Stress Responses and Behavior in Sheep. *Animals* **2019**, *9*, 30. [CrossRef] [PubMed]

35. Marini, D.; Cowley, F.; Belson, S.; Lee, C. The Importance of an Audio Cue Warning in Training Sheep to a Virtual Fence and Differences in Learning when Tested Individually or in Small Groups. *Appl. Anim. Behav. Sci.* **2019**, *221*, 104862. [CrossRef]

36. Campbell, D.L.M.; Marini, D.; Lea, J.M.; Keshavarzi, H.; Dyall, T.R.; Lee, C. The Application of Virtual Fencing Technology Effectively Herds Cattle and Sheep. *Anim. Prod. Sci.* **2021**, *61*, 1393–1402. [CrossRef]

Conclusion

This study describes the use of three different conservation technologies for wildlife monitoring, nature management, and wildlife research. The first article provides preliminary results demonstrating the use of drones with thermal imaging to conduct population surveys of European hare (*Lepus europaeus*). The second article provides a quantitative method that can be utilized to analyze data from camera–based monitoring systems and factually determine which behaviors lead to an increased collision risk. This method was utilized in the third article to quantify species-specific flight behavior in association with turbine collision risk. These results can be used to identify risk prone species based on flight behavior and phylogenetic relatedness. However, collision risk is also site-specific and these results should, therefore, be used to give a general indication of risk prone species. Thus, suggesting which species are relevant to further investigate in site-specific contexts. The last article demonstrated the use of virtual fencing as an effective tool for confining a herd of cattle without compromising their welfare. Thus, supporting the potential for virtual fencing as a viable alternative to physical electrical fencing for conservation grazing in Denmark.

This study demonstrates how technology can provide biologists with novel tools, including specific management tools, e.g. IdentiFlight and Nofence, and tools for collecting more and better data, thereby improving wildlife monitoring and research that can assist in management decisions. Thus, suggesting how technology can help solve existing management problems, such as, protecting environmentally sensitive areas during conservation grazing and preventing bird fatalities due to collisions with wind turbines. The data presented in this study also demonstrates how technology can enable the collection of large amounts of data, and all four articles confirm the need for tools to manage, process, and analyze these large amounts of data. Other technologies, such as bio-logging, bio-telemetry, acoustic recording, and camera traps, also effectuate the collection of large amounts of data. Thus, to maximize the output of these technological methods and fully capitalize on their potential, future research should focus on further developing tools to manage, process, and analyze these types of data. Moreover, researchers should focus not only on applying existing technology to wildlife conservation, but also on actively seeking to create novel technologies to provide conservation tools and solutions. This requires biologists, with first–hand knowledge of local wildlife conservation needs and obstacles, to work closely with technologists, able to develop and implement new solutions. Thus, bridging the gap between the conservation community and technology industry.